Title	Molecular Imaging Probes and Radiation-Activated Prodrugs Targeting Tumor Hypoxic Microenvironments: Molecular Design, Synthesis, and Evaluation(Dissertation_　　)
Author(s)	Hirata, Nao
Citation	Kyoto University (　　　)
Issue Date	2009-07-23
URL	http://dx.doi.org/10.14989/doctor.k14870
Right	
Type	Thesis or Dissertation
Textversion	author

Molecular Imaging Probes and Radiation-Activated Prodrugs Targeting Tumor Hypoxic Microenvironments: Molecular Design, Synthesis, and Evaluation

Nao Hirata

2009

Contents

General Introduction

1. *Background*

Due to the development of bioscience research and the progress of genome sequencing project, intracellular messengers and their host molecules have been continuously identified and characterized. Recently, as represented in a term "post-genome age", it has identified all of the chemical pieces of the human genome, the blueprint of life. This genome information has also revealed roles of bimolecules functioning in specific location or time. Therefore, there has been increasing demand to readily detect and visualize the dynamical behavior of biologically active molecules (metal ion,[1–6] sugar chain,[7] cAMP,[8] nitric oxide,[9] enzyme,[10–12] and so on) in living cells or tissues. Because of these backgrounds, fluorescent imaging techniques have been developed and widely used in view of their high sensitivity, high resolution, and convenient means, and hundreds of fluorescent probes to specifically recognize biomolecules in living body have been created for biological and medical application. Most of these fluorescent imaging probes are based on the fluorescence resonance energy transfer (FRET) or the photoinduced electron transfer (PeT) mechanism, resulting in suppression of non-specific fluorescence within an organism. In view of these characteristics, high-sensitive and versatile fluorescent probes have been developed for visualization of biologically active species and vital functions (Figure 1).
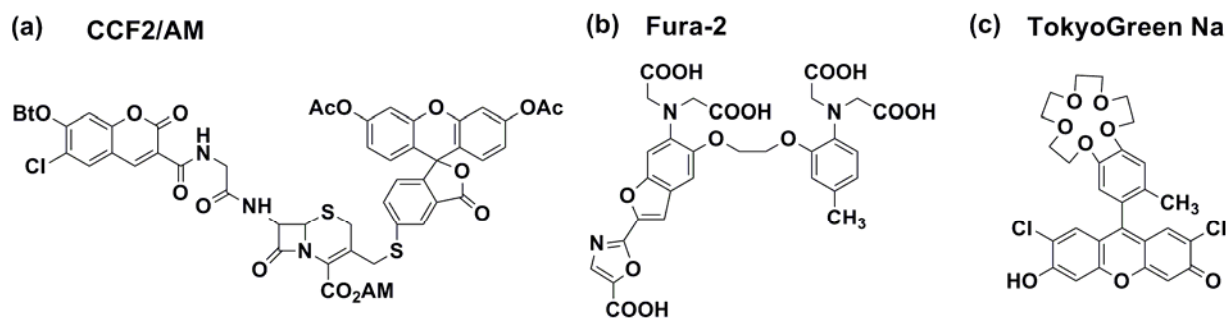

Figure 1. Examples of commercially available fluorescent-probes for detecting (a) hydrolysis activity of β-lactamase, (b) intracellular calcium ion, and (c) intracellular sodium ion.

2. *Imaging probes for visualization of biologically active species*

2-1. Calcium ion probe

Intracallular Ca^{2+} acts as a second messenger that regulates numerous physiological cellular phenomena including development, differentiation and apoptosis. Thus, there were increasing demand for quantitive measurement and visualization of cytosolic free Ca^{2+} and comparison with varied stimuli and cell responses. In 1985, Tsien and co-workers synthesized a new family of higher fluorescent indicator for cytosolic free Ca^{2+} (named **Fura-2**[1]) (Figure 2). The compound combined an 8-coordinate tetracarboxylate chelating site with stilbene chromophores. Incorporation of the ethylenic linkage of the stilbene into a heterocyclic ring enhanced the quantum efficiency and photochemical stability of the fluorophore. The greatest characteristic of **Fura-2** is that the fluorescence excitation spectra shift to shorter wavelengths as Ca^{2+} increases. The fluorescence intensity at the 355-nm excitation was increased, whereas that of the 380-nm excitation was decreased as increasing Ca^{2+} concentration.
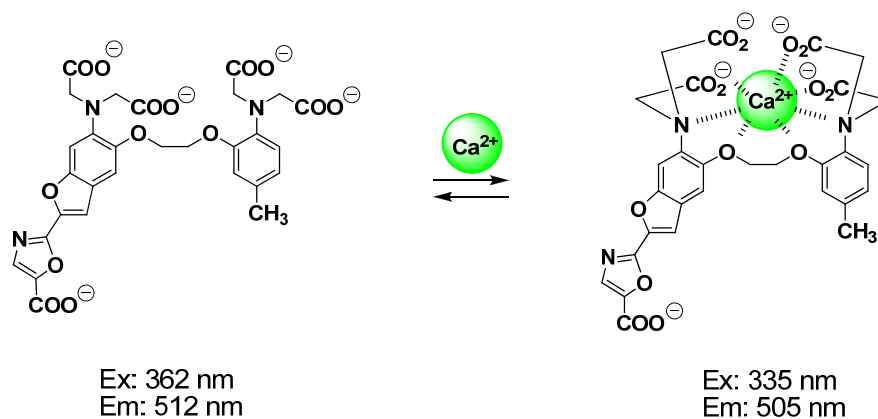
Ex: 362 nm
Em: 512 nm

Ex: 335 nm
Em: 505 nm

Figure 2. Schematic representation of **Fura-2**.

Consequently, Ca^{2+} concentration at each point in a cell was determined and visualized by measuring the fluorescence intensity (500 nm, emission) with excitation at 340 nm and at 380 nm, subsequently image processing of the fluorescence ratio (340/380). This ratiometric imaging technique has tremendously influenced later fluorescent imaging research.

In the mid-1990s, Green fluorescent protein (GFP) became popular for biological application. In 1997, Tsien and co-worker developed a new class of fluorescent indicator for Ca^{2+} based on GFP and the exchange of FRET efficiency[2] (named "cameleon", Figure 3). They consisted of tandem fusioins of a cyan-emitting mutant of the GFP,[13] calumodulin,[14] the calmodulin-binding peptide M13,[15] and an enhanced yellow-emitting GFP.[16] Binding Ca^{2+} makes calmodulin wrap around the M13 domain, increasing the FRET between the flanking GFPs. They have succeeded to visualize free Ca^{2+} dynamics in the cytosol, nucleus and endoplacmic of single HeLa cells by using this system. After that, FRET type fluorescent probes using GFP have been created, and most of those have been based on the principle of the fluorescent ratiometric measuring. Because of his outstanding achievements, Tsien received Nobel Prize in chemistry in 2008.
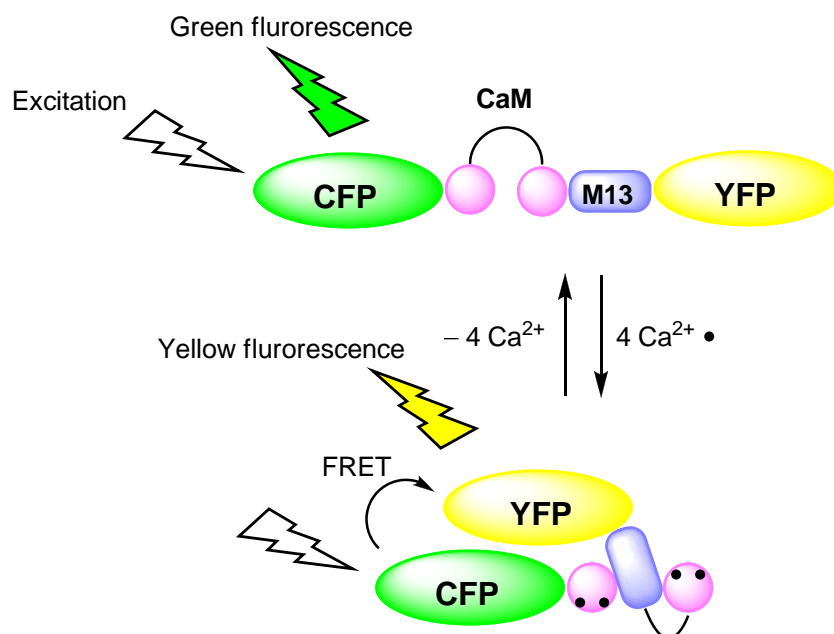

Figure 3. Schematic illustration of cameleon structure and its recognition of Ca^{2+} based on FRET mechanism.

2-2. Zinc ion probe

Zinc is the second most abundant "trace" element in the body. This metal ion is vital for normal cellular function as a cofactor in numerous enzymes, in transcription factors, in the immune system, and in the reproductive system.[17] In the brain, synaptically released zinc has physiological and pathological relevance;[18] the level of free zinc ions after release may reach a range of 10–100 µM in the synaptic cleft.[19] Although zinc plays important biological roles, little was known about the processes of distribution of this metal in the body or the incorporation of zinc into a variety of metalloproteins. Kikuchi and co-workers have designed and synthesized a series of fluorescent Zn^{2+} sensor molecules based on an aminofluorescein possessing *N, N, N', N'*-tetrakis(2-pyridyl-methyl)ethylenediamine (TPEN) as the acceptor of Zn^{2+} (named **ZnAF-2**, **ZnAF-2DA**[4]) (Figure 4). **ZnAF-2** recognizes Zn^{2+} based on the PeT mechanism, that is, aminofluorescein itself does not fluoresce due to the high HOMO level of its electron-donating group, whereas the HOMO level is lowered because electron donation is hindered by complex formation with Zn^{2+}, resulting in fluorescence with a high quantum yield. Indeed, **ZnAF-2** showed almost no fluorescence; however, upon addition of Zn^{2+}, the fluorescence intensity was increased by 51-fold. **ZnAF-2** showed no response to biologically important metal ions, such as Ca^{2+} and Mg^{2+}. **ZnAF-2** modified membrane-permeable acetyl ester derivative (**ZnAF-2DA**) were also prepared for the intracellular Zn^{2+} detection. This compound can easily penetrate through the cell membrane into cytosol, where the acetyl groups are hydrolyzed by esterase to afford the Zn^{2+} sensors. Kikuchi and co-worker confirmed the intracellular localization of endogenous Zn^{2+} in rat hippocampal slices by using **ZnAF-2DA**.
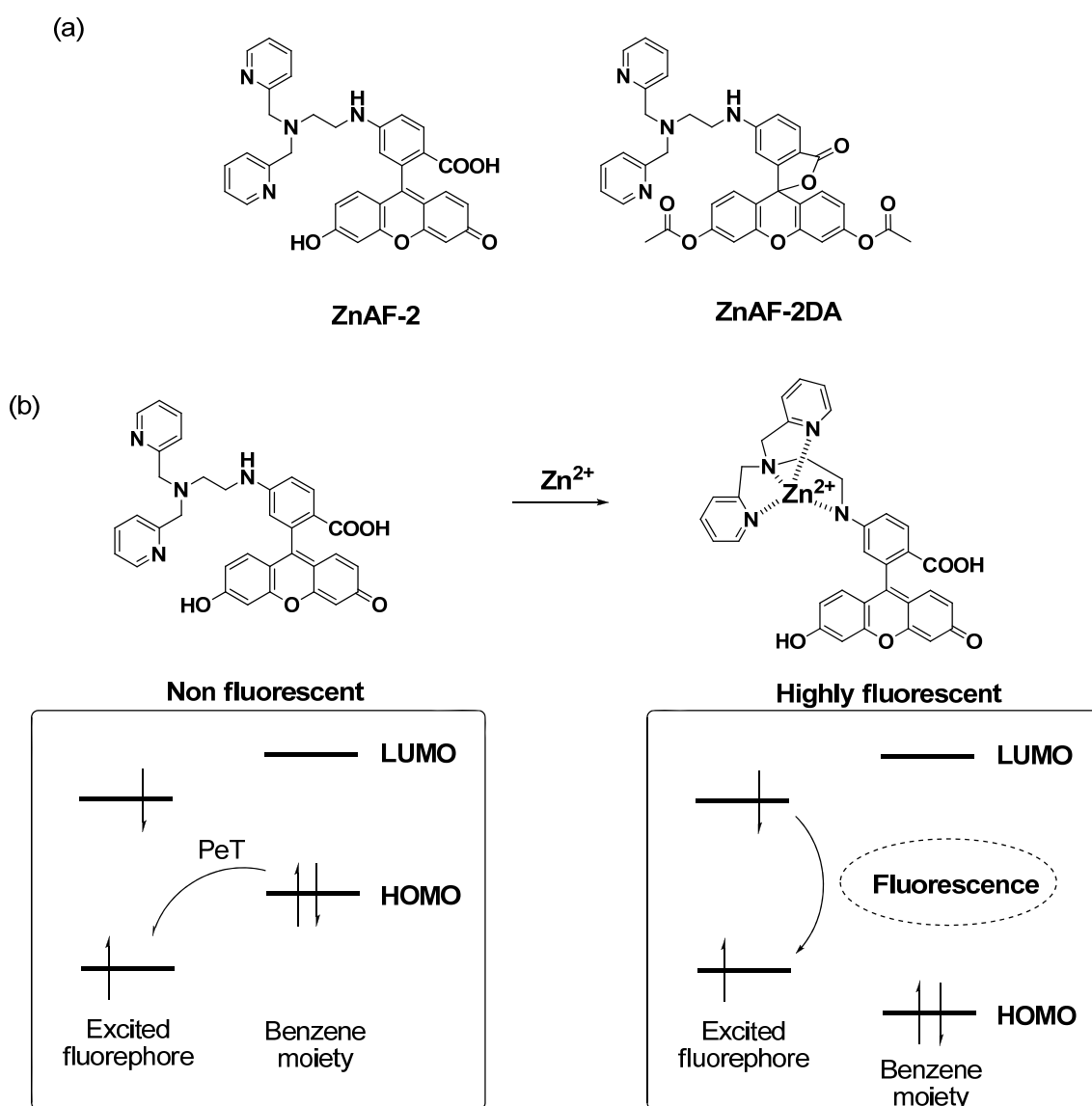
Figure 4. (a) Structures of zinc ion probes; **ZnAF-2** and **ZnAF-2DA**. (b) Schematic of PeT mechanism.

As described above, two remarkable imaging probes have been created and practically used for detecting intracellular Ca^{2+} and Zn^{2+} distribution. Other than those probes, fluorescent imaging probes for detecting intracellular Mg^{2+}, Na^+, Cu^+, Hg^{2+} have been reported,[5] moreover, dual imaging probe for Mg^{2+} and Na^+ has been also developed.[6] These imaging probes have been expected to enormously contribute the biological, physiological, and pathological research.

2-3. cAMP imaging probe

Most of fluorescent indicator dyes tended to be available only for simple inorganic ions such as Ca^{2+}, H^+, Na^+, Zn^{2+}, and Mg^{2+}. However, Tsien and co-workers have been reported a fluorescent indicator for biologically active molecule, adenosine 3',5'-cyclic monophosphate (cAMP) signaling pathway.[8] The sensor consists of cAMP-dependent protein kinase[20] in which the catalytic (C) and regulatory (R) subunits were each labeled with a different fluorescent dye such as fluorescein or rhodamine capable of fluorescence resonance energy transfer (FRET) in the holoenzyme complex R_2C_2 (named **FlCRhR**). When cAMP molecules bind to the R subunits of **FlCRhR**, the C subunits dissociate, thereby eliminating energy transfer (Figure 5).
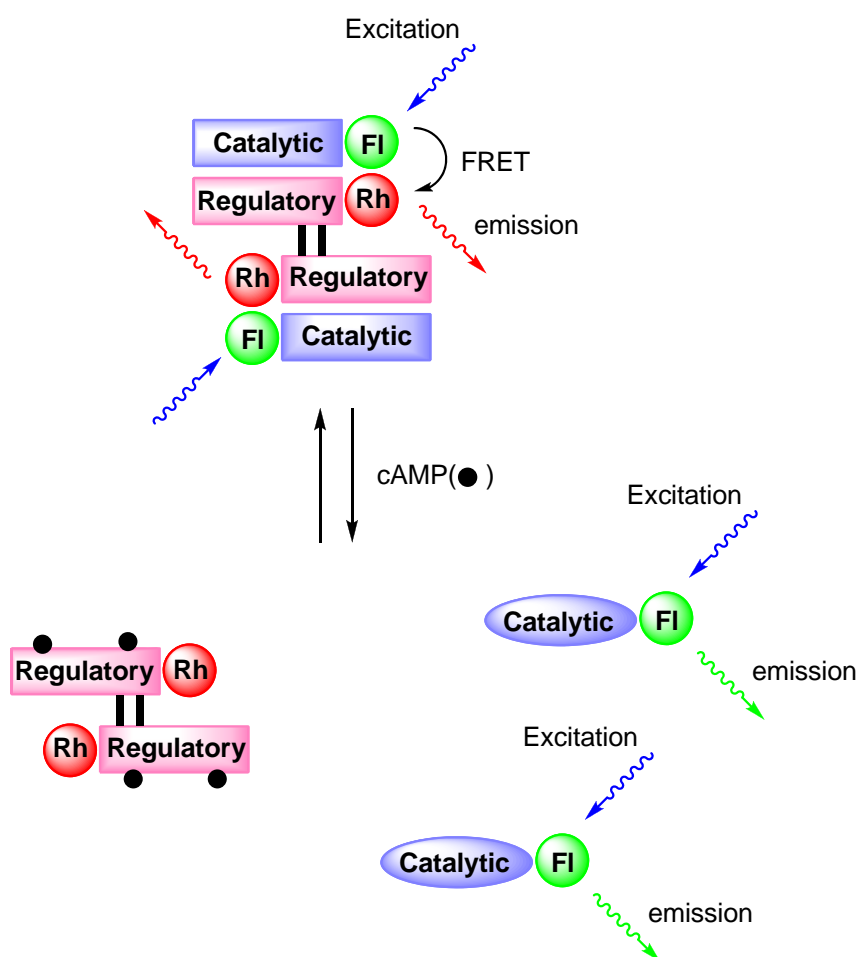

Figure 5. Schematic diagram showing how to detect cAMP using FRET mechanism

8

Indeed, in the holoenzyme, the dyes were close enough so that excitation of the fluorescein donor at 480–495 nm results in detectable emission from the rhodamine acceptor moiety as a result of resonance energy transfer. Cyclic AMP liberated the C subunits, effectively increase the donor–acceptor distance to infinity, and thereby energy transfer is prevented. Excitation of the fluorescein gave brighter emission of that dye at 500–570 nm and less emission at the 570–620 nm wavelengths characteristic of rhodamine. Therefore, cAMP changed the ratio of emission amplitudes of **FlCRhR** at two wavelength bands. In this way, the change in shape of the fluorescence emission spectrum allowed cAMP concentrations and the activation of kinase to be nondestructively visualized in single living cells microinjected with the labeled holoenzyme.

Other than these remarkable imaging probes for visualizing intracellular Ca^{2+}, Zn^{2+}, and cAMP, some unique imaging systems have been succeeded in detecting intracellular sugar chains,[7] or nitric oxide,[9] which deeply relates to vasorelaxant effect.

3. *Imaging probes for visualization of vital functions*

3-1. Imaging of β-galactosidase activity

β-Galactosidase is widely used reporter enzyme, but although several substrates are available for *in vitro* detection, its application for *in vivo* optical imaging remains a challenge. To obtain a probe suitable for *in vivo* use, Nagano and co-worker have developed activatable fluorescence probe.[11] First, they have synthesized and characterized various derivatives (TokyoGreens) whose electron density of the benzene moiety was tuned in a fine manner by introducing methyl and methoxy groups into the benzene moiety. Consequently, the fluorescence quantum yield was greatly altered, depending on the oxidation potential and the HOMO energy level of the benzene moiety. 2-Me-4-MeO TokyoGreen exists mainly as an anion form under neutral to basic conditions, because the pK_a value of the xanthene fluorophore is around 6.2, and it

fluoresced almost fully at neutral pH, while under acidic conditions it was almost nonfluorescent. This is because the oxidation potential of 3-methxytoluene, which is the benzene moiety of this derivative, lies between the fluorescence on/off thresholds of the neutral and anion forms of the fluorophore. In view of this, they have conjugated 2-Me-4-OMe TokyoGreen with *O*-β-galactoside (named **TG-βGal**) as a novel fluorescence probe for β-galactosidase. Before the reaction, the quantum efficiency of fluorescence was very small and the probe was almost nonfluorescent. Upon encounter with the target β-galactosidase, hydrolysis occurred efficiently to afford highly fluorescent **TG-βGal** (Figure 6). In the application of **TG-βGal** to GP293 cells transduced with or without LNCX2-*lacZ* (*lacZ*-positive or *lacZ*-negative cells, β-galactosidase is the gene product of *lacZ*.), a bright image of *lacZ*(+) cells was obtained by using **TG-βGal** without any fixation or other compicated technique. These results clearly show the advantages of **TG-βGal** for fluorescence imaging of β-galactosidase activity in living cells.
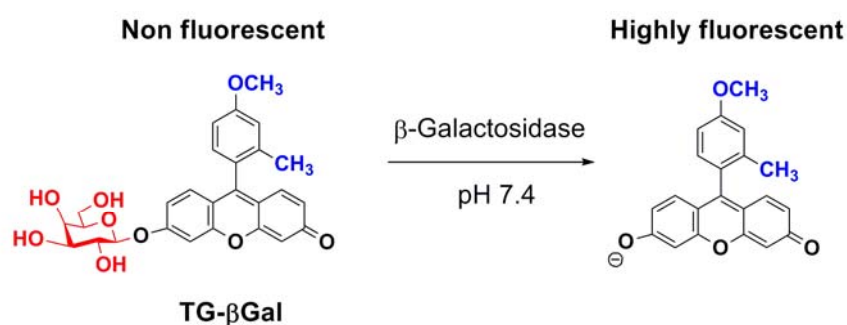
Figure 6. Reaction scheme of TG-βGal before and after the reaction with β-galactosidase

3-2. imaging of β-lactamase activity

β-Lactamases are a family of bacterial enzymes that cleave penicillins and cephalosporins very efficiently. Because of thier clinical importance in mediating antibiotic resistance, much is known about thier three dimensional structure, mechnism, optimal substrates, and inhibitors. Although colorimetric substrates for β-lactamase were known,[21] fluorogenic substrates that could detect the enzyme within living cells were reported. Zlokarnik and co-workers have designed a

10

fluorescent β-lactamase substrates called **CCF2** incorporated with 7-hydroxycoumarin, cephalosporin β-lactam ring, and fluorescein moiety, and also synthesized its ester derivative (named **CCF2/AM**[12]). Figure 7 shows a schematic representation of substrate loading into cells in culture.

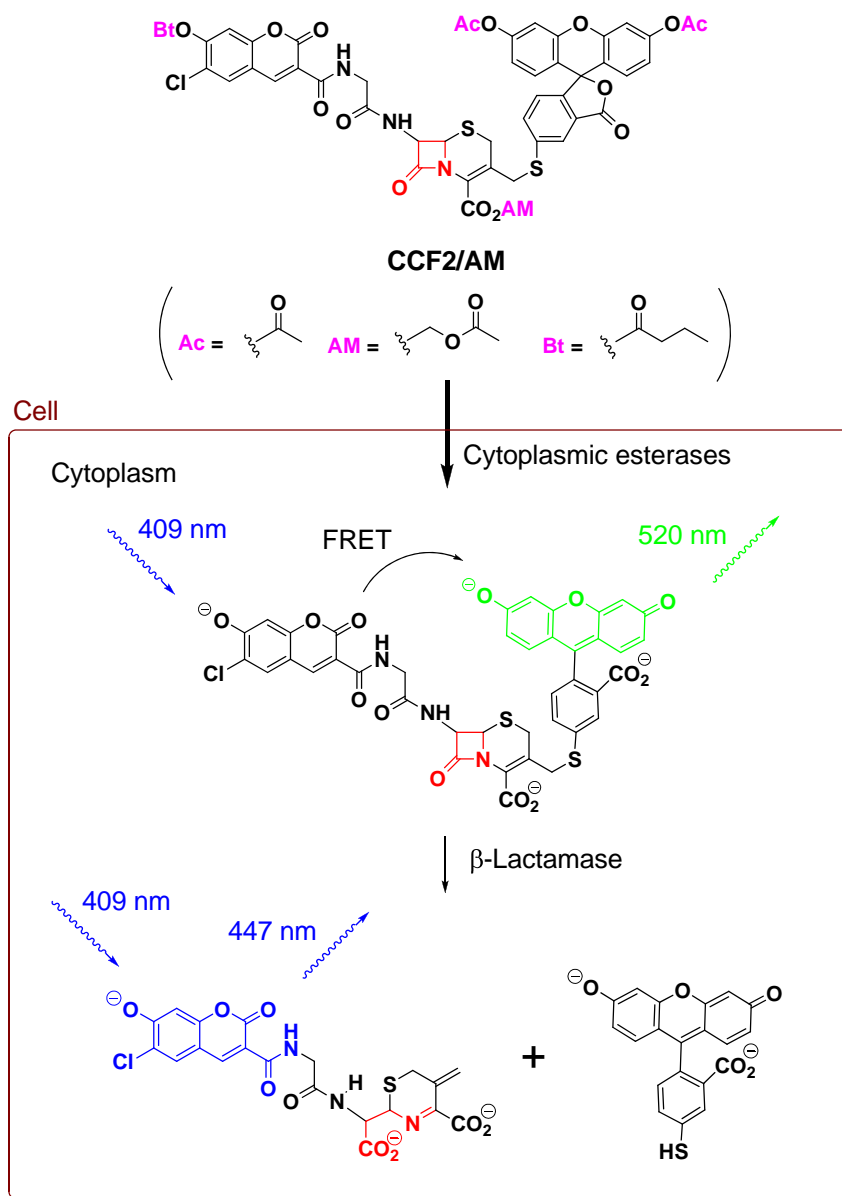**Figure 7.** Schematic representation of **CCF2/AM** loading into cells in culture.

CCF2/AM diffuses across the cell's plasma membrane where cytoplasmic activities catalyze the hydrolysis of its ester functionalities (Ac, acetyl; Bt, butyryl; AM, acetoxymethyl), releasing the polyanionic β-lactamase substrate **CCF2**, which is trapped due to its charges. In the intact substrates, excitation of the coumarin donor at 409 nm leads to FRET to the fluorescein acceptor and reemission of green light. β-Lactamase-catalyzed hydrolysis of the substrate separates donor and acceptor. The donor then emits blue fluorescence whereas the acceptor is quenched. Indeed in the application of **CCF2/AM** to Jurket cells transfected with or without β-lactamase gene, wild type Jurket cells lacking β-lactamase remained green-fluorescent, whereas Jurket cells transfected β-lactamase caused to turn blue-green by loading **CCF2**. These results demonstrate the use of β-lactamase and a membrane-permeant, fluorogenic substrates ester (**CCF2/AM**) to measure gene expression in single live mammlian cells with high sensitivity and real-time response.

4. New fluorescent imaging systems

BRET imaging system

The unique optical properties of quantum dots, such as high quantum yields, large molar extinction coefficients, size-dependent tunable emission and high photostability,[22] make them appealing as fluorescent probes for biological imaging.[23] However, the utility of existing quantum dots for *in vivo* imaging is limited because they require excitation from external illumination sources to fluoresce, which results in a strong autofluorescence background and paucity of excitation light at non superficial locations. In view of these issues, Rao and co-workers have created a new class of quantum dot conjugates that luminesce by bioluminescence resonance energy transfer (BRET) in the absence of external excitation.[24] The conjugates are prepared by coupling carboxylate- presenting quantum dots to a mutant of the bioluminescent protein *Renilla reniformis* luciferase (named **QD655-Luc8**). Figure 8 shows a schematic of a quantum dot that is covalently coupled to a BRET donor, Luc8. The bioluminescence energy of Luc8-catalyzed oxidation of

coelenterazine is transferred to the quantum dots, resulting in quantum dot emission. Indeed, **QD655-Luc8** have been succeed to emit long-wavelength (from red to near-infrared) bioluminescent light in cells and in animals, even in deep tissues, and suitable for multiplexed *in vivo* imaging.
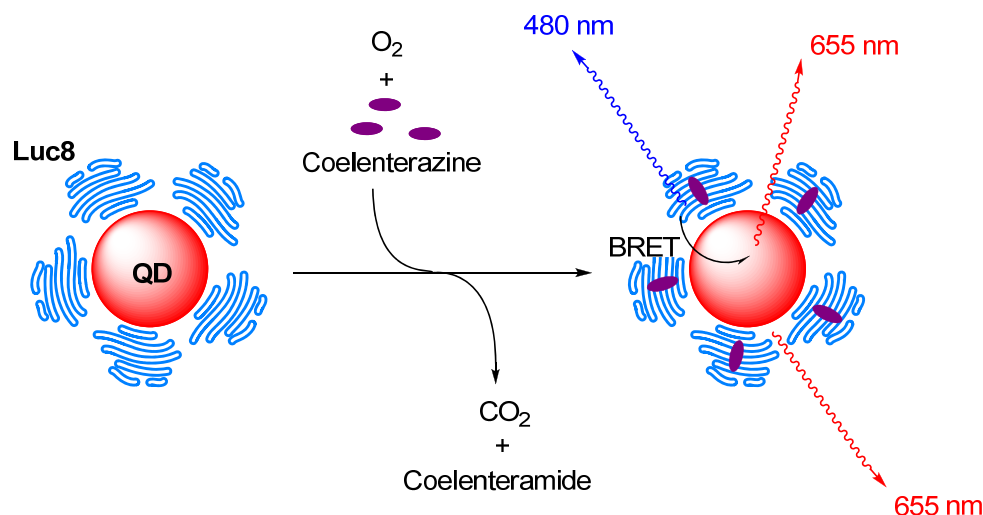

Figure 8. Schematic of QD that is covalently coupled to BRET donor, Luc8. The bioluminescence energy of Luc8-catalyzed oxidation of coelenterazine is transferred to the QD, resulting in QD emission.

As described above, many kinds of imaging probes have been developed for visualizing biologically active species and vital functions in living cells or tissues, and actually used for biological, medical and pathological applications. However, many biological molecules and its functions are still unknown. As an example, dissolved oxygen and its distribution in biological functions are quoted. A partial pressure of oxygen has been known to be maintained at proper level by homeostatic systems,[25] and an imbalance of oxygen homeostasis has been reported to cause various diseases. Especially, a hypoxia profoundly relates to cerebrovascular disease,[26] cardiovascular disease,[27] and solid tumors.[28]   In view of these, there has been increasing demands for convenient imaging systems, or high-sensitive prodrugs targeting hypoxia region in living body. In this thesis, new classes of molecular imaging probes and radiation-activated prodrugs have been designed, synthesized, and evaluated for targeting tumor hypoxic microenvironments.

Survey of this thesis

Chapter 1 shows a development of a hypoxia imaging probe conjugated with indolequinone derivative and fluorescent coumarin chromophore (IQ-Cou). Indolequinone derivatives have been identified as quenchers for the adjacent fluorescent molecules and removable substitutes *via* one-electron reduction under hypoxic conditions. Therefore, IQ-Cou showed a weak fluorescence due to a photoinduced electron transfer (PeT) quenching of indolequinone unit to coumarin chromophore. Upon a treatment of a HT1080-cell lysate under hypoxic conditions, however, IQ-Cou underwent a one-electron reduction triggered by intrinsic NADPH:cytochrome P450 reductase to release a fluorescent coumarin chromophore, whereupon an intense fluorescence emission with a maximum intensity at 420 nm was observed.

Chapter 2 demonstrates the expansion of the indoelequinoen characteristics to fluorescent-labeled avidin chromophore systems. An indolequinone derivative possessing biotin and C-5 linker units was newly synthesized (named **C5-IQ-Btn**) and incorporated into fluorescein isothiocyanate (FITC) labeled avidin (AF) systems. Upon the enzymatic treatment by NADPH:cytochrome P450 reductase, **C5-IQ-Btn** and avidin-FITC complex (**AF-IQ-Btn**) caused the enhanced emission of FITC in a hypoxia-selective manner.

Chapter 3 illustrates the application of indolequinone characteristics to magnetic nanoparticles (MNP) incorporating an FITC-labeled avidin system. An avidin-FITC chromophore (AF) was tethered with the efficient quencher of MNP by using a hypoxia-responsible linker of indolequinone-biotin derivative (**C5-IQ-Btn**). The system of the combination of AF, MNP and **C5-IQ-Btn** units was named as **AF-IQ-Btn@MNP**. Upon the enzymatic treatment by NADPH:cytochrome P450 reductase, **AF-IQ-Btn@MNP** caused the enhanced emission of FITC in a hypoxia-selective manner.

Chapter 4 reports the development of a novel radiation-activated prodrug, incorporating a 2-oxopropyl group to an anti-tumour agent of cytarabine (named **oxo-ara-C**) that targeted hypoxic tumour tissues with selective cytotoxicity. The prodrug **oxo-ara-C** had dramatically reduced

cytotoxicity against human lung adenocarcinoma A549 cells relative to **ara-C** because of the effect of 2-oxopropyl substituent. In contrast, X-ray treatment of hypoxic A549 cells containing **oxo-ara-C** enhanced the cytotoxic effect, indicating that toxic **ara-C** was preferentially released in hypoxic cells *via* radiolytic one-electron reduction by hydrated electrons (e_{aq}^-).

Chapter 5 characterizes tyrosine derivative possessing a 2-oxoalkyl group (Tyr(Oxo)) to evaluate its radiolytic reactivity caged amino acids and proteins. Upon hypoxic X-irradiation, Tyr(Oxo) released a 2-oxopropyl group to form the corresponding uncaged tyrosine. In addition, radiolysis of dipeptides containg Tyr(Oxo) revealed that the efficiency of radiolytic removal of 2-oxopropyl group increased significantly by the presence of neighboring aromatic amino acids.

References

(1)   (a) Grynkiewicz, G.; Poenie, M.; Tsien, R. Y. *J. Biol. Chem.* **1985**, *260*, 3440–3450. (b) Williams, D. A.; Fogarty, K. E.; Tsien, R. Y.; Fay, F. S. *Nature* **1985**, *318*, 558–561.

(2)   (a) Miyawaki, A.; Llopis, J.; Heim, R.; McCaffery, J. M.; Ikura, M.; Tsien, R. Y. *Nature* **1997**, *388*, 882–887. (b) Truong, K.; Sawano, A.; Mizuno, H.; Hama, H.; Tong, K. L.; Miyawaki, A.; Ikura, M. *Nat. Struct. Biol.* **2001**, *8*, 1069–1073. (c) Nagai, T.; Yamada, S.; Tominaga, T.; Miyawaki, A. *Proc. Natl. Acad. Sci. USA.* **2004**, *101*, 10554–10559. (d) Nagai, T.; Sawano, A.; Park, E. S.; Miyawaki, A. *Proc. Natl. Acad. Sci. USA.* **2001**, *98*, 3197–3202.

(3)   (a) Bozym, R. A.; Thompson, R. B.; Fierke, C. A. *ACS. Chem. Biol.* **2006**, *1*, 103–111. (b) Ojida, A.; Mito-oka, Y.; Hamachi, I. *J. Am. Chem. Soc.* **2002**, *124*, 6256–6258. (c) Ojida, A.; Inoue, M.; Mito-oka, Y.; Hamachi, I. *J. Am. Chem. Soc.* **2003**, *125*, 10184–10185. (d) Kinoshita, E.; Takahashi, M.; Shiro, M.; Koike, T. *Dalton Trans.* **2004**, *8*, 1189–1193.

(4)   (a) Komatsu, K.; Kikuchi, K.; Kojima, H.; Urano, Y.; Nagano, T. *J. Am. Chem. Soc.* **2005**, *127*, 10197–10204. (b) Kawabata, E.; Kikuchi, K.; Urano, Y.; Kojima, H.; Odani, A.; Nagano, T. *J. Am. Chem. Soc.* **2005**, *127*, 818–819.

(5)   (a) Komatsu, H.; Iwasawa, N.; Citterio, D.; Suzuki, Y.; Kubota, T.; Kitamura, Y.; Oka, K.; Suzuki, K. *J. Am. Chem. Soc.* **2004**, *126*, 16353–16360. (b) Kenmoku, S.; Urano, Y.; Kanda, K.; Kojima, H.; Kikuchi, K.; Nagano, T. *Tetrahedron* **2004**, *60*, 11067–11073. (c) Yang, L.; McRae, R.; Henary, M. M.; Patel, R.; Lai, B.; Vogt, S.; Fahrni, C. J. *Proc. Natl. Acad. Sci. USA.* **2005**, *102*, 11179–11184. (d) Zhang, Z.; Wu, Di.; Guo, X.; Qian, X.; Lu, Z.; Xu, Q.; Yang, Y.; Duan, L.; He, Y.; Feng, Z. *Chem. Res. Toxicol.* **2005**, *18*, 1814–1820.

(6)   Komatsu, H.; Miki, T.; Citterio, D.; Kubota, T.; Shindo, Y.; Kitamura, Y.; Oka, K.; Suzuki, K. *J. Am. Chem. Soc.* **2005**, *127*, 10798–10799.

(7)   Nakata, E.; Koshi, Y.; Koga, E.; Hamachi, I. *J. Am. Chem. Soc.* **2005**, *127*, 13253–13261.

(8)   (a) Adams, S. R.; Harootunian, A. T.; Buechler, Y. J.; Taylor, S. S.; Tsien, R. Y. *Nature* **1991**, *349*, 694–697. (b) Dunn, T. A.; Wang, C.; Colicos, M. A.; Zaccolo, M.; DiPilato, L. M.; Zhang, J.; Tsien, R. Y.; Feller, M. B. *J. Neurosci.* **2006**, *26*, 12807–12815.

(9)   (a) Kojima, H.; Urano, Y.; Kikuchi, K.; Higuchi, T.; Hirata, Y.; Nagano, T. *Angew. Chem. Int. Ed*. **1999**, *38*, 3209–3212. (b) Nakatsubo, N.; Kojima, H.; Kikuchi, K.; Nagoshi, H.; Hirata, Y.; Maeda, D.; Irimura, T.; Nagano, T. *FEBS. Lett*. **1998**, *427*, 263–266.

(10)   (a) Zhang, J.; Ma, Y.; Taylor, S. S.; Tsien, R. Y. *Proc. Natl. Acad. Sci. USA*. **2001**, *98*, 14997–15002. (b) Lin, C.-W.; Ting, A. Y. *Angew. Chem. Int. Ed*. **2004**, *43*, 2940–2943. (c) Kunkel, M. T.; Toker, A.; Tsien, R. Y.; Newton, A. C. *J. Biol. Chem*. **2007**, *282*, 6733–6742. (d) Takakusa, H.; Kikuchi, K.; Urano, Y.; Nagano, T. *Chem. Eur. J*. **2003**, *9*, 1479–1485. (e) Takakusa, H.; Kikuchi, K.; Urano, Y.; Yamaguchi, K.; Nagano, T. *J. Am. Chem. Soc*. **2002**, *124*, 1653–1657. (f) Takemoto, K.; Nagai, T.; Miyawaki, A.; Miura, M. *J. Cell. Biol*. **2003**, *160*, 235–243.

(11)   Urano, Y.; Kamiya, M.; Kanda, K.; Ueno, T.; Nagano, T. *J. Am. Chem. Soc*. **2005**, *127*, 4888–4894.

(12)   Zlokarnik, G.; Negulescu, P. A.; Knapp, T. E.; Mere, L.; Burres, N.; Feng, L.; Whitney, M.; Tsien, R. Y. *Science* **1998**, *279*, 84–88.

(13)   (a) Heim, R.; Pracher, D. C.; Tsien, R. Y. *Proc. Natl. Acad. Sci. USA*. **1994**, *91*, 12501–12504. (b) Heim, R.; Tsien, R. Y. *Curr. Biol*. **1996**, *6*, 178–182.

(14)   (a) Crivici, A.; Ikura, M. *Annu. Rev. Biophys. Biomol. Struct*. **1995**, *24*, 85–116. (b) Babu, Y.; Bugg, C. E.; Cook, W. J. *J. Mol. Biol*. **1988**, *204*, 191–204. (c) Falke, J. J.; Drake, S. K.; Hazard, A. L.; Peersen, O. B. *Rev. Biophys*. **1994**, *27*, 219–290.

(15)   Ikura, M.; Clore, G. M.; Gronenborn, A. M.; Zhu, G.; Klee, C. B.; Bax, A. *Science* **1992**, *256*, 632–638.

(16)   (a) Heim, R.; Cubitt, A. B.; Tsien, R. Y. *Nature* **1995**, *373*, 663–664. (b) Cormack, B. P.; Valdivia, R. H.; Falkow, S. *Gene* **1996**, *173*, 33–38. (c) Ormo, M.; Cubitt, A. B.; Kallio, K.; Gross, L. A.; Tsien, R. Y.; Remington, S. J. *Science* **1996**, *273*, 1392–1395.

(17)   (a) Vallee, B. L.; Falchuk, K. H. *Physiol. Rev*. **1993**, *73*, 79–118. (b) Berg, J. M.; Shi, Y. *Science* **1996**, *271*, 1081–1085. (c) O'Halloran, T. V. *Science* **1993**, *261*, 715–725. (d) Fraker, P. J.; Telford, W. G. *Proc. Soc. Exp. Biol. Med*. **1997**, *215*, 229–236. (e) Costello, L. C.;

Franklin, R. B. *The Prostate* **1998**, *35*, 285–296.

(18) (a) Frederickson, C. J.; Hemandez, M. D.; McGinty, J. F. *Brain Res*. **1998**, *480*, 317–321. (b) Frederickson, C. J. *Int. Rev. Neurobiol.* **1989**, *31*, 145–238. (c) Frederickson, C. J.; Bush, A. I. *BioMetals* **2001**, *14*, 353–366. (d) Choi, D. W.; Koh, J. Y. *Annu. Rev. Neurosci.* **1998**, *21*, 347–375.

(19) Vogt, K.; Mellor, J.; Tong, G.; Nicoll, R. *Neuron* **2000**, *26*, 187–196.

(20) Taylor, S. S.; Buechler, J. A.; Yonemoto, W. *A. Rev. Biochem.* **1990**, *59*, 971–1005.

(21) (a) O'Callaghan, C. H.; Morris, A.; Kirby, S. M.; Shingler, A. H. *Antimicrob. Agent. Chemother.* **1972**, *1*, 283–288. (b) Moore, J. T.; Davis, S. T.; Dev, I. K. *Anal. Biochem.* **1997**, *247*, 203–209.

(22) (a) Dabbousi, B. O.; RodriguezViejo, J.; Mikulec, F. V.; Heine, J. R.; Mattoussi, H.; Ober, R.; Jensen, K. F.; Bawendi, M. G. *J. Phys. Chem. B* **1997**, *101*, 9463–9475. (b) Leatherdale, C. A.; Woo, W. K.; Mikulec, F. V.; Bawendi, M. G. *J. Phys. Chem. B* **2002**, *106*, 7619–7622. (c) Bruchez, M.; Moronne, M.; Gin, P.; Weiss, S.; Alivisatos, A. P. *Science* **1998**, *281*, 2013–2016. (d) Chan, W. C. W.; Nie, S. *Science* **1998**, *281*, 2016–2018. (e) Niemeyer, C. M. *Angew. Chem. Int. Ed.* **2001**, *40*, 4128–4158.

(23) (a) Medintz, I. L.; Uyeda, H. T.; Goldman, E. R.; Mattoussi, H. *Nat. Mater.* **2005**, *4*, 435–446. (b) Pinaud, F.; King, D.; Moore, H.-P.; Weiss, S. *J. Am. Chem. Soc.* **2004**, *126*, 6115–6123. (c) Mamedova, N. N.; Kotov, N. A.; Rogach, A. L.; Studer, J. *Nano. Lett.* **2001**, *1*, 281–286. (d) Wu, X. Y.; Liu, H. J.; Liu, J. Q.; Haley, K. N.; Treadway, J. A.; Larson, J. P.; Ge, N. F.; Peale, F.; Bruchez, M. P. *Nat. Biotechnol*. **2003**, *21*, 41–46. (e) Dubertret, B.; Skourides, P.; Norris, D. J.; Noireaux, V.; Brivanlou, A. H.; Libchaber, A. *Science* **2002**, *298*, 1759–1762.

(24) So, M.; Xu, C.; Loening, A. M.; Rao, J. *Nat. biotechnol*. **2006**, *24*, 339–343.

(25) (a) Semenza, G. L. *Annu. Rev. Cell. Dev. Biol.* **1999**, *15*, 551–578. (b) Ke, Q.; Costa, M. *Mol. Pharmacol.* **2006**, *70*, 5, 1469–1480. (c) Li, X. Y.; Takasaki, C.; Satoh, Y.; Kimura, S.; Yasumoto, K.; Sogawa, K. *J. Biochem.* **2008**, *144*, 555–561. (d) Downie, B. R.; Sanchez, A.; Knotgen, H.; Contreras-Jurado, C.; Gymnopoulos, M.; Weber, C.; Stuhmer, W.; Pardo, L. A. *J.*

Biol. Chem. **2008**, *283*, 36234–36240. (e) Masson, N.; Ratcliffe, P. J. *J. Cell Sci.* **2003**, *116*, 3041–3049.

(26)　(a) Manabe, T.; Katayama, T.; Sato, N.; Gomi, F.; Hitomi, J.; Yanagita, T.; Kudo, T.; Honda, A.; Mori, Y.; Matsuzaki, S.; Imaizumi, K.; Meyeda, A.; Tohyama, M. *Cell Death Differ.* **2003**, *10*, 698–708. (b) Sato, N.; Hori, O.; Yamaguchi, A.; Lambert, J.-C.; Chartier-Harlin, M.-C.; Robinson, P. A.; Delacourte, A.; Schmidt, A. M.; Furuyama, T.; Imaizumi, K.; Tohyama, M.; Takagi, T. *J. Neurochem.* **1999**, *72*, 2498–2505. (c) Higashide, S.; Morikawa, K.; Okumura, M.; Kondo, S.; Oagata, M.; Murakami, T.; Yamashita, A.; Kanemoto, S.; Manabe, T.; Imaizumi, K. *J. Neurochem.* **2004**, *91*, 1191–1198. (d) Paschen, W.; Mengesdorf, T. *Phrmacol. Therapeut.* **2005**, *108*, 362–375.

(27)　(a) Haunstetter, A.; Izumo, S. *Circ. Res.* **1998**, *82*, 1111–1129. (b) Chen, C.-J.; Yu, W.; Fu, Y.-C.; Wang, X.; Li, J.-L.; Wang, W. *Biochem. Biophys. Res. Commun.* **2009**, *378*, 389–393. (c) Bonavita, F.; Stefanelli, C.; Giordano, E.; Columbaro, M.; Facchini, A.; Bonafe, F.; Caldarera, C. M.; Guarnieri, C. *FEBS. lett.* **2003**, *536*, 85–91.

(28)　Vaupel, P.; Kallinowski, F.; Okunieff, P. *Cancer Res.* **1989**, *49*, 6449–6465.

Chapter 1

Emission under Hypoxia:
One-Electron Reduction and Fluorescence Characteristics of
# an Indolequinone-Coumarin Conjugate

Abstract: A characteristic feature of the reactivity of indolequinone derivatives, substituents of which can be removed by one-electron reduction under hypoxic conditions, was applied to the development of a new class of fluorescent probes for disease-relevant hypoxia. A reducing indolequinone parent molecule conjugated with fluorescent coumarin chromophores could suppress efficiently the fluorescence emission of the coumarin moieties by an intramolecular electron-transfer quenching mechanism and a conventional internal-filter effect. Under hypoxic conditions, however, the conjugate, denoted IQ-Cou, underwent a one-electron reduction triggered by X irradiation or the action of a reduction enzyme to release a fluorescent coumarin chromophore, whereupon an intense fluorescence emission with a maximum intensity at 420 nm was observed. The one-electron reduction of IQ-Cou was suppressed by molecular oxygen under aerobic conditions. IQ-Cou also showed intense fluorescence in a hypoxia-selective manner upon incubation with a cell lysate of the human fibrosarcoma cell line HT-1080. The IQ-Cou conjugate has several unique properties that are favorable for a fluorescent probe of hypoxia-specific imaging.

Introduction

Most cellular functions rely on the continuous and adequate supply of oxygen molecules from blood vessels. A stable oxygen supply is preserved in normal tissues by so-called oxygen homeostasis. An inadequate oxygen supply to cells induces hypoxia, which is one of the well-known pathophysiological characteristics of cardiac ischemia,[1] inflammatory diseases,[2] and solid tumors.[3] Tumor hypoxia is of particular importance, as it has been associated closely with the malignant phenotype of cancer cells, resistance to cancer therapies, and the low mortality rate of cancer patients.[3] Therefore, there has been increasing demand for hypoxia-specific molecular probes as useful indicators for the pathophysiological analysis of diseases.

We have developed prodrugs of the well-documented antitumor agents 5-fluorouracil (5-FU) and 5-fluorodeoxyuridine (5-FdUrd), which release 5-FU and 5-FdUrd, respectively, upon hypoxic X irradiation.[4] One 5-FdUrd prodrug with an indolequinone structure showed strong cytotoxicity against hypoxic tumor cells.[4a] Indolequinone derivatives have been identified by other research groups as a new class of hypoxia-specific prodrugs that can be activated to eliminate cytotoxic substituent components (active drugs) selectively by bioreduction or radiolytic reduction under hypoxic conditions.[5] These findings prompted us to investigate the development of hypoxia-imaging molecular probes containing a reducing indolequinone skeleton. Two coumarin chromophores were thus conjugated with an indolequinone unit through a 2,6-bis(hydroxymethyl)-*p*-cresol linker[6] to produce IQ-Cou, the indolequinone unit of which undergoes one-electron reduction to liberate three functional components through the spontaneous cyclization of a free-amine intermediate and the rearrangement of the resulting phenol derivative to the corresponding 1,4-quinone methide (Scheme 1). IQ-Cou itself showed weak fluorescence, because the fluorescent excited singlet state of the coumarin unit is quenched efficiently by the indolequinone unit located intramolecularly in close proximity. Upon the one-electron reduction of the indolequinone unit, the coumarin chromophore was eliminated and no longer affected by the fluorescence quenching action of the indolequinone unit; thus, an intense fluorescence emission was

observed. With these reaction characteristics, IQ-Cou might be applicable as a fluorescent probe for the molecular imaging of disease-relevant hypoxia.
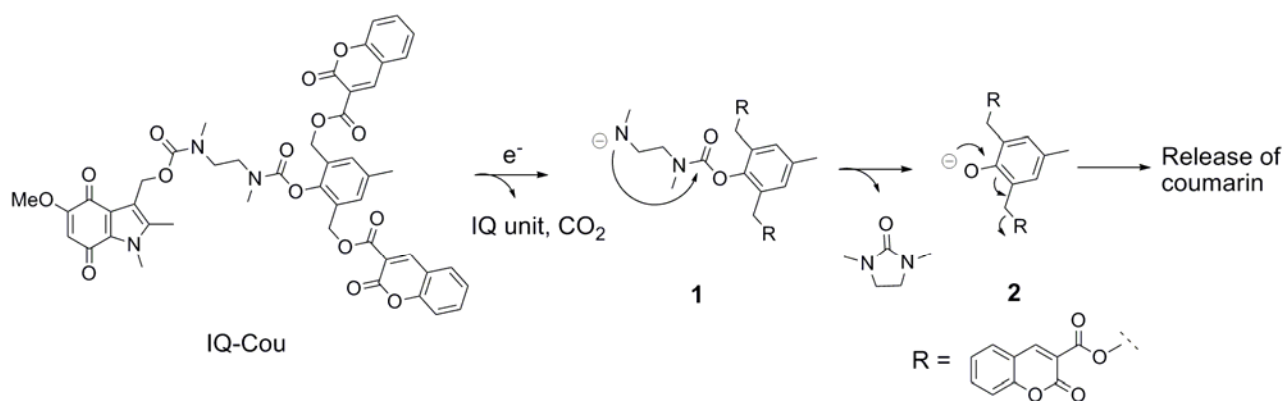
Scheme 1. Mechanism for the activation of IQ-Cou to release a fluorescent coumarin chromophore under reductive conditions.

Results and Discussion

The synthetic route to IQ-Cou is outlined in Scheme 2. The diol **3** was prepared by a previously described method[6] and coupled with the acid chloride **8** to form **4**. The diester **4** was converted into the free amine under acidic conditions and then coupled with the indolequinone derivative **7** (prepared from the alcohol **6**[7]) to give IQ-Cou.
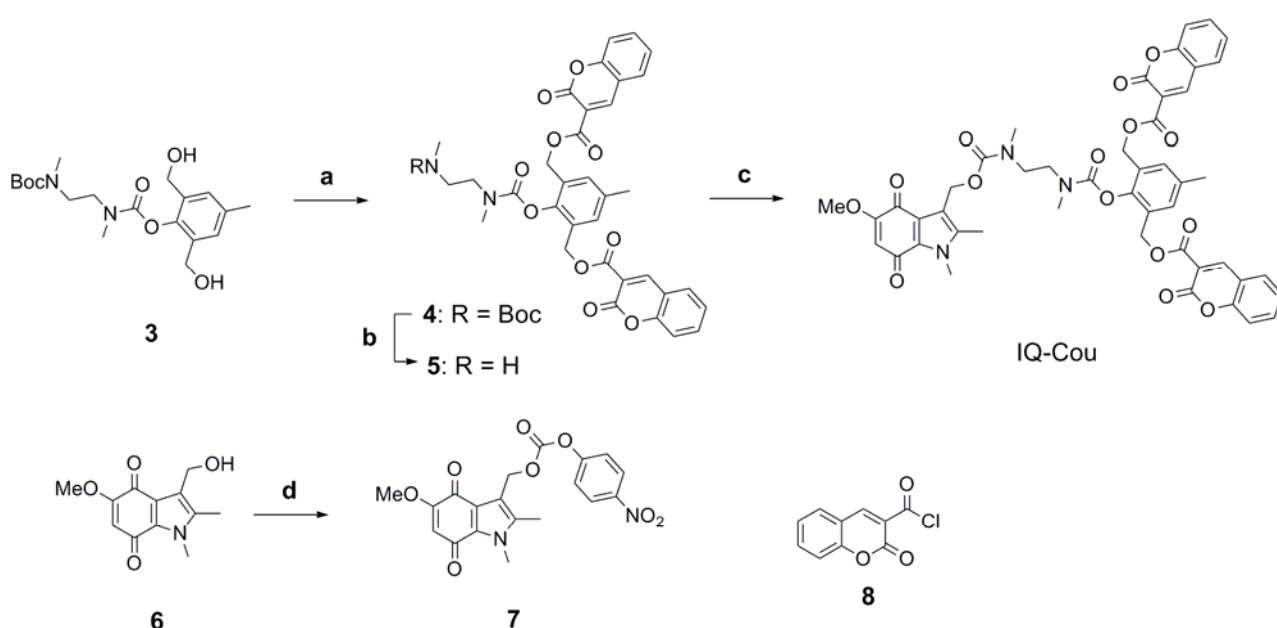
Scheme 2. Reagents and conditions: a) **8**, TEA, CH$_2$Cl$_2$, room temperature, 62%; b) HCl, MeOH, room temperature; c) **7**, Et$_3$N, CH$_2$Cl$_2$, room temperature, 39% (two steps); d) 4-nitrophenyl chloroformate, Et$_3$N, CH$_2$Cl$_2$, 0 °C, 37%. Boc = *tert*-butoxycarbonyl.

We first compared the fluorescence spectrum of IQ-Cou with that of the reference compound coumarin-3-carboxylic acid (Figure 1A). Whereas coumarin-3-carboxylic acid showed an intense fluorescence emission at about 420 nm upon excitation at a wavelength of 300 nm, the apparent fluorescence intensity of IQ-Cou was extremely weak: The formal fluorescence quantum yields (Φ_F) of coumarin-3-carboxylic acid and IQ-Cou were 0.042 and 0.002, respectively. These

results indicate that the fluorescence of the coumarin chromophore in IQ-Cou is quenched intramolecularly by the neighboring indolequinone unit and predict that fluorescence emission will be restored upon the one-electron reduction of IQ-Cou to release a coumarin-3-carboxylic acid fragment.

The suppressed fluorescence emission of IQ-Cou is attributable to two modes of action of the indolequinone unit. First, a conventional internal filter effect due to the presence of the indolequinone unit could lead to a decrease in the apparent fluorescence quantum yield of the counterpart coumarin chromophore by about a third in view of the similarity of the molar extinction coefficients at 300 nm of coumarin-3-carboxylic acid and the indolequinone **6** (ε = 6206 and 5863 M^{-1} cm^{-1}, respectively).[8] Second, a photoinduced electron transfer (PeT) process[9] should be operative as a key mechanism for modulating the fluorescence properties of IQ-Cou. The PeT that leads to fluorescence quenching can occur between the excited states of an electron-withdrawing (electron-donating) fluorophore and an electron-donating (electron-withdrawing) quencher. The feasibility of the process depends on the relative ordering of the energy levels of the highest occupied molecular orbitals (HOMO) and the lowest unoccupied molecular orbitals (LUMO) of the fluorophore and the quencher.[10] The MO energy levels of 3-methoxycarbonylcoumarin and the indolequinone **6** were estimated by ab initio calculations at the B3LYP/6-31G(d) level, which revealed that the LUMO energy level of **6** (−2.94 eV) is lower than that of coumarin (−2.25 eV), whereas the HOMO energy level of **6** (−6.15 eV) is higher than that of coumarin (−6.77 eV). These calculation results suggest strongly that an intramolecular electron transfer from coumarin in the excited state to the indolequinone unit in the ground state is feasible thermodynamically in IQ-Cou.

We also carried out laser flash photolysis studies to gain further insight into the suppressed fluorescence emission of IQ-Cou. Figure 1B shows the transient absorption spectra observed in the laser flash photolysis at 355 nm of IQ-Cou in acetonitrile. The transient absorption appeared 1 μs after the laser flash. An absorption in the region 360–390 nm was assigned to the semiquinone radical anion.[4a, 5d] We also observed a transient absorption at 410–440 nm that may be assigned to the coumarin radical cation.[11] This absorption decayed in a similar way to that of the

semiquinone radical anion. These results indicate that the photolysis of IQ-Cou induces electron transfer from the excited coumarin unit to the indolequinone unit. Thus, we concluded that indolequinone could suppress efficiently the fluorescence emission of coumarin by an intramolecular electron-transfer mechanism.
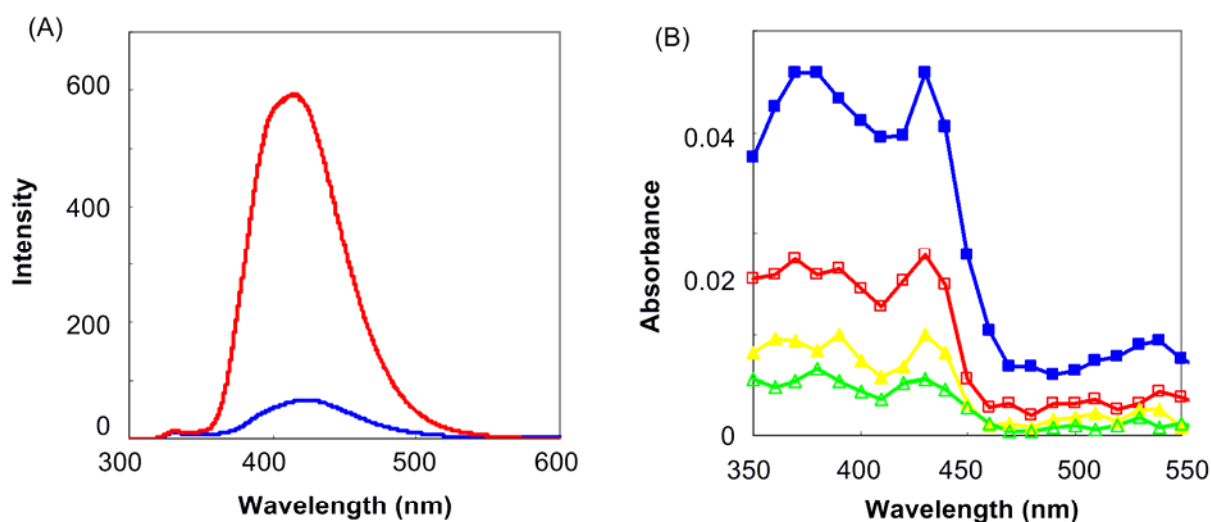

Figure 1. (A) Fluorescence spectra of IQ-Cou (10 μM; blue line) and coumarin-3-carboxylic acid (10 μM; red line) in acetonitrile. The fluorescence spectra were measured with excitation at 300 nm. (B) Transient absorption spectra observed upon the excitation at 355 nm of IQ-Cou (30 μM) in acetonitrile; 1 (blue line), 10 (red line), 20 (yellow line) and 30 μs (green line) after flash photolysis.

We measured the changes in the fluorescence spectrum of IQ-Cou upon X irradiation. An argon-purged aqueous solution of IQ-Cou in the presence of excess 2-methyl-2-propanol was used for these experiments. Under these conditions, IQ-Cou undergoes one-electron reduction, whereby the indolequinone unit, with a lower LUMO energy level, may capture reducing hydrated electrons (e_{aq}^-) generated as a primary intermediate of water radiolysis.[12, 13] As shown representatively in Figure 2, the intensity of the fluorescence at about 420 nm assigned to coumarin-3-carboxylic acid increased with increasing irradiation dose upon hypoxic X irradiation of IQ-Cou. The fluorescence

after 720 Gy of X irradiation was three times as intense as that of IQ-Cou in the absence of irradiation (Figure 2A). These results indicate clearly that IQ-Cou is activated to release coumarin-3-carboxylic acid from the indolequinone quencher by radiolytic one-electron reduction by e_{aq}^- with the restoration of fluorescence.
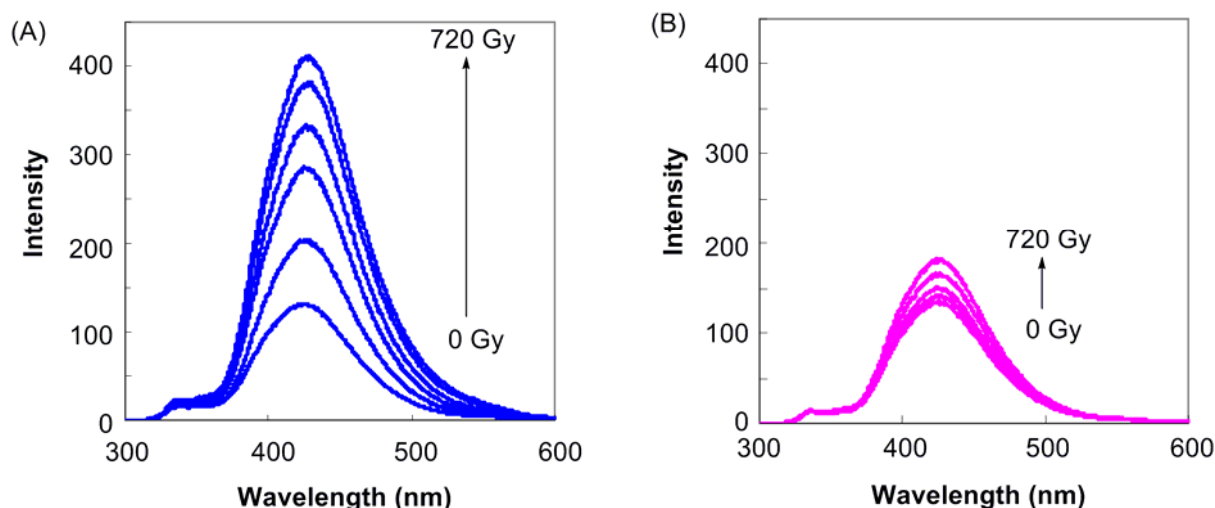

Figure 2. Changes in the fluorescence spectrum of IQ-Cou upon X irradiation. IQ-Cou (100 μM) was irradiated, and then the fluorescence spectra were measured with excitation at 300 nm. (A) Fluorescence spectra observed after hypoxic irradiation of IQ-Cou (from bottom to top: 0, 72, 144, 288, 528, 720 Gy). (B) Fluorescence spectra observed after aerobic irraidation of IQ-Cou (from bottm to top: 0, 72, 144, 288, 528, 720 Gy).

A smaller enhancement in fluorescence emission occurred upon aerobic irradiation: The sample solution showed only a 1.5-fold increase in fluorescence intensity upon exposure to 720 Gy of X irradiation (Figure 2B). This oxygen effect on the activation of IQ-Cou can be accounted for by the reactivity of molecular oxygen, which captures efficiently reducing e_{aq}^- species to form a superoxide anion radical ($O_2^{\bullet-}$). Furthermore, recent studies on the reductive activation of indolequinone prodrugs suggest that a semiquinone anion radical intermediate generated by the one-electron reduction of the indolequinone unit could reduce molecular oxygen to form the original indolequinone and $O_2^{\bullet-}$, a process that would lead to a decrease in the net yield of the released drug.[4a] Because of the reaction characteristics of molecular oxygen, the described

26

radiolytic activation of IQ-Cou to enhance the fluorescence emission is likely to occur substantially under hypoxic conditions.

We also monitored the course of the radiolytic reduction of IQ-Cou and release of coumarin-3-carboxylic acid with time by a reversed-phase HPLC (Figure 3). Upon the hypoxic X irradiation of an argon-purged, aqueous solution of IQ-Cou in the presence of excess 2-methyl-2-propanol, the concentrations of decomposed IQ-Cou and released coumarin-3-carboxylic acid increased with increasing radiation dose. G values[13] of 218.9 and 15.2 nmol J^{-1} were found for the decomposition of IQ-Cou and the release of coumarin, respectively.[14] Consistent with the smaller change in fluorescence intensity in the aerobic irradiation of IQ-Cou, the decomposition of IQ-Cou was suppressed to a G value of 16.5 nmol J^{-1} and the release of coumarin-3-carboxylic acid was not detected under aerobic conditions. Thus, the concentration change of coumarin-3-carboxylic acid upon irradiation correlates well with the change in fluorescence intensity.
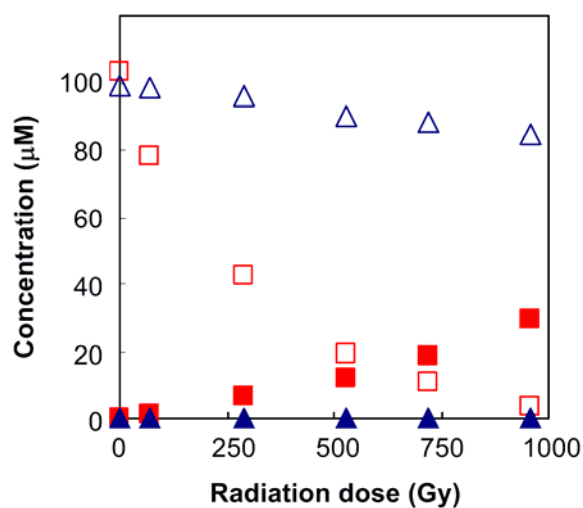

Figure 3. X-Radiolysis (4.0 Gy min^{-1}) of IQ-Cou (100 μM; open symbols) in aqueous solution containing 30% 2-methyl-2-propanol at ambient temperature under hypoxic (square) and aerobic (triangle) conditions, with the release of coumarin-3-carboxylic acid (filled symbols).

To characterize the biological one-electron reduction of IQ-Cou, we subjected IQ-Cou to enzymatic reduction. NADPH:cytochrome P450 reductase is an electron-donating protein that catalyzes the one-electron reduction of quinone derivatives to semiquinone anion radicals. Evidence that NADPH:cytochrome P450 reductase is expressed in many pathological tissues[15] stimulated us to carry out the bioreduction of IQ-Cou. We incubated IQ-Cou with NADPH:cytochrome P450 reductase and the cofactor β-NADPH at three different oxygen concentrations (<0.5, 8.2, and >20 mg L^{-1}). An intense fluorescence emission was observed for the solution of IQ-Cou incubated with <0.5 mg L^{-1} oxygen as a model of hypoxia (Figure 4). At an oxygen concentration of 8.2 mg L^{-1}, as under aerobic conditions, the extent of enhanced fluorescence intensity diminished significantly as a result of the competitive scavenging by molecular oxygen of hydrated electrons, e_{aq}^-, and the semiquinone radical to inhibit partially the reductive fragmentation of IQ-Cou. Thus, IQ-Cou was activated by NADPH:cytochrome P450 reductase in a hypoxia-selective manner, in accord with the results of radiolytic reduction. We also confirmed the hypoxia-selective release of coumarin-3-carboxylic acid from IQ-Cou upon treatment with NADPH:cytochrome P450 reductase, as monitored by HPLC (Figure 5).

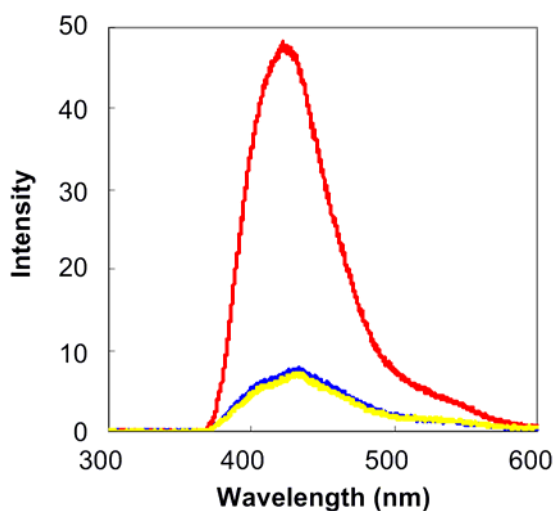**Figure 4.** Fluorescence spectra of IQ-Cou after treatment with reductase. IQ-Cou (500 μM) was incubated with NADPH:cytochrome P450 reductase (10.6 μg mL^{-1}) and β-NADPH (2 mM) at 37 °C for 45 min at three different oxygen concentrations (<0.5 mg L^{-1}: red line; 8.2 mg L^{-1}: blue line; >20 mg L^{-1}: yellow line). The fluorescence spectra were measured with excitation at 300 nm.
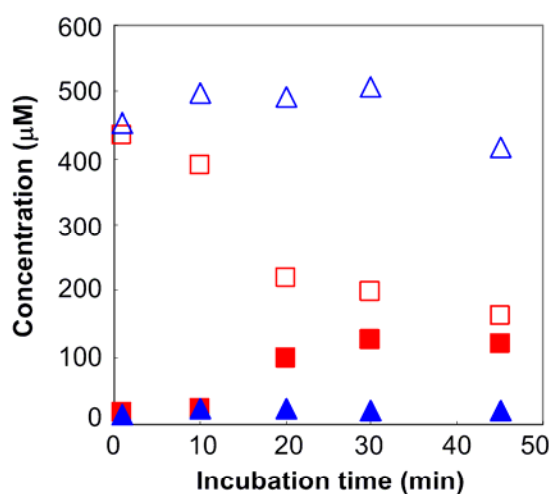
Figure 5. Enzymatic reduction of 500 μM IQ-Cou (open symbols) in 25 mM phosphate buffer (pH 7.4) to release coumarin-3-carboxylic acid (closed symbols) by NADPH:cytochrome P450 reductase (10.6 μg mL^{-1}) and β-NADPH coenzyme (2 mM) at 37 °C under hypoxic (square) and aerobic (triangle) conditions.

To further assess the function of IQ-Cou, we studied the reaction of IQ-Cou upon treatment with a cell lysate. IQ-Cou was incubated at 37 °C for 4 h under hypoxic and aerobic conditions with a lysate of the human fibrosarcoma cell line HT-1080. After incubation, the samples were filtered and analyzed by fluorescence spectrophotometry and HPLC. An intense fluorescence emission at about 420 nm was observed for the sample incubated under hypoxic conditions (Figure 6A). The intensity of the emission was four times as strong as that of the sample incubated under aerobic conditions. The difference in the fluorescence intensity of the two samples correlates well with the corresponding yields of coumarin-3-carboxylic acid from IQ-Cou, as quantified independently by HPLC (Figure 6B). We also confirmed that the incubation of IQ-Cou in a buffer solution resulted in a similar fluorescence intensity to that observed for the sample incubated aerobically. These results indicate strongly that IQ-Cou undergoes one-electron reduction by intracellular reductase to release fluorescent coumarin-3-carboxylic acid under hypoxic conditions.
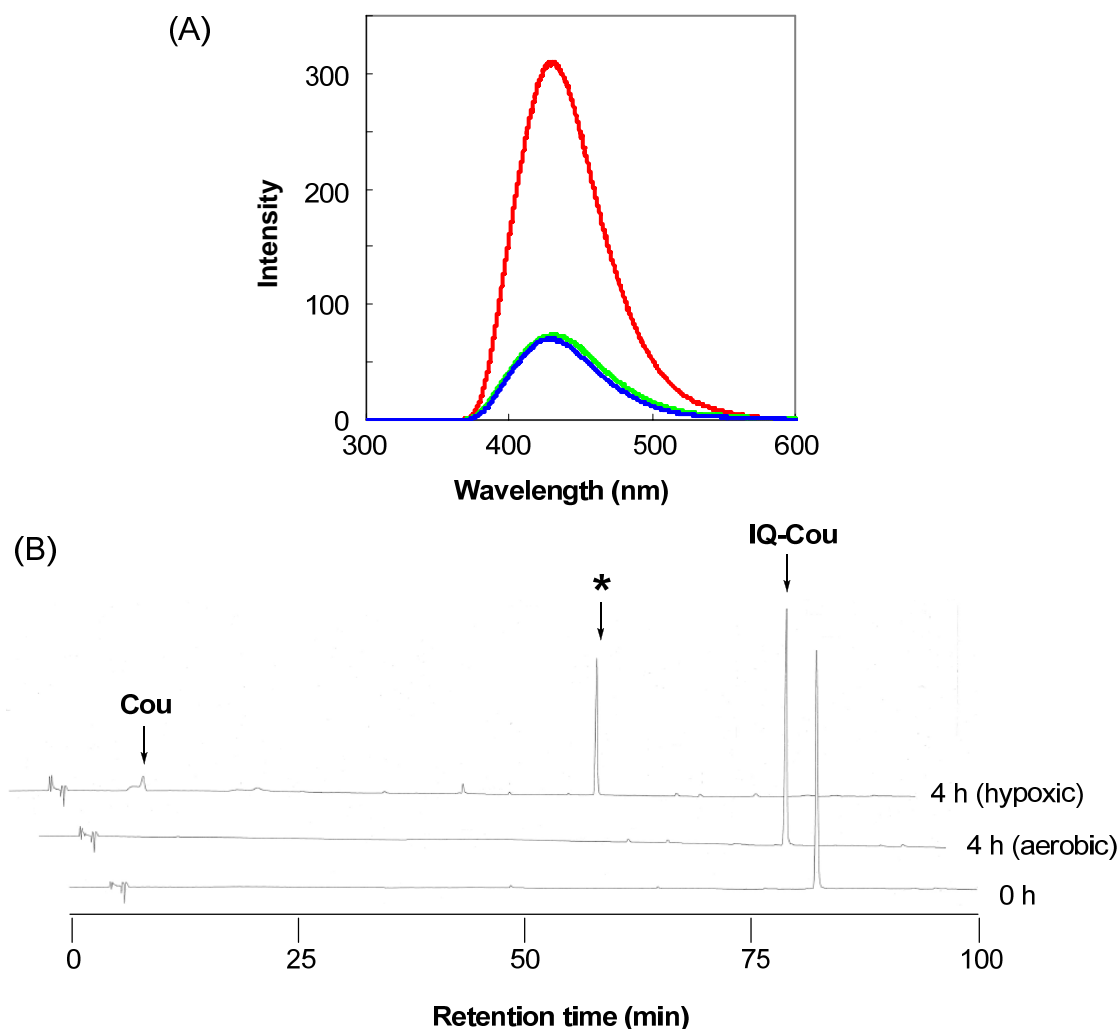
Figure 6. Treatment of IQ-Cou with a cell lysate obtained from the human fibrosarcoma cell line HT-1080. IQ-Cou (500 μM) was incubated with cell lysate for 4 h at 37 °C under hypoxic or aerobic conditions. (A) The fluorescence spectra[16] of IQ-Cou upon treatment with the cell lysate under hypoxic (red line) or aerobic conditions (blue line). IQ-Cou was also incubated alone in a buffer solution as a control (green line). The fluorescence spectra were measured with excitation at 300 nm. (B) HPLC profiles of IQ-Cou (500 μM) upon treatment with cell lysate for 0 and 4 h under hypoxic or aerobic conditions. The HPLC signal indicated "Cou" was identified as coumarin-3-carboxylic acid. The HPLC signal indicated with the symbol "*" possibly corresponds to a reaction intermediate; however, the compound could not be identified because of its low stability and prompt degradation.

In this study, we developed a new type of hypoxia-specific fluorescence imaging probe. IQ-Cou is activated efficiently by intracellular reductase under hypoxic conditions. Although low expression of NADPH:cytochrome P450 reductase was reported for the HT-1080 cell line,[17] an intense fluorescence emission was observed for IQ-Cou even upon treatment with HT-1080 cell lysate under hypoxic conditions. IQ-Cou may therefore be expected to show more intense fluorescence emission when incorporated in certain hypoxic tumor cells with higher reductase expression. In view of the hypoxia-specific fluorescence emission of IQ-Cou, the one-electron reduction of indolequinone derivatives could be a promising strategy for the detection of disease-relevant hypoxia. However, IQ-Cou has some drawbacks: First, an inner-filter effect due to the overlapping of the absorption of indolequinone with that of coumarin leads to the apparent suppression of fluorescence emission. Therefore, fluorescent molecules that absorb in a wavelength region that does not coincide with the absorption of indolequinone should be employed to establish a highly sensitive hypoxia-specific fluorescence imaging probe. Second, the fluorescence spectrum of coumarin-3-carboxylic acid occurs at around 420 nm, that is, at wavelengths that are too short to be applied to the imaging of deep-seated malignant tissues. One of the key strategies for in vivo optical imaging is the employment of near-infrared (NIR) light, because hemoglobin, as a principle absorber of visible light, and water and lipids, as principle absorbers of infrared light, have their lowest absorption in the NIR region, at around 650–900 nm.[18] Moreover, tissue autofluorescence observed in the NIR region has a minimum intensity. From this point of view, it is essential to apply dyes with fluorescence at NIR wavelengths to the present strategy with indolequinone derivatives.

Conclusions

In summary, we have characterized the reactivity by one-electron reduction of IQ-Cou, which was synthesized as a hypoxia specific fluorescence probe. IQ-Cou consists of a hypoxia-sensitive reducing indolequinone parent unit, two fluorescent coumarin chromophores, and a 2,6-bis(hydroxymethyl)-*p*-cresol linker. Both radiolytic and enzymatic one-electron reduction under hypoxic conditions leads to the efficient decomposition of IQ-Cou, with the release of coumarin-3-carboxylic acid accompanied by intense fluorescence. A similar enhancement in fluorescence emission was also observed in a hypoxia-selective manner upon the incubation of IQ-Cou with an HT-1080 cell lysate. Thus, it appears that IQ-Cou can be activated by intracellular reductase. Although IQ-Cou is a promising candidate as a hypoxia-specific fluorescence imaging tool, the absorption and emission of the coumarin fluorophore at relatively short wavelengths is a disadvantage. Furthermore, it is necessary to characterize the reactivity of the probe with potentially reactive species in living cells in detail to establish a molecular system for hypoxia imaging. Our current studies focus on the construction of a hypoxia-specific imaging probe that is sensitive to NIR light and thereby applicable to *in vivo* optical imaging.

Experimental Section

General Methods.

NMR spectra were recorded on 270-MHz JMN-AL-270 (JEOL), 300-MHz JMN-AL-300 (JEOL) or 400-MHz JMN-AL-400 (JEOL) spectrophotometer at ambient temperature. Chemical shift are reported in ppm relative to the residual solvent peak. Multiplicity is designated as singlet (s), doublet (d), triplet (t), doublet-doublet (dd), broad-singlet (brs) or multiplet (m). Mass spectra were recorded on a JMS-SX102A (JEOL) mass spectrometer, with a glycerol or *m*-nitrobenzyl alcohol (NBA) matrix as an internal standard. All reactions were carried out under a dry nitrogen atmosphere with freshly distilled solvents, unless otherwise noted. Reagents were purchased from Aldrich, Wako Pure Chemical Industries or Nacalai Tesque, and used without purification. NADPH:cytochrome P450 reductase and β-NADPH coenzyme were obtained from Oxford Biomedical Research and Oriental Yeast CO., respectively. Tetrahydrofuran was distilled under a nitrogen atmosphere from sodium/benzophenone ketyl immediately prior to use. Ultrapure water was obtained from Yamato WR-600A water purifier. Precoated TLC (Merck silica gel 60 F_{254}) plates were used for monitoring the reactions. Wako gel (C-300, Wako Pure Chemical Industries) was used for column chromatography. A Rigaku Radioflex-350 X-ray generator was employed for X radiolysis at ambient temperature. High-performance liquid chromatography (HPLC) was carried out with a Shimadzu HPLC system (SPD-10A UV-VIS detector, CT0-10A column oven, two LC-10AS pumps, C-R6A chromatopac). Sample solutions were injected onto a reversed-phase column (Inertsil ODS-3, GL Science Inc., ϕ 4.6 × 150 mm). The following solvent program was used: of 88.9% B (20 min) followed by 88.9–16.7% B (a linear gradient over 70 min; solution A: 95% acetonitrile; solution B: 5% acetonitrile containing 0.1 M triethylammonium acetate (TEAA) buffer, pH 5). Fluorescent spectra were recorded with excitation at 300 nm on Shimadzu RF-5300PC spectrofluorophotometer at ambient temperature, whereby a UV-33 glass filter (Toshiba Glass CO.) was set on the detector side to cut off the excitation peak at 300 nm. The amount of dissolved oxygen (DO) was measured with an OM-51 DO meter (Horiba) at 37 °C. Compounds **7**

was prepared from compound **6** as reported elsewhere.[7] The human fibrosarcoma cell line, HT-1080, was purchased from American Type Culture Collection (Manassas, VA) and maintained in Dulbecco Modified Eagle Medium (Invitrogen) containing fetal bovine serum (10%) in a humidified incubator with 5% CO_2, 95% air at 37 °C.

Preparation of Compound 4

Coumarin-3-carboxylic acid (510 mg, 2.68 mmol) was dissolved in thionyl chloride (5 mL), and the resulting mixture was stirred at 100 °C for 2.5 h. The mixture was then concentrated by evaporation to give the acid chloride **8**, which was used immediately, without purification, in the next step.

The crude acid chloride **8** was added as a solution in dichloromethane (2 mL) and triethylamine (TEA; 1 mL) to a solution of **3** (254 mg, 0.66 mmol) in dichloromethane (3 mL), and the resulting mixture was stirred at 0 °C for 15 min, and then at ambient temperature for 3 h. The reaction mixture was then diluted with saturated aqueous sodium hydrogen carbonate and extracted with chloroform. The organic layer was washed with brine, dried over anhydrous magnesium sulfate, filtered, and concentrated in vacuo. The crude product was purified by flash chromatography (SiO_2, 33% hexane/ethyl acetate) to give **4** (300 mg, 62%) as a brown oil. ^{1}H NMR (300 MHz, $CDCl_3$; as a result of restricted rotation about the amide bond adjacent to the linker, two signals were observed for some atoms): δ 8.49 and 8.46 (s, 2H), 7.57–7.49 (m, 4 H), 7.29–7.17 (m, 6 H), 5.22 (s, 4 H), 3.54–3.23 (m, 4 H), 3.08, 2.83, and 2.67 (s, 6 H), 2.28 (s, 3H), 1.32, and 1.29 (s, 9H); ^{13}C NMR (68 MHz, $CDCl_3$; as a result of restricted rotation about the amide bond adjacent to the linker, two signals were observed for some atoms): δ 162.0, 156.3, 154.9, 154.0, 149.0, 148.9, 145.9, 136.0, 135.9, 134.3, 131.7, 131.4, 129.5, 128.4, 124.7, 117.6, 117.4, 117.3, 116.5, 79.6, 62.6, 62.5, 47.5, 47.1, 46.3, 35.5, 35.3, 34.9, 29.6, 28.4, 20.9, 14.2; FABMS (NBA/$CHCl_3$): *m/z* 727 [(M + H)$^+$]; HRMS: *m/z* calcd. for $C_{39}H_{39}N_2O_{12}$: 727.2498 [(M + H)$^+$]; found: 727.2505.

Preparation of IQ-Cou

Compound **4** (155 mg, 0.21 mmol) was added to 0.5 M HCl/MeOH (2 mL), and the mixture was

stirred for 14 h at ambient temperature. The solvent was then removed under reduced pressure to give **5** (181 mg) as a colorless oil. The crude product **5** was dissolved in *N, N*-dimethylformamide (DMF; 1 mL).

The indolequinone derivative **7** (177 mg, 0.44 mmol) in DMF (1 mL) was added to the solution of **5** in DMF, and the resulting mixture was stirred at ambient temperature for 8 h. The mixture was then diluted with saturated aqueous sodium hydrogen carbonate and extracted with ethyl acetate. The organic layer was washed with brine, dried over anhydrous magnesium sulfate, filtered, and concentrated in vacuo. The crude product was purified by flash chromatography (SiO$_2$, from 16.7% ethyl acetate/hexane to 100% ethyl acetate) to give IQ-Cou (72.1 mg, 39%) as an orange oil. ^{1}H NMR (300 MHz, CDCl$_3$, room temperature; as a result of restricted rotation about the amide bonds, two signals were observed for some atoms): δ 8.55 and 8.51 (s, 2H), 7.58–7.53 (m, 4H), 7.31–7.20 (m, 6H), 5.52–5.39 (m, 1H), 5.24–5.04 (m, 6H), 3.83–3.66 (m, 6H), 3.58– 2.74 (m, 10H), 2.31 (s, 3 H), 2.24, and 2.19 (s, 3H); ^{1}H NMR (400 MHz, DMSO-*d*$_6$, 120 °C): δ 8.62 (s, 2H), 7.83 (d, *J* = 0.02 Hz, 2 H), 7.72 (t, *J* = 0.02 Hz, 2H), 7.38 (t, *J* = 0.02 Hz, 6H), 5.61 (s, 1H), 5.27–5.13 (br, 4H), 5.11 (s, 2H), 3.74 (s, 3H), 3.71 (s, 3H), 3.48–3.33 (m, 5H), 2.92–2.69 (m, 5H), 2.36 (s, 3H), 2.19 (s, 3H); ^{13}C NMR (100 MHz, CDCl$_3$, room temperature; as a result of restricted rotation about the amide bonds, two signals were observed for some atoms): δ 178.4, 177.0, 162.1, 159.3, 156.4, 155.0, 154.1, 149.3, 149.0, 145.7, 138.1, 136.0, 134.3, 131.4, 129.6, 129.0, 128.5, 124.7, 121.6, 117.77, 117.75, 117.3, 116.6, 106.5, 62.5, 57.5, 56.3, 47.2, 46.7, 35.7, 35.3, 35.0, 32.3, 21.0, 9.6, 9.4; ^{13}C NMR (100 MHz, DMSO-*d*$_6$, 120 °C): δ 177.3, 176.3, 163.0, 161.5, 158.9, 155.1, 154.2, 152.8, 147.8, 145.1, 137,5, 134.6, 133.8, 129.8, 129.5, 128.3, 127.8, 124.2, 120.6, 117.2, 117.1, 115.6, 115.1, 106.2, 61.4, 56.7, 55.8, 46.3, 45.8, 34.2, 33.9, 31.3, 19.8, 8.3; FABMS (NBA/CHCl$_3$): *m/z* 888 [(M + H)$^+$]; HRMS: *m/z* calcd. for C$_{47}$H$_{42}$N$_3$O$_{15}$: 888.2610 [(M + H)$^+$]; found: 888.2604.

Measurement of extinction coefficients

The extinction coefficients (ε) of compound **6** and coumarin-3-carboxylic acid were calculated according to the Beer–Lambert law. UV spectra of the samples in acetonitrile (final concentration:

120 µM) were recorded with a Jasco V-530 UV/Vis spectrometer.

Fluorescence spectrophotometry

Fluorescence spectra of IQ-Cou and coumarin-3-carboxylic acid in acetonitrile (final concentration: 10 µM) were recorded with a Shimadzu RF-5300PC fluorescence spectrophotometer with excitation at 300 nm.

Measurement of fluorescence quantum yield

The fluorescence quantum yield (Φ_F) was determined by using Coumarin 153, with a known Φ_F value of 0.42 in methanol, as a reference. The area of the emission spectrum was integrated by using instrumentation software, and the quantum yield was calculated according to Equation (1), in which $\Phi_{F(S)}$ and $\Phi_{F(R)}$ are the fluorescence quantum yields of the sample and the reference, respectively, the terms $A_{(S)}$ and $A_{(R)}$ refer to the area under the fluorescence spectra, $(Abs)_{(R)}$ and $(Abs)_{(S)}$ are the optical densities of the sample and reference solutions at the excitation wavelength, and $n_{(S)}$ and $n_{(R)}$ are the refractive indices of the solvents used for the sample and the reference.

$$\Phi_{F(S)}/\Phi_{F(R)} = \frac{A_{(S)}}{A_{(R)}}\frac{(Abs)_{(R)}}{(Abs)_{(S)}}\frac{n_{(S)}^2}{n_{(R)}^2} \tag{1}$$

Laser flash photolysis

Laser flash photolysis was carried out with a Unisoku TSP-601 flash spectrometer. A continuum Surelite-I Nd-YAG (Q-switched) laser with the fourth harmonic at 355 nm was employed for flash photoirradiation. The probe beam from a Hamamatsu 150-W xenon short-arc lamp was guided with an optical fiber scope to a perpendicular orientation with respect to the excitation laser beam. The probe beam was monitored with a Unisoku MD200 photomultiplier tube through a Hamamatsu DG535 image-intensifier controller (1024 photodiodes). The timing of the excitation pulse laser, the probe beam, and the detection system was achieved through a Tektronix model TDS 3012 digital

phosphor oscilloscope interfaced to an IBM Windows XP computer. A solution of IQ-Cou (30 μM) in acetonitrile was deaerated by bubbling argon through it prior to laser flash photolysis.

Radiolytic reduction

To establish hypoxia, an aqueous solution of IQ-Cou (100 μM) containing 2-methyl-2-propanol (30%) was purged with argon for 30 min and then irradiated in a sealed glass ampoule at ambient temperature with an X-ray source (4.0 Gy min^{-1}). After irradiation, aliquots were taken at appropriate time intervals for fluorescence spectrophotometry, and then diluted by 33% with Milli-Q water for analytical HPLC. A control air-saturated sample solution was irradiated and analyzed in a similar manner.

Bioreduction by NADPH−P450 reductase

To establish hypoxia, a solution of NADPH:cytochrome P450 reductase (final concentration: 10.6 μg mL^{-1}) and β-NADPH (final concentration: 2 mM) in phosphate buffer (25 mM, pH 7.4) was purged with argon for 10 min at 37 °C. IQ-Cou (final concentration: 500 μM) was added to the resulting solution, which was then incubated at 37 °C. For analytical HPLC, aliquots were taken at appropriate time intervals and diluted by 10% with Milli-Q water/acetonitrile (1:1). The reaction mixture was extracted with ethyl acetate to remove β-NADPH coenzyme, and florescence spectra of the organic layer were measured with excitation at 300 nm. A control aerobic sample solution was irradiated and analyzed in a similar manner.

Bioreductive activation of IQ-Cou by HT-1080 cell lysate

HT-1080 cells were cultured in six dishes (90% confluent in dishes of 100 mm in diameter) and washed twice with ice-cold phosphatebuffered saline. The cell lysate was then harvested with ice-cold CelLytic M cell lysis reagent (2 mL; Sigma-Aldrich), maintained at ambient temperature for 15 min, and centrifuged at 14000 rpm for 5 min to remove the cell debris. The resulting supernatant was kept in a Bactron II anaerobic environmental chamber (Sheldon Manufacturing,

Cornelius, OR; 94% N_2, 5% CO_2, 1% H_2) at 37 °C for 22 h for hypoxic treatment. IQ-Cou (final concentration: 500 μM) was added to the hypoxic lysate, which was then incubated at 37 °C for 4 h. Aliquots were taken at appropriate time intervals, diluted by 10% with a 1:1 mixture of Milli-Q water and acetonitrile, and then diluted by 50% with acetonitrile. All solutions were filtered with a Cosmonice Filter S (Nacalai Tesque, Kyoto, Japan) for analytical HPLC and fluorescence spectrophotometry. Normoxic lysate, which was kept in a well-oxygenated incubator (95% air, 5% CO_2, 37 °C), and lysis buffer alone were mixed in a similar way with IQ-Cou and analyzed as negative controls.

References and Notes

(1)   (a) Semenza, G. L. *Annu. Rev. Med.* **2003**, *54*, 17–28. (b) Semenza, G. L. *Trends Mol. Med.* **2001**, *7*, 345–350. (c) Semenza, G. L. *Pediatr. Res.* **2001**, *49*, 614–617.

(2)   Murdoch, C.; Muthana, M.; Lewis, C. E. *J. Immunol.* **2005**, *175*, 6257–6263.

(3)   (a) Kizaka-Kondoh, S.; Inoue, M.; Harada, H.; Hiraoka, M. *Cancer Sci.* **2003**, *94*, 1021–1028. (b) Harris, A. L. *Nat. Rev. Cancer* **2002**, *2*, 38–47.

(4)   (a) Tanabe, K.; Makimura, Y.; Tachi, Y.; Imagawa-Sato, A.; Nishimoto, S. *Bioorg. Med. Chem. Lett.* **2005**, *15*, 2321–2324. (b) Shibamoto, Y.; Tachi, Y.; Tanabe, K.; Hatta, H.; Nishimoto, S. *Int. J. Radiat. Oncol. Biol. Phys.* **2004**, *58*, 397–402. (c) Tanabe, K.; Mimasu, Y.; Eto, A.; Tachi, Y.; Sakakibara, S.; Mori, M.; Hatta, H.; Nishimoto, S. *Bioorg. Med. Chem.* **2003**, *11*, 4551–4556. (d) Shibamoto, Y.; Zhou, L.; Hatta, H.; Mori, M.; Nishimoto, S. *Int. J. Radiat. Oncol. Biol. Phys.* **2001**, *49*, 407–413. (e) Mori, M.; Hatta, H.; Nishimoto, S. *J. Org. Chem.* **2000**, *65*, 4641–4647. (f) Shibamoto, Y.; Zhou, L.; Hatta, H.; Mori, M.; Nishimoto, S. *Jpn. J. Cancer Res.* **2000**, *91*, 433–438.

(5)   (a) Hernick, M.; Flader, C.; Borch, R. F. *J. Med. Chem.* **2002**, *45*, 3540–3548. (b) Everett, S. A.; Swann, E.; Naylor, M. A.; Stratford, M. R. L.; Patel, K. B.; Tian, A.; Newman, R. G.; Vojnovic, B.; Moody, C. J.; Wardman, P. *Biochem. Pharmacol.* **2002**, *63*, 1629–1639. (c) Swann, E.; Barraja, P.; Oberlander, A. M.; Gardipee, W. T.; Hundnott, A. R.; Beall, H. D.; Moody, C. J. *J. Med. Chem.* **2001**, *44*, 3311–3319. (d) Naylor, M. A.; Swann, E.; Everett, S. A.; Jaffar, M.; Nolan, J.; Robertson, N.; Lockyer, S. D.; Patel, K. B.; Dennis, M. F.; Stratford, M. R. L.; Wardman, P.; Adams, G. E.; Moody, C. J.; Stratford, I. J. *J. Med. Chem.* **1998**, *41*, 2720–2731.

(6)   Shamis, M.; Lode, H. N.; Shabat, D. *J. Am. Chem. Soc.* **2004**, *126*, 1726–1731.

(7)   Zhang, Z.; Tanabe, K.; Hatta, H.; Nishimoto, S. *Org. Biomol. Chem.* **2005**, *3*, 1905–1910.

(8)   As two coumarin chromophores are conjugated with an indolequinone unit in IQ-Cou, the indolequinone unit could absorb about 1/3 of the total incident UV light at 300 nm to suppress the apparent fluorescence quantum yield of the counterpart coumarin chromophore

to about 2/3 of the intrinsic quantum yield in the absence of an indolequinone unit.

(9)   (a) Ueno, T.; Urano, Y.; Setsukinai, K.; Takakusa, H.; Kojima, H.; Kikuchi, K.; Ohkubo, K.; Fukuzumi, S.; Nagano, T. *J. Am. Chem. Soc*. **2004**, *126*, 14079–14085. (b) Miura, T.; Urano, Y.; Tanaka, K.; Nagano, T.; Ohkubo, K.; Fukuzumi, S. *J. Am. Chem. Soc*. **2003**, *125*, 8666–8671. (c) Tanaka, K.; Miura, T.; Umezawa, N.; Urano, Y.; Kikuchi, K.; Higuchi, T.; Nagano, T. *J. Am. Chem. Soc*. **2001**, *123*, 2530–2536.

(10)   Kavarnos, G. J. Fundamentals of Photoinduced Electron Transfer; VCH, Weinheim, **1993**.

(11)   The transient signals of the radical cations of coumarin derivatives were reported to appear at 390–450 nm; see: (a) Chen, L.; Wood, P. D.; Mnyusiwalla, A.; Marlinga, J.; Johnston, L. J. *J. Phys. Chem. B* **2001**, *105*, 10927–10935. (b) Wood, P. D.; Johnston, L. J. *J. Phys. Chem. A* **1998**, *102*, 5585–5591. (c) Priyadarsini, K. I.; Naik, D. B.; Moorthy, P. N. *Chem. Phys. Lett*. **1988**, *148*, 572–576.

(12)   Radiolysis of a dilute aqueous solution at about pH 7.0 produces primary water radicals, such as oxidizing hydroxyl radicals ($^\bullet$OH), reducing hydrated electrons (e_{aq}^-), and reducing hydrogen atoms ($^\bullet$H) with the G values (see ref. 10) 280, 280, and 60 nmol J^{-1}, respectively. In the presence of excess 2-methyl-2-propanol, oxidizing $^\bullet$OH is scavenged, and reduction proceeds almost exclusively.

(13)   The G value is defined as the number of moles produced or changed per 1 J of radiation energy absorbed by the reaction system.

(14)   Hydrated electrons were reported to show high reactivity toward carbonyl groups: (a) Hart, E. J.; Fielden, E. M.; Anbar, M. *J. Phys. Chem*. **1967**, *71*, 3993–3998. (b) Garrison, W. M. *Chem. Rev*. **1987**, *87*, 381–398. This side reaction may be one of the reasons for the low yield of free coumarin upon hypoxic X irradiation.

(15)   Yu, L. J.; Matis, J.; Scudiero, D. A.; Hite, K. M.; Monk, A.; Sausville, E. A.; Waxman, D. J. *Drug Metab. Dispos*. **2001**, *29*, 304–312.

(16)   The fluorescence emission of coumarin-3-carboxylic acid was influenced by the pH variation. Fluorescence quantum yield of this fluorophore at pH 3.6, 7.4 and 11.8 were 0.012, 0.0016

and 0.0015, respectively. To avoid the pH effect on the fluorescence spectra, we measured fluorescence of the sample after extraction or dilution by organic solvents. (see Experimental Section).

(17)   Cowen, R. L.; Williams, K. J.; Chinje, E. C.; Jaffar, M.; Sheppard, F. C. D.; Telfer, B. A.; Wind, N. S.; Stratford, I. J. *Cancer Res*. **2004**, *64*, 1396–1402.

(18)   Weissleder, R.; Ntziachristos, V. *Nat. Med*. **2003**, *9*, 123–128.

Chapter 2

Hypoxia Imaging Probe:
One-electron Reduction and Fluorescence Characteristics
of a Complex of Avidin-FITC and Biotin-Indolequinone Conjugate

Abstract: 3-Substituted indolequinone analogs readily remove the substituents *via* one-electron reduction under hypoxic conditions, whereas the removal of the substituents is suppressed under aerobic conditions. Moreover, indolequinone derivatives have an ability of quenching the fluorescence through the photoinduced electron transfer (PeT) mechanism. In view of these characteristics, we have developed a new class of a hypoxic detection probe by means of incorporating indolequinone derivatives into avidin-biotin complex. We conjugated biotin compound at a 3-position and C-5 linker at a 5-position of an indolequinone unit (**C5-IQ-Btn**). The indolequinone moiety was confirmed to be released from **C5-IQ-Btn** *via* one-electron reduction by X-irradiation or a treatment of NADPH:cytochrome P450 reductase under hypoxic conditions, indicating that biotin conjugated at a 3-position of indolequinone was simultaneously released. According to the HABA analysis, synthesized **C5-IQ-Btn** was confirmed to retain sufficiently the binding affinity to avidin in spite of the substituent such as indolequinone moiety. The fluorescence intensity of the fluorescein isothiocyanate (FITC) labeled avidin complex containing **C5-IQ-Btn** was suppressed due to the adjacent quenching unit of indolequinone moiety. **C5-IQ-Btn** was confirmed to decrease the fluorescence of other fluorescent-labeled (7-amino-4-methylcoumarin-3-acetic acid, Texas Red, and rhodamine) avidin chromophore in a similar way. In addition, **C5-IQ-Btn** could quench the emission of an FITC-labeled streptavidin chromophore, suggesting that indoelquinone derivatives can efficiently suppress the fluorescence of the adjacent chromophore in spite of the wide range of fluorescent maximum or the different structures between avidin and streptavidin. Upon enzymatic treatment by NADPH:cytochrome P450 reductase, the

avidin-FITC and **C5-IQ-Btn** complex (**AF-IQ-Btn**) caused the enhanced emission, suggesting that indolequinone moiety is removed *via* one-electron reduction under hypoxic conditions. The **AF-IQ-Btn** system has several unique properties that are favorable for a fluorescent probe of hypoxic microenvironment.

Introduction

A partial pressure of oxygen within a living body attracts the attention in physiological action and pathological alteration. A partial pressure of oxygen is maintained at proper level by homeostatic systems,[1] and an imbalance of oxygen homeostasis has been reported to cause various diseases. Especially, a hypoxia profoundly relates to cerebrovascular disease,[2] cardiovascular disease,[3] and solid tumors.[4] In view of this, hypoxia detectable systems, an immunohistochemical detecting method based on pimonidazole[5] or a cloning technique based on hypoxia-specific fusion proteins,[6] have been developed in two decades. These systems are substantially superior in selectivity; however, more concise and quantitatively excellent systems will be able to contribute enormously to biological and pathological study. This motivation stimulates us to create a novel hypoxia-specific probe.

Indolequinone derivatives have been identified as quenchers for the adjacent fluorescent molecules[7] and removable substitutes *via* one-electron reduction under hypoxic conditions.[8] We have developed a new indolequinone derivative conjugated with two chromophore of coumarin-3-carboxylic acid (IQ-Cou) for a hypoxia detectable probe.[9] Upon the treatment with a cell lysate of the human fibrosarcoma cell line HT-1080 (expressing NADPH:cytochrome P450 reductase), IQ-Cou showed an enhanced fluorescence under hypoxic conditions, whereas the fluorescence remained weak under aerobic treatment. Therefore, IQ-Cou would be a candidate to imaging hypoxic microenvironments. However, IQ-Cou had some drawbacks: First, fluorescence emission at around 420 nm of coumarin-3-carboxylic acid was too short to be applied in substantial application. Second, IQ-Cou hardly dissolved in water, resulting in precipitates. Therefore, living

cells would be suffered from adverse effects by existing precipitates.

To overcome these defects, we have newly designed an indolequinone derivative possessing biotin in order to incorporate a fluorescent-labeled avidin (Figure 1). Multicolor fluorescent-labeled avidin proteins have been developed and used for many purposes and situations. Furthermore, an indolequinone derivative is expected to be soluble in water due to incorporating avidin protein. In view of these, we have chosen a fluorescent-labeled avidin, avidin-FITC, as a chromophore group. We conjugated a biotin at a 3-position and 1-Propanol moiety at a 5-position of an indolequinone (**C5-IQ-Btn**), to introduce other functional groups at C-5 terminus; quenching agents, fluorescence molecules and so on. A carbon-carbon bond at a 3-position of the indolequinone moiety was cleaved to release the biotin *via* one-electron reduction by radiolytic or enzymatic reduction under hypoxic conditions. Because of strong binding affinity to avidin protein, **C5-IQ-Btn** was expected to form a complex with avidin-FITC. Indeed, the fluorescence intensity derived from fluorescein was decreased due to the adjacent indolequinone unit. **C5-IQ-Btn** was confirmed to decrease the fluorescence of other fluorescent-labeled (7-amino-4-methylcoumarin-3-acetic acid, Texas Red, and rhodamine) avidin chromophore in a similar way. In addition, **C5-IQ-Btn** could quench the emission of an FITC-labeled streptavidin chromophore, suggesting that indoelquinone derivatives can efficiently suppress the fluorescence of the adjacent chromophore in spite of the wide range of fluorescent maximum or the different structures between avidin and streptavidin. An enzymatic treatment by NADPH:cytochrome P450 reductase to the complex of avidin-FITC and **C5-IQ-Btn** (**AF-IQ-Btn**) causes the enhanced emission in a hypoxia-selective manner, suggesting that indolequinone moieties are removed *via* one-electron reduction under hypoxic conditions. With these characteristics, a complex of a fluorescent-labeled avidin and **C5-IQ-Btn** might be applicable as multicolor fluorescent probes for the molecular imaging of disease-relevant hypoxia.
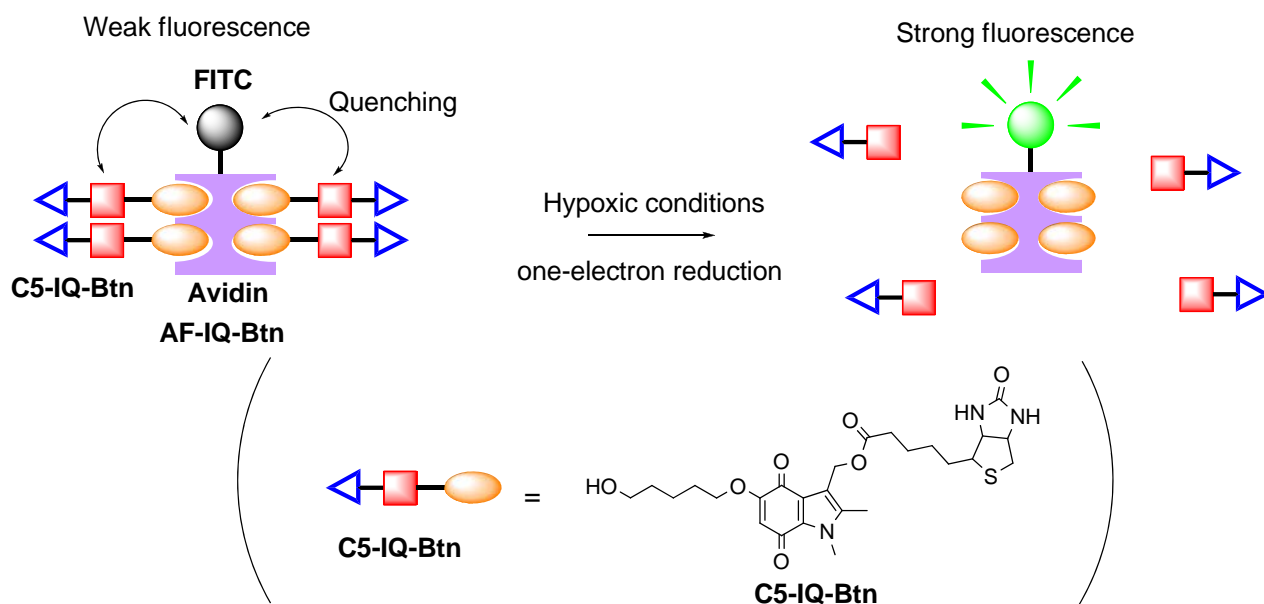
Figure 1. Schematic illustration of a complex of FITC-labeled avidin and biotin conjugated with a reducing indolequinone unit (**C5-IQ-Btn**). A fluorescence intensity of the avidin-FITC and **C5-IQ-Btn** complex (**AF-IQ-Btn**) is suppressed due to the adjacent indolequinone units, whereas an enhanced fluorescence is emitted upon one-electron reduction under hypoxic conditions because of the removal of indolequinone moieties.

Results and discussion

Synthesis of **C5-IQ-Btn** is outlined in Scheme 1. The indole derivative **1** as a starting material was prepared by the reported method.[10] After introduction of 5-bromo-1-pentanol protected by *tert*-butyldimethylsilyl group, nitration at the C(4) position of **2** accompanied the deprotection of the hydroxyl group to provide **3**. Reduction of nitro group into amino group purely furnished **4** without purification by flash column chromatography. Following reprotection of the hydroxyl group of **4**, LAH reduction afforded the alcohol **6**. Oxidation of the 4-aminoindole **6** with Fremy's salt gave the indolequinone **7**. The carboxylic ester **8** was readily obtained direct coupling with biotin using uronium methodology. Desilylation with weak acid transformed silyl ether into desired **C5-IQ-Btn** in excellent yield. As an index sample in radiolytic reduction, **C5-IQ** was obtained by desilylation of indolequinone **7**.
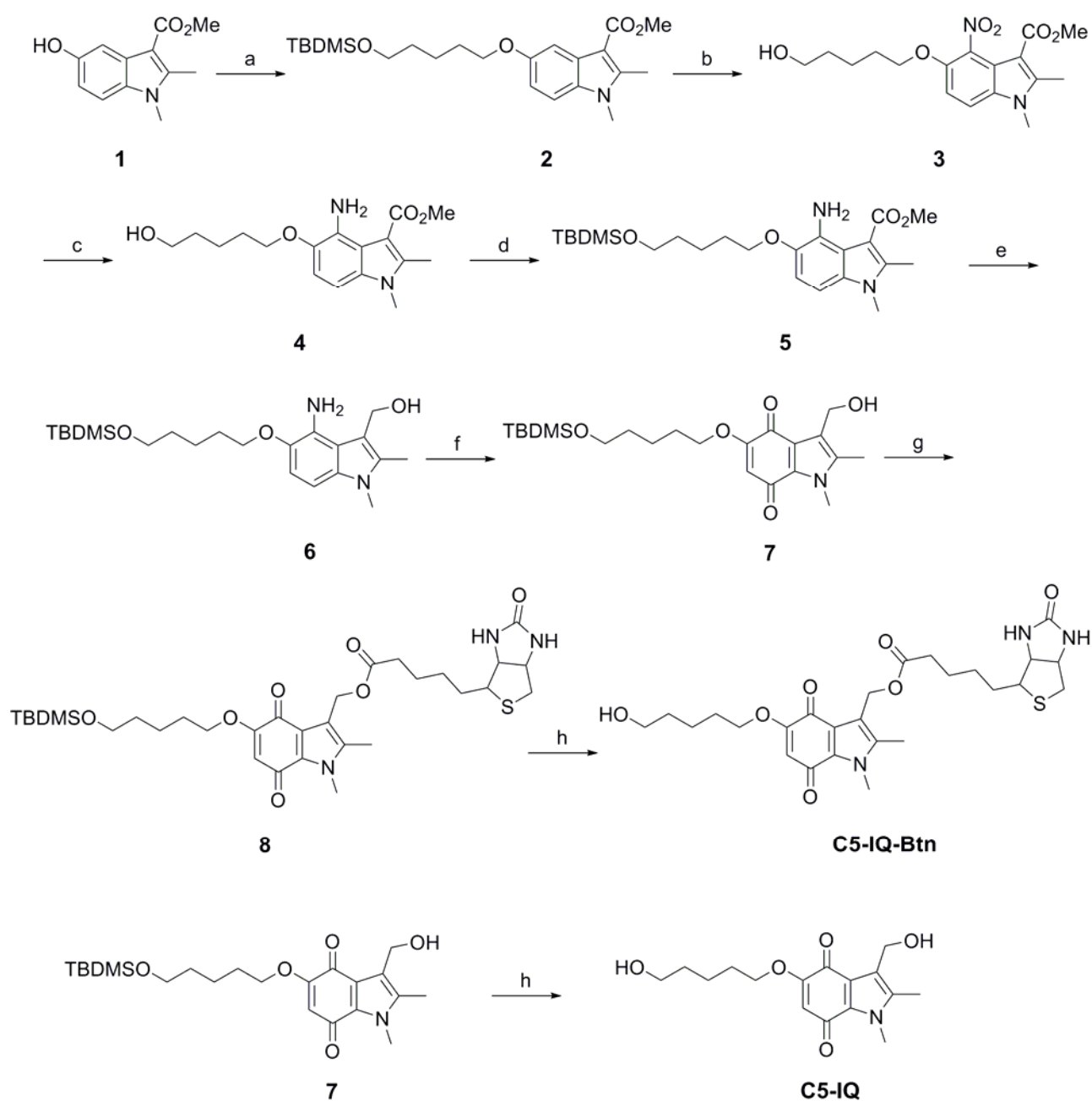
Scheme 1. Reagents and conditions: (a) 5-Bromo-1-*tert*-butyldimethylsilyloxypentane, NaH, DMF, 0 °C to room temperature, overnight, 38%; (b)HNO₃, AcOH, CH₂Cl₂, 0 °C to room temperature, 4 h, 63%; (c)Sn, HCl, EtOH, reflux at 80 °C, 2 h, 95%; (d) TBDMS-Cl, imidazole, DMF, 0 °C to room temperature, 3.5 h, 85%; (e) LAH, THF, 0 °C, 30 min; (f) Fremy's salt, NaH₂PO₄, THF, 0 °C, 20 min, 79% in 2 steps; (g) Biotin, TATU, DIPEA, DMAP, DMF, 0 °C to room temperature, overnight, 93%; (h) AcOH-H₂O-THF (13:7:3), room temperature, overnight, 81% (**C5-IQ-Btn**), 90% (**C5-IQ**).

To assess the reductive characteristics of **C5-IQ-Btn**, we performed one-electron reduction of **C5-IQ-Btn** by X-radiolysis of an argon-purged aqueous solution containing excess 2-methyl-2-propanol as the scavenger of oxidizing hydroxyl radicals. Reducing hydrated electrons (e_{aq}^-) are generated as the major active species under these radiolysis conditions, in which the yield of reducing hydrogen atoms is much less than those of hydrated electron and oxidizing hydroxyl radicals.[11] Figure 2 shows a representative reaction profile analyzed by HPLC of the radiolytic one-electron reduction of **C5-IQ-Btn** by the resulting e_{aq}^- under hypoxic conditions. The appearance of a single new peak in Figure 2 was attributable to the formation of **C5-IQ**, as confirmed by the overlap injection of authentic samples in the HPLC analysis. Indolequinone derivatives possessing leaving groups at the 3-position have been reported to generate iminium ions derived from indolequinone moieties after release of leaving groups *via* one-electron reduction. And subsequently, the iminium ions rapidly react with water molecules to regenerate indolequinone moieties.[7] Therefore, it is reasonable to form the fragment of **C5-IQ**. Unfortunately, the other fragment of biotin didn't be detectable by HPLC analysis because of its low UV-Vis absorption around 260 nm, but it strongly suggests that biotin molecules are released as much as the formation of **C5-IQ** *via* one-electron reduction.
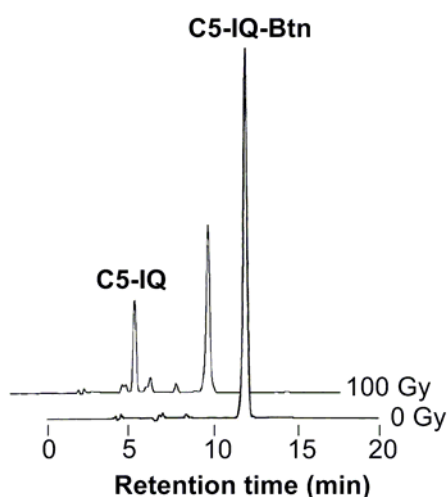

Figure 2. HPLC profiles of radiolytic reduction (0 and 100 Gy) of 100 μM **C5-IQ-Btn** in aqueous solution containing 30% 2-methyl-2-propanol under hypoxic conditions.

The G values[12] were 552 nmol J^{-1} for the decomposition of **C5-IQ-Btn** and 182 nmol J^{-1} for the formation of corresponding **C5-IQ**, respectively. Thus, 33% of the decomposed **C5-IQ-Btn** was converted to **C5-IQ** upon hypoxic X-irradiation. The radiolytic reactivity of **C5-IQ-Btn** was significantly greater than that of previous reported indolequinone derivatives; IQ-FdUrd[13] (140 nmol J^{-1} for the decomposition, 38 nmol J^{-1} for the formation of FdUrd), IQ-Cou[9] (219 nmol J^{-1} for the decomposition, 15 nmol J^{-1} for the formation of fluorescent coumarin molecules). These results imply that higher electron affinity of the substituents such as FdUrd and coumarin, compared to biotin moiety, causes lower reductive reactivity of indolequinone. In the case of the aerobic conditions, the radiolytic decomposition of **C5-IQ-Btn** was dramatically suppressed (Figure 3); the G values were evaluated as 25 nmol J^{-1} for the decomposition of **C5-IQ-Btn** and 7 nmol J^{-1} for the formation of the corresponding **C5-IQ**, respectively. This oxygen effect on the activation of **C5-IQ-Btn** is accounted for by the reactivity of molecular oxygen that captures efficiently reducing species of e_{aq}^{-} into superoxide anion radical ($O_2^{\bullet-}$).[7] These results indicate that **C5-IQ-Btn** is activated to lead to the cleavage between indolequinone and biotin moieties, thus the biotin molecules are released in a hypoxia selective manner, as were observed in the cases of the IQ-FdUrd[13] and CPT4 prodrugs.[14]
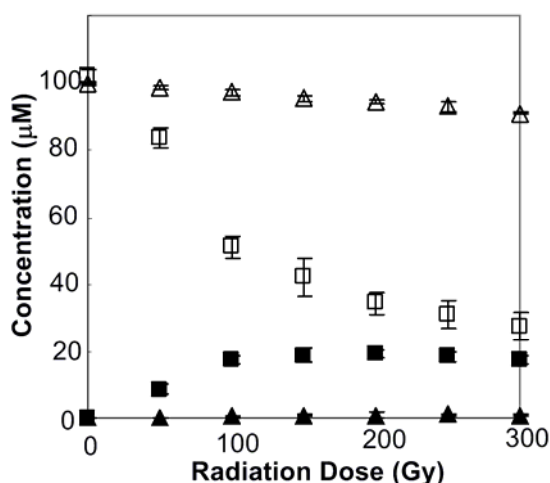

Figure 3. X-radiolysis (5.0 Gy min^{-1}) of 100 μM **C5-IQ-Btn** (open square and triangle) in aqueous solution containing 30% 2-methyl-2-propanol to release **C5-IQ** (closed square and triangle) at ambient temperature under hypoxic (square) and aerobic (triangle) conditions. Results are shown with the mean ± S.D (n = 3)

To further characterize one-electron reduction of **C5-IQ-Btn**, we performed an enzymatic reduction of **C5-IQ-Btn**. NADPH:cytochrome P450 reductase, which is expressed in many pathological tisses,[15] is an electron-donating protein that catalyzes one-electron reduction of quinone derivatives to form semiquinone anion radicals. We incubated **C5-IQ-Btn** (final concentration; 500 μM) with NADPH:cytochrome P450 reductase (final concentration; 22.7 μg mL^{-1}) and cofactor β-NADPH (final concentration; 2 mM) at 37 °C for 5 min under hypoxic or aerobic conditions. Figure 4 shows a representative reaction profile analyzed by HPLC of the one-electron reduction of **C5-IQ-Btn** by NADPH:cytochrome P450 reductase under each condition. As shown in Figure 4, **C5-IQ-Btn** was preferentially reduced under hypoxic conditions to appear a new peak represented as a symbolic " * " in the HPLC profiles. This peak was confirmed to be a product of two-electron reduction by the overlap injection of authentic samples, thereby a hydroquinone derivative was predicted to generate after reacting the indolequinone moiety.[7] These results suggest that **C5-IQ-Btn** readily proceeds in two steps of one-electron reduction by NADPH:cytochrome P450 reductase, consequently releases the biotin in a similar way of previous reports.[7,8]
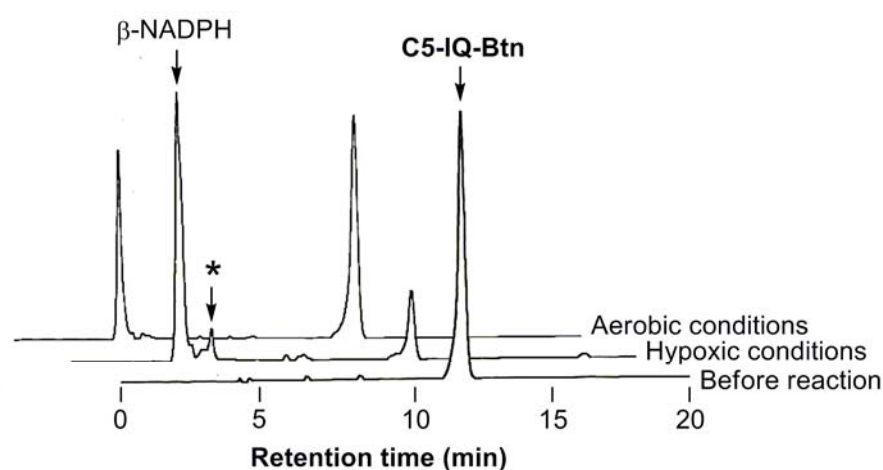

Figure 4. HPLC profiles of the enzymatic reduction of 500 μM **C5-IQ-Btn** in 25 mM phosphate buffer (pH 7.4) by NADPH:cytochrome P450 reductase (22.7 μg mL^{-1}) and β-NADPH coenzyme (2 mM) at 37 °C under hypoxic or aerobic conditions. The HPLC signal indicated with "*" corresponds to a product of two-electron reduction.

49

Under aerobic conditions, the reduction of **C5-IQ-Btn** was dramatically suppressed. As suggested by the recent studies on reductive activation of indolequinone prodrugs, a semiquinone anion radical intermediate generated by one-electron reductioin of indolquinone unit could exhibit reducing reactivity toward molecular oxygen to form original indolequinone and $O_2^{\bullet-}$. These results indicate that the reductive activity of **C5-IQ-Btn** can be controlled by the environmental O_2 concentration.

To examine an affinity of the synthesized **C5-IQ-Btn** to avidin, we compared the binding affinity of **C5-IQ-Btn** to that of a biotin by using 4-hydoroxyazobenzene-2'-carboxylic acid (HABA) analysis.[16]
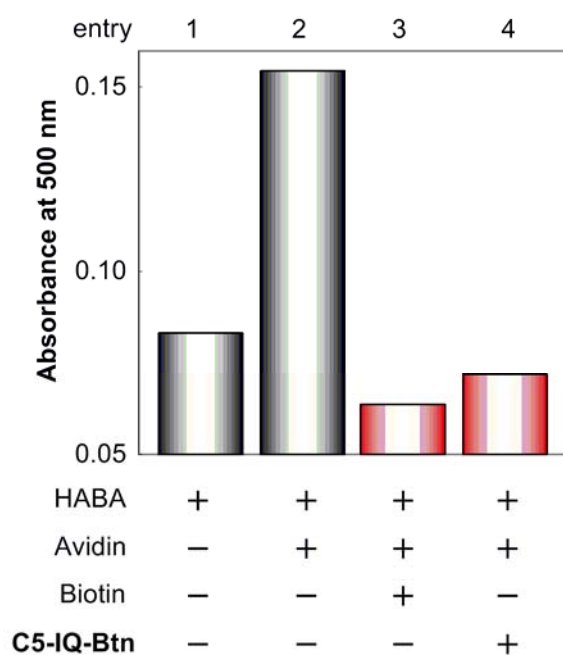

Figure 5. Compared binding affinity of the synthesized **C5-IQ-Btn** to biotin. Biotin or **C5-IQ-Btn** (final concentration: 80 μM, respectively) was added to a solution of 4-hydroxyazobenzene-2'-carboxylic acid (HABA, final concentration: 160 μM) and avidin (final concentration: 0.8 μM) in PBS buffer (pH 7.4). HABA and avidin complex had discriminative absorbance at 500 nm (entry 2), whereas only HABA compound had lower absorption (entry 1). Addition of biotin to avidin-HABA complex caused to reduce the absorbance at 500 nm because of the replacement of HABA to biotin (entry 3). Addition of **C5-IQ-Btn** to avidin-HABA complex resulted in suppression of the absorbance at 500 nm, indicating that **C5-IQ-Btn** has strong binding affinity to avidin similar to biotin.

It has been known that HABA forms a complex with avidin to enhance an absorbance at 500 nm. The interaction between HABA and avidin is comparatively weak, thus HABA incorporated into avidin is readily replaced with biotin, resulting that the intense absorbance at 500 nm is perceptively decreased. Therefore, the difference of the absorbance at 500 nm reflects quantitatively the binding affinity to avidin. Biotin or **C5-IQ-Btn** (final concentration: 80 μM, respectively) was added to a mixture of HABA (final concentration: 160 μM) and avidin (final concentration: approximately 0.8 μM) in PBS buffer (pH 7.4). We monitored the difference of the absorbance at 500 nm (Figure 5). HABA and avidin complex showed discriminative absorbance at 500 nm (entry 2), whereas only HABA compound had lower absorption (entry 1). Addition of biotin to avidin-HABA complex caused to reduce the absorbance at 500 nm because of the replacement of HABA to biotin (entry 3). In a similar way, addition of **C5-IQ-Btn** to avidin-HABA complex resulted to suppress the absorbance at 500 nm, indicating that **C5-IQ-Btn** has strong binding affinity toward avidin similar to biotin.

To evaluate the fluorescence characteristics, we measured the fluorescence intensity of 500 ng mL^{-1} avidin-FITC containing with 10 μM biotin, 10 μM **C5-IQ-Btn**, and the mixutre of 10 μM biotin and 10 μM **C5-IQ** in 25 mM phosphate buffer (pH 7.4). As shown in Figure 6A, an intense fluorescence emission of avidin-FITC in the presence of biotin was confirmed, whereas the fluorescence intensity of avidin-FITC containing **C5-IQ-Btn** was dramatically decreased. Avidin-FITC and **C5-IQ-Btn** are considered to form a complex each other due to high affinity of **C5-IQ-Btn** to avidin protein. Moreover, considering the strong fluorescence of avidin-FITC containing the mixture of biotin and **C5-IQ**, these fluorescence spectra clearly suggest that the fluorescence of avidin-FITC is quenched by spatially adjacent indolequinone moiety due to biotin conjugate.
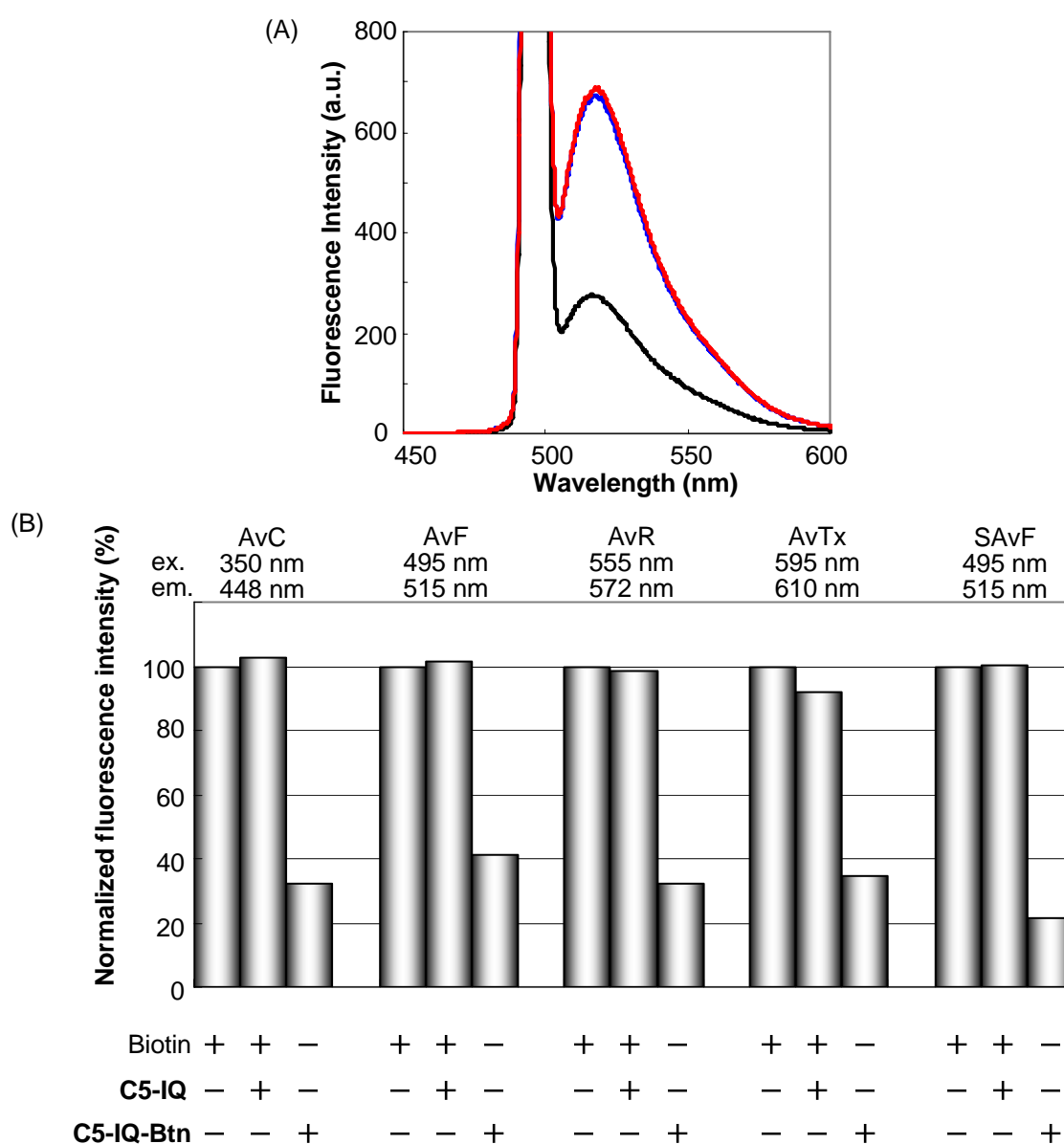
Figure 6. (A) Fluorescence spectra of 500 ng mL^{-1} avidin-FITC containing with 10 μM biotin (red line), 10 μM **C5-IQ-Btn** (black line), and the mixutre of 10 μM biotin and 10 μM **C5-IQ** (blue line) in 25 mM phosphate buffer (pH 7.4). The fluorescence spectra were measured with excitation at 495 nm. (B) The fluorescence intensities of fluorescent-labeled avidin chromophore; 7-amino-4-methylcoumarin-3-acetic acid-avidin (AvC, ex. 350 nm, em. 448 nm), FITC-avidin (AvF, ex. 495 nm, em. 515 nm), rhodamine-avidin (AvR, ex. 555 nm, em. 572 nm), Texas Red-avidin (AvTx, ex. 595 nm, em. 610 nm), and FITC-streptavidin (SAvF, ex. 495 nm, em. 515 nm). All spectra were normalized with the fluorescence intensity of each fluorescent-labeled avidin chromophore including biotin (left bar of each section). The fluorescence intensities were all suppressed by existing the **C5-IQ-Btn** (right bar of each section), whereas the strong fluorescence was observed in the case of each fluorescent-labeled avidin chromophore including biotin and **C5-IQ** (middle bar of each section).

To evaluate the versatility of these systems, we similarly investigated the fluorescence characteristics of other fluorescent-labeled avidin chromophore; 7-amino-4-methylcoumarin-3-acetic acid-avidin (AvC, $\lambda_{max(ex)}$ = 350 nm, $\lambda_{max(em)}$ = 448 nm), rhodamine-avidin (AvR, $\lambda_{max(ex)}$ = 555 nm, $\lambda_{max(em)}$ = 572 nm), Texas Red-avidin (AvTx, $\lambda_{max(ex)}$ = 595 nm, $\lambda_{max(em)}$ = 610 nm), and FITC-streptavidin (SAvF, $\lambda_{max(ex)}$ = 495 nm, $\lambda_{max(em)}$ = 515 nm). These fluorescence characteristics are summarized in Figure 6B. All spectra were normalized with the fluorescence intensity of each fluorescent-labeled avidin chromophore including biotin (left bar of each section). These fluorescence intensities were all suppressed by existing **C5-IQ-Btn** (right bar of each section), whereas the strong fluorescence was observed for the samples of each fluorescent-labeled avidin chromophore including biotin and **C5-IQ** (middle bar of each section). These results clearly suggest that indoelquinone derivatives can efficiently suppress the fluorescence of the adjacent chromophore in spite of the wide range of fluorescent maximum or the different structures between avidin and streptavidin. Thus, these systems incorporating **C5-IQ-Btn** into fluorescent-labeled avidin chromophore are expected to be widely used for many purposes and situations.

To evaluate the reductive characteristics of the avidin-FITC and **C5-IQ-Btn** complex (**AF-IQ-Btn**), we conducted an enzymatic reduction to **AF-IQ-Btn** under hypoxic or aerobic conditions. We added **C5-IQ-Btn** (final concentration; 1 μM) to avidin-FITC solution (final concentration; 500 ng mL^{-1}) containing cofactor β-NADPH (final concentration; 2 mM), and then treated the mixture with NADPH:cytochrome P450 reductase (final concentration; 22.7 μg mL^{-1}). After the enzymatic reduction, we measured the fluorescence intensity, normalized by the fluorescence of avidin-FITC (final concentration; 500 ng mL^{-1}) containing biotin (final concentration; 1 μM). As shown in Figure 7, the fluorescence intensity of avidin-FITC containing **C5-IQ-Btn** was lower than that of avidin-FITC coexisting with biotin as described above (compare entries 1 and 2). After the enzymatic reduction of **AF-IQ-Btn** under hypoxic conditions, the fluorescence intensity was increased (entry 3), indicating that indolequinone derivative is removed from **C5-IQ-Btn** *via* one-electron reduction by enzymatic reduction, thereby leading to restoration of fluorescence. In contrast, such an enhancement of fluorescence emission occurred to less extent

under aerobic conditions (entry 4). These results suggest that **C5-IQ-Btn** incorporated in the avidin-FITC complex is reduced by NADPH:cytochrome P450 reductase to release the indolequinone derivative *via* one-electron reduction under hypoxic conditions, whereas one-electron reduction for **C5-IQ-Btn** is suppressed by dissolved oxygen. In view of the hypoxia-specific fluorescence activity of **AF-IQ-Btn**, one-electron reduction of indolequinone derivatives could be a promising strategy to discriminate the hypoxic microenvironment. However, the **AF-IQ-Btn** system has drawbacks in high background. Our current study focuses on modification of more powerful quenchers, black hole quencher (BHQ), Au-nanoparticles or magnetic nanoparticles, at C-5 terminus.
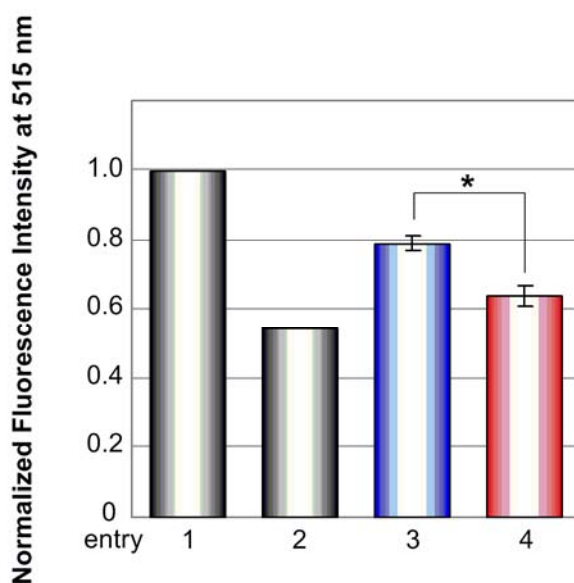

Figure 7. Relative fluorescence intensity normalized with the fluorescence of 500 ng mL^{-1} avidin-FITC at 515 nm (entry 1). Avidin-FITC containing with 1 μM **C5-IQ-Btn** (entry 2) in 25 mM phosphate buffer (pH 7.4) was treated by NADPH:cytochrome P450 reductase (22.7 μg mL^{-1}) and β-NADPH coenzyme (2 mM) at 37 °C under hypoxic (entry 3) and aerobic (entry 4) conditions. These fluorescence intensities were measured with excitation at 495 nm. Results are shown with the mean ± S.D. (n = 3) (* P < 0.01).

Conclusion

In this study, we have designed and synthesized the new hypoxic imaging probe based on an avidin-biotin complex incorporated with an indolequinone derivative. We conjugated biotin at a 3-position and C-5 linker at a 5-position of an indolequinone unit (**C5-IQ-Btn**). The cleavage between the indolequinone and biotin moieties of the synthesized **C5-IQ-Btn** was confirmed by X-radiolytic and enzymatic reduction in a hypoxia selective manner. The fluorescence of the avidin-FITC and **C5-IQ-Btn** complex (**AF-IQ-Btn**) was weak because of the quenching effect of the indolequinone derivative. In addition, **C5-IQ-Btn** could also suppress the fluorescence of other fluorescent-labeled avidin chromophore; 7-amino-4-methylcoumarin-3-acetic acid-avidin ($\lambda_{\max(ex)} = 350$ nm, $\lambda_{\max(em)} = 448$ nm), rhodamine-avidin ($\lambda_{\max(ex)} = 555$ nm, $\lambda_{\max(em)} = 572$ nm), Texas Red-avidin ($\lambda_{\max(ex)} = 595$ nm, $\lambda_{\max(em)} = 610$ nm), and FITC-streptavidin ($\lambda_{\max(ex)} = 495$ nm, $\lambda_{\max(em)} = 515$ nm). Thus, these systems incorporating **C5-IQ-Btn** into fluorescent-labeled avidin chromophore are expected to be versatility. The enhanced emission of **AF-IQ-Btn** reductively-activated under hypoxic conditions was greater than that of under aerobic conditions, indicating that indolequinone derivative is preferentially removed *via* one-electron reduction by NADPH:cytochrome P450 reductase to increase the AF fluorescence. The specific cleavage of indolequinone derivatives under hypoxic conditions could be a promising strategy to develop the hypoxia targeting probe. However, in order to establish the more sensitive probe for hypoxia, we need the modification to conjugate a more effective quencher at C-5 terminus.

Experimental Section

General Methods.

All reactions were carried out under a dry nitrogen atmosphere using freshly distilled solvents unless otherwise noted. Reagents were purchased from Aldrich, Wako pure chemical industries and Nacalai tesque, and used as received. NADPH:cytochrome P450 reductase and β-NADPH coenzyme were obtained from Oxford Biomedical Research and Oriental Yeast CO., respectively. Ultrapure water was obtained from YAMATO WR-600A. Precoated TLC (Merck silica gel 60 F_{254}) plates were used for monitoring the reactions. Column chromatography was carried out on Wakogel C-300 (Wako pure chemical industries). ^{1}H NMR spectra were measured with JEOL JMN-AL-300 (300 MHz) or JEOL JMN-AL-400 (400 MHz) spectrophotometers at ambient temperature. ^{13}C NMR spectra were measured with JEOL JMN-AL-300 (75.5 MHz) or JEOL JMN-AL-400 (100 MHz) spectrophotometers at ambient temperature. Coupling constants (J values) are reported in Hertz. The chemical shifts are expressed in ppm downfield from tetramethylsilane, using residual chloroform (δ = 7.24 in ^{1}H NMR, δ = 77.0 in ^{13}C NMR) and dimethylsulfoxide (δ = 2.49 in ^{1}HNMR, δ = 39.5 in ^{13}C NMR) as an internal standard. Multiplicity is designed as singlet (s), doublet (d), triplet (t), doublet-doublet (dd), or multiplet (m). FAB Mass spectra were recorded on JEOL JMS-SX102A spectrometer, using *m*-nitrobenzyl alcohol (NBA) matrix. A Rigaku RADIOFLEX-350 was used for X-irradiation. High-performance liquid chromatography (HPLC) was performed with Shimadzu LC-10AS system. Sample solutions were injected on a reversed phase column (Inertsil ODS-3, GL Science Inc., ϕ 4.6 × 150 mm). The 0.1 M triethylamine (TEA) 40 vol% acetonitrile/water solution containing acetic acid, pH 7.0 was delivered as mobile phase at a flow rate of 0.6 mL min^{-1} at 40 °C. The elution peaks were monitored at 290 nm wavelength. Fluorescent spectra were recorded on Shimadzu RF-5300PC spectrofluorophotometer at ambient temperature. UV spectra were recorded with a Jasco V-530 UV/Vis spectrometer at ambient temperature.

5-[5-(*tert*-Butyldimethylsilanyloxy)pentoxy]-1,2-dimethyl-1*H*-indole-3-carboxylic acid methyl ester (2)

To a solution of the alcohol **1** (14.5 g, 66 mmol) in DMF (200 mL) cooled in ice-water bath (0 °C) was added 50–72% sodium hydride in oil (2.71 g, 55–79 mmol) followed by stirring at same temperature. To the resultant mixture was added (5-bromopenthyl)-*tert*-butyldimethylsilane (31.2 g, 110 mmol) followed by stirring at room temperature for overnight. The reaction was quenched with saturated aqueous $NaHCO_3$ and extracted with EtOAc. The combined organic layer was washed with brine, dried over anhydrous $MgSO_4$, filtered, concentrated under reduced pressure. The residue was purified by flash column chromatography (silica gel, EtOAc:Hexane = 1:10) to give the title compound (10.6 g, 38% yield). A yellow oil; R_f = 0.74 (50% EtOAc-Hexane); ^1H NMR (400 MHz, $CDCl_3$) δ 7.55 (d, *J* = 2.4 Hz, 1H), 7.10 (d, *J* = 8.8 Hz, 1H), 6.80 (dd, *J* = 2.4, 8.9 Hz, 1H), 3.99 (t, *J* = 6.6 Hz, 2H), 3.86 (s, 3H), 3.60 (s, 3H), 3.59 (t, *J* = 6.6 Hz, 2H), 2.67 (s, 3H), 1.78 (m, 2H), 1.50 (m, 4H), 0.84 (s, 9H), 0 (s, 6H); ^{13}C NMR (100 MHz, $CDCl_3$) δ 166.6, 155.1, 145.3, 131.6, 127.3, 112.1, 109.6, 104.7, 103.4, 68.6, 63.1, 50.6, 32.6, 29.7, 29.2, 26.0, 22.4, 18.4, 12.0, −5.3; FABMS *m/z* 419 [M$^+$]; HRMS calcd. for $C_{23}H_{38}NO_4Si$ [(M + H)$^+$] 420.2565, found 420.2580.

5-(5-Hydroxypentoxy)-1,2-dimethyl-4-nitro-1*H*-indole-3-carboxylic acid methyl ester (3)

To a solution of the indole **2** (4.33 g, 10 mmol) and acetic acid (1.8 mL, 30 mmol) in CH_2Cl_2 (50 mL) cooled in ice-water bath (0 °C) was added 61% nitric acid (1.2 mL, 15 mmol) followed by stirring at room temperature for 4 h. The reaction was quenched with saturated aqueous $NaHCO_3$ and extracted with $CHCl_3$. The combined organic layer was washed brine, dried over $MgSO_4$, filtered, concentrated under reduced pressure. The residue was purified by flash column chromatography (silica gel, EtOAc:hexane = 4:1) to give the title compound (2.22 g, 63% yield). A brown solid; mp 83–87 °C; R_f = 0.09 (50% EtOAc-Hexane); ^1H NMR (400 MHz, DMSO-d_6) δ 7.73 (d, *J* = 9.0 Hz, 1H), 7.20 (d, *J* = 9.0 Hz, 1H), 4.35 (t, *J* = 5.1 Hz, 4.9 Hz, 1H), 4.09 (t, *J* = 6.3 Hz, 6.6 Hz, 2H), 3.76 (s, 3H), 3.63 (s, 3H), 3.38 (q, *J* = 6.1, 5.4, 6.1 Hz, 2H), 2.66 (s, 3H), 1.66 (m, *J* = 7.3, 6.8 Hz, 2H), 1.44–1.38 (m, 4H); ^{13}C NMR (100 MHz, DMSO-d_6) δ 164.0, 147.7, 145.5, 132.2,

116.7, 113.3, 109.5, 101.3, 101.1, 70.2, 60.6, 50.0, 32.0, 30.2, 28.5, 21.8, 11.7; FABMS *m/z* 350 [M$^+$]; HRMS calcd. for C$_{17}$H$_{23}$N$_2$O$_6$ [(M + H)$^+$] 351.1551, found 351.1554.

4-Amino-5-(5-hydroxypentoxy)-1,2-dimethyl-1*H*-indole-3-carboxylic acid methyl ester (4)

To a solution of the nitro compound **3** (2.21 g, 6.3 mmol) in EtOH (50 mL) were added Sn (3.75 g, 32 mmol) and 35% HCl (13 mL, 147 mmol). The reaction was refluxed with stirring at 80 °C for 2 h. The reaction was quenched with saturated aqueous NaHCO$_3$ and extracted with EtOAc. The combined organic layer was washed with brine, dried over anhydrous MgSO$_4$, filtered, concentrated under reduced pressure to give the title compound (1.91 g, 95% yield). An off-white solid; mp 103–105 °C; R$_f$ = 0.50 (80% EtOAc-Hexane); ^{1}H NMR (300 MHz, DMSO-*d*$_6$) δ 6.83 (d, *J* = 8.8 Hz, 1H), 6.59 (d, *J* = 8.6 Hz, 1H), 5.72 (bs, 2H), 4.35 (t, *J* = 5.1, 5.3 Hz, 1H), 3.89 (t, *J* = 6.6, 6.4 Hz, 2H), 3.80 (s, 3H), 3.58 (s, 3H), 3.41 (m, 2H), 2.60 (s, 3H), 1.72 (m, 2H), 1.48–1.45 (m, 4H); ^{13}C NMR (75.5 MHz, DMSO-*d*$_6$) δ 166.7, 144.1, 139.2, 133.6, 131.0, 113.5, 111.0, 102.9, 96.6, 69.8, 60.6, 51.0, 32.3, 29.8, 29.1, 22.2, 12.7; FABMS *m/z* 320 [M$^+$]; HRMS calcd. for C$_{17}$H$_{25}$N$_2$O$_4$ [(M + H)$^+$] 321.1809, found 321.1804.

4-Amino-5-[5-(*tert*-butyldimethylsilanyloxy)pentoxy]-1,2-dimethyl-1*H*-indole-3-carboxylic acid methyl ester (5)

To a solution of the alcohol **4** (4.0 g, 12.5 mmol) and imidazole (1.84 g, 27 mmol) in DMF (50 mL) cooled in ice-water bath (0 °C) was added *tert*-butyldimethylsilychloride (3.94 g, 26 mmol) followed by stirring at room temperature for 3.5 h. The reaction was quenched with saturated aqueous NaHCO$_3$ and extracted with EtOAc. The combined organic layer was washed with brine, dried over anhydrous MgSO$_4$, filtered, concentrated under reduced pressure. The residue was purified by flash column chromatography (silica gel, EtOAc:hexane = 1:4) to give the title compound (4.61 g, 85% yield). An off-white solid; mp 90–91 °C; R$_f$ = 0.91 (80% EtOAc-Hexane); ^{1}H NMR (300 MHz, DMSO-*d*$_6$) δ 6.80 (d, *J* = 8.6 Hz, 1H), 6.56 (d, *J* = 8.6 Hz, 1H), 5.68 (bs, 2H), 3.86 (m, 2H), 3.58 (s, 3H), 3.56 (m, 5H) 3.28 (s, 3H), 2.57 (s, 3H), 1.69 (m, 2H), 1.46 (m, 4H), 0.83

(s, 9H), 0.01 (s, 6H); ^{13}C NMR (75.5 MHz, DMSO-d_6), δ 166.7, 144.0, 139.2, 133.6, 131.0, 113.5, 111.0, 102.9, 96.6, 69.7, 62.4, 51.0, 32.1, 29.8, 29.0, 25.8, 22.0, 17.9, 12.7, −5.3; FABMS m/z 435 [(M + H)$^+$]; HRMS calcd. for $C_{23}H_{39}N_2O_4Si$ [(M + H)$^+$] 435.2674, found 435.2673.

{4-Amino-5-[5-(*tert*-butyldimethylsilanyloxy)pentoxy]-1,2-dimethyl-1*H*-indole-3-yl}methanol (6)

To a solution of the ester **5** (4.61 g, 11 mmol) in THF (50 mL) cooled in ice-water bath (0 °C) was added LAH (800 mg, 21 mmol) followed by stirring at the same temperature for 30 min. The reaction was quenched by ice-water. The reaction mixture was extracted with EtOAc. The combined organic layer was washed with brine, died over anhydrous MgSO$_4$, filtered, concentrated under reduced pressure. The given compound was immediately reacted for the next step without purification.

5-[5-(*tert*-Butyldimethylsilanyloxy)pentoxy]-3-hydroxymethyl-1,2-dimethyl-1*H*-indole-4,7-dione (7)

To a solution of the 4-aminoindole **6** (4.31 g, crude) and trioctylmethylammonium chloride (8.6 g, 21 mmol) in THF (22 mL) cooled in ice-water bath (0 °C) was added potassium nitrosodisulfonate (Fremy's salt) (7.18 g, 27 mmol) in aqueous sodium dihydrogenphosphate (0.3 M, 22 mL) followed by stirring at the same temperature for 20 min. The reaction was quenched saturated aqueous NaHCO$_3$, extracted with EtOAc. The combined organic layer was washed with brine, dried over anhydrous MgSO$_4$, filtered, concentrated under reduced pressure. The residue was purified by flash column chromatography (silica gel, EtOAc:hexane = 1:2) to give the title compound (3.52 g, 79% yield in 2 steps). A red oil; R$_f$ = 0.63 (80% EtOAc-Hexane); ^{1}H NMR (400 MHz, DMSO-d_6), δ 5.68 (s, 1H), 4.58 (d, J = 4.9 Hz, 1H), 4.54 (s, 2H), 3.88 (t, J = 6.3 Hz, 2H), 3.80 (s, 3H), 3.56 (t, J = 6.1, 5.9 Hz, 2H), 2.20 (s, 3H), 1.74–1.68 (m, 2H), 1.48-1.39 (m, 4H), 0.83 (s, 9H), 0 (s, 6H); ^{13}C NMR (100 MHz, DMSO-d_6) δ 177.5, 159.0, 154.7, 135.0, 126.0, 122.5, 120.4, 104.5, 69.4, 62.3, 54.4, 31.9, 31.8, 27.6, 25.8, 21.8, 17.9, 9.2, −5.3; FABMS m/z 421 [M$^+$]; HRMS calcd. for $C_{22}H_{36}NO_5Si$

[(M + H)$^+$] 422.2357, found 422.2354.

Indolequinone derivatives conjugated with biotin (8)

To a solution of the indolequinone **7** (1.73 g, 4.1 mmol) and biotin (2.03 g, 8.3 mmol) in DMF (23 mL) cooled in ice-water bath (0 °C) were added TATU (2.71 g, 8.4 mmol), DMAP (612 mg, 5 mmol), and DIPEA (1.44 mL, 8.2 mmol) followed by stirring at room temperature for overnight. The reaction was quenched with saturated aqueous NaHCO$_3$ and extracted with CHCl$_3$. The combined organic layer was washed with brine, dried over anhydrous MgSO$_4$, filtered, concentrated under reduced pressure. The residue was purified by flash column chromatography (silica gel, MeOH:CHCl$_3$ = 1:20) to give the title compound (2.48 g, 93% yield). An orange solid, mp 109–110 °C; R$_f$ = 0.54 (9% MeOH-CHCl$_3$); ^{1}H NMR (400 MHz, DMSO-d_6) δ 6.37 (s, 1H), 6.32 (s, 1H), 5.72 (s, 1H), 5.10 (s, 2H), 4.26 (t, J = 7.6, 5.4 Hz, 1H), 4.08 (m, 1H), 3.89 (t, J = 6.3 Hz, 2H), 3.81 (s, 3H), 3.81 (m, J = 5.6, 2.2, 3.9 Hz, 2H), 3.02 (m, 1H), 2.67 (dd, J = 12.4, 5.1 Hz, 1H), 2.53 (d, J = 12.4 Hz, 1H), 2.24–2.21 (m, 5H), 1.72–1.69 (m, 2H), 1.49–1.41 (m, 8H), 1.27 (m, 2H), 0.82 (s, 9H), 0 (s, 6H); ^{13}C NMR (100 MHz, DMSO-d_6) δ 178.3, 177.1, 172.7, 162.6, 158.5, 138.4, 128.1, 120.8, 114.8, 106.9, 69.1, 62.3, 61.0, 59.1, 56.0, 55.3, 40.1, 33.3, 32.1, 31.9, 27.91, 27.89, 27.6, 25.8, 24.6, 21.8, 17.9, 9.2, −5.3; FABMS m/z 648 [(M + H)$^+$]; HRMS calcd. for C$_{32}$H$_{50}$N$_3$O$_7$SSi [(M + H)$^+$] 648.3133, found 648.3135.

Preparation of C5-IQ-Btn

To a solution of the indolequinone derivative **8** (209 mg, 0.32 mmol) was added a solution of 10 mL AcOH:H$_2$O:THF (13:7:3) followed by stirring at room temperature for overnight. The reaction was quenched with saturated aqueous NaHCO$_3$ and extracted with CHCl$_3$. The combined organic layer was washed with brine, dried over anhydrous MgSO$_4$, filtered, concentrated under reduced pressure. The residue was purified by flash column chromatography (silica gel, MeOH:CHCl$_3$ = 1:10) to give the title compound (140 mg, 81% yield). An orange solid; mp 163–166 °C; R$_f$ = 0.23 (9% MeOH-CHCl$_3$); ^{1}H NMR (400 MHz, DMSO-d_6) δ 6.38 (s, 1H), 6.33 (s, 1H), 5.73 (s, 1H), 5.12 (s,

2H), 4.37 (t, J = 4.9, 5.4 Hz, 1H), 4.27 (t, J = 7.8, 5.1 Hz, 1H), 4.09 (m, 1H), 3.90 (t, J = 6.3, 6.6 Hz, 2H), 3.83 (s, 3H), 3.39 (m, 5.9, 5.4, 6.1 Hz, 2H), 3.04 (m, 1H), 2.79 (dd, J = 12.4, 5.1 Hz, 1H), 2.55 (d, J = 12.4 Hz, 1H), 2.26–2.23 (m, 5H), 1.73–1.69 (m, 2H), 1.54–1.39 (m, 8H), 1.29–1.28 (m, 2H); ^{13}C NMR (100 MHz, DMSO-d_6) δ 178.3, 177.2, 172.7, 162.6, 158.4, 138.5, 128.1, 120.8, 114.8, 106.9, 69.2, 61.0, 60.5, 59.1, 56.0, 55.3, 40.1, 33.2, 32.1, 32.0, 27.91, 27.89, 27.8, 24.5, 22.0, 9.1; FABMS m/z 534 [(M + H)$^+$]; HRMS calcd. for $C_{26}H_{36}N_3O_7S$ [(M + H)$^+$] 534.2268, found 534.2286.

Preparation of C5-IQ

To a solution of the indolequinone **7** (88 mg, 0.21 mmol) was added a solution of 3 mL AcOH:H$_2$O:THF (13:7:3) followed by stirring at room temperature overnight. The reaction was quenched with saturated aqueous NaHCO$_3$ and extracted with CHCl$_3$. The combined organic layer was washed with brine, dried over anhydrous MgSO$_4$, filtered, concentrated under reduced pressure. The residue was purified by flash column chromatography (silica gel, MeOH:CHCl$_3$ = 1:20) to give the title compound (58 mg, 90% yield). A red oil; R$_f$ = 0.49 (9% MeOH-CHCl$_3$); ^{1}H NMR (400 MHz, DMSO-d_6) δ 5.68 (s, 1H), 4.60 (t, J = 5.6 Hz, 1H), 4.54 (d, J = 5.6 Hz, 2H), 4.37 (t, J = 5.1 Hz, 1H), 3.89 (t, J = 6.9, 6.3 Hz, 2H), 3.80 (s, 3H), 3.39 (q, J = 6.1, 5.4, 6.1 Hz, 2H), 2.21 (s, 3H), 1.71 (m, 2H), 1.42 (m, 4H); ^{13}C NMR (100 MHz, DMSO-d_6) δ 178.2, 177.6, 158.4, 137.0, 127.5, 121.7, 120.4, 106.8, 69.1, 60.5, 53.2, 32.0, 31.9, 27.8, 22.0, 9.2; FABMS (matrix: NPOE) m/z 308 [(M + H)$^+$]; HRMS (matrix: NPOE) calcd. for $C_{16}H_{22}NO_5$ [(M + H)$^+$] 308.1492, found 308.1523.

Radiolytic reduction

To establish hypoxia, aqueous solutions of **C5-IQ-Btn** (100 μM) containing 30% 2-methyl-2-propanol were purged argon for 30 min and then irradiated in a sealed glass ampoule at ambient temperature with an X-ray source (5.0 Gy min^{-1}). After irradiation, aliquots were sampled at appropriate time intervals for analytical HPLC. A control air-saturated sample solution was irradiated and analyzed in a similar manner.

Bioreduction by NADPH:cytochrome P450 reductase.

To establish hypoxia, a solution of **C5-IQ-Btn** (final concentration: 500 μM) and β-NADPH (final concentration: 2mM) in 25 mM phosphate buffer (pH 7.4), which was preliminarily purged with argon for 30 min, were kept in anaerobic environmental glove box (0.1–0.4% O_2) for 3 h at ambient temperature. To the resulting solution, NADPH:cytochrome P450 reductase (final concentration: 22.7 μg mL^{-1}) was added and incubated for 5 min at 37 °C. For analytical HPLC, the reaction mixture was diluted 10% by acetonitrile/milli Q (1:1). As a control sample, air-saturated buffer was used and analyzed in a similar manner.

Fluorescence spectrophotometry

Fluorescence spectra of fluorescent-labeled avidin chromophore (AvC, 1.5 μg mL^{-1}; AvF, 0.5 μg mL^{-1}; AvR, 2.5 μg mL^{-1}; AvTx, 1.3 μg mL^{-1}; SAvF, 1.0 μg mL^{-1}) containing with 10 μM biotin, 10 μM **C5-IQ-Btn**, and the mixutre of 10 μM biotin and 10 μM **C5-IQ** in 25 mM phosphate buffer (pH 7.4) were taken on a SHIMADZU RF-5300PC fluorescence spectrophotometry.

Bioreductive activation of the complex of avidin-FITC and C5-IQ-Btn (AF-IQ-Btn)

A mixture of β-NADPH, avidin-FITC, and **C5-IQ-Btn** (final concentration: 2 mM, 500 ng mL^{-1} and 1 μM, respectively) in 25 mM phosphate buffer (pH 7.4), which was preliminarily purged with argon for 30 min, were kept in anaerobic environmental glove box (0.1–0.9% O_2) for 3 h at ambient temperature to establish hypoxia. To the resulting solution was added NADPH:cytochrome P450 reductase (final concentration: 22.7 μg mL^{-1}) and incubated for 5 min at 37 °C. After the reaction, aliquots were sampled and diluted 10% by 25 mM phosphate buffer (pH 7.4) for quenching the reaction and measuring the fluorescent spectra. Fluorescence spectra were taken with excitation at 495 nm and detected at 515 nm. As a control sample, air-saturated buffer was used and analyzed in a similar manner. All fluorescence intensities were normalized with intensity at 515 nm of avidin-FITC (final concentration; 500 ng mL^{-1}) containing biotin (final concentration; 1 μM).

References and Notes

(1) (a) Semenza, G. L. *Annu. Rev. Cell. Dev. Biol.* **1999**, *15*, 551–578. (b) Ke, Q.; Costa, M. *Mol. Pharmacol.* **2006**, *70*, 5, 1469–1480. (c) Li, X. Y.; Takasaki, C.; Satoh, Y.; Kimura, S.; Yasumoto, K.; Sogawa, K. *J. Biochem.* **2008**, *144*, 555–561. (d) Downie, B. R.; Sanchez, A.; Knotgen, H.; Contreras-Jurado, C.; Gymnopoulos, M.; Weber, C.; Stuhmer, W.; Pardo, L. A. *J. Biol. Chem.* **2008**, *283*, 52, 36234–36240. (e) Masson, N.; Ratcliffe, P. J. *J. Cell Sci.* **2003**, *116*, 3041–3049.

(2) (a) Manabe, T.; Katayama, T.; Sato, N.; Gomi, F.; Hitomi, J.; Yanagita, T.; Kudo, T.; Honda, A.; Mori, Y.; Matsuzaki, S.; Imaizumi, K.; Meyeda, A.; Tohyama, M. *Cell Death Differ.* **2003**, *10*, 698–708. (b) Sato, N.; Hori, O.; Yamaguchi, A.; Lambert, J.; Chartier-Harlin, M.; Robinson, P. A.; Delacourte, A.; Schmidt, A. M.; Furuyama, T.; Imaizumi, K.; Tohyama, M.; Takagi, T. *J. Neurochem.* **1999**, *72*, 2498–2505. (c) Higashide, S.; Morikawa, K.; Okumura, M.; Kondo, S.; Oagata, M.; Murakami, T.; Yamashita, A.; Kanemoto, S.; Manabe, T.; Imaizumi, K. *J. Neurochem.* **2004**, *91*, 1191–1198. (d) Paschen, W.; Mengesdorf, T. *Phrmacol. Therapeut.* **2005**, *108*, 362–375.

(3) (a) Haunstetter, A.; Izumo, S. *Circ. Res.* **1998**, *82*, 1111–1129. (b) Chen, C.; Yu, W.; Fu, Y.; Wang, X.; Li, J.; Wang, W. *Biochem. Biophys. Res. Commun.* **2009**, *378*, 389–393. (c) Bonavita, F.; Stefanelli, C.; Giordano, E.; Columbaro, M.; Facchini, A.; Bonafe, F.; Caldarera, C. M.; Guarnieri, C. *FEBS. lett.* **2003**, *536*, 85–91.

(4) Vaupel, P.; Kallinowski, F.; Okunieff, P. *Cancer Res.* **1989**, *49*, 6449–6465.

(5) (a) Durand, R. E.; Raleigh, J. A. *Cancer Res.* **1998**, *58*, 3547–3550. (b) Raleigh, J. A.; Calkins-Adams, D. P.; Rinker, L. H.; Ballenger, C. A.; Weissler, M. C.; Fowler, W. C.; Novotny, J. D. B.; Varia, M. A. *Cancer Res.* **1998**, *58*, 3765–3768. (c) Samoszuk, M. K.; Walter, J.; Mechetner, E. *J. Histochem. Cytochem.* **2004**, *52*, 6, 837–839. (d) Hofer, S. O. P.; Mitchell, G. M.; Penington, A. J.; Morrison, W. A.; RomeoMeeuw, R.; Keramidaris, E.; Palmer, J.; Knight, K. R. *Br. J. Plast. Surg.* **2005**, *58*, 1104–1114.

(6) (a) Liu, J.; Qu, R.; Ogura, M.; Shibata, T.; Harada, H.; Hiraoka, M. *J. Radiat. Res.* **2005**, *46*,

93–102. (b) Harada, H.; Kizaka-Kondoh, S.; Itasaka, S.; Shibuya, K.; Morinibu, A.; Shinomiya, K.; Hiraoaka, M. *Biochem. Biophys. Res. Commun.* **2007**, *360*, 791–796.

(7)　Everett, S. A.; Swann, E.; Naylor, M. A.; Stratford, M. R. L.; Patel, K. B.; Tian, N.; Newman, R. G.; Vojnovic, B.; Moody, C. J.; Wardman, P. *Biochem. Pharmacol.* **2002**, *63*, 1629–1639.

(8)　Newsome, J. J.; Swann, E.; Hassani, M.; Bray, K. C.; Slawin, A. M. Z.; Beall, H. D.; Moody, C. J. *Org. Biomol. Chem.* **2007**, *5*, 1629–1640.

(9)　(a) Tanabe, K.; Hirata, N.; Harada, H.; Hiraoka, M.; Nishimoto, S. *ChemBioChem* **2008**, *9*, 426–432. (b) Tanabe, K.; Zhang, Z.; Ito, T.; Hatta, H.; Nishimoto, S. *Org. Biomol. Chem.* **2007**, *23*, 5, 3721–3876.

(10)　Patrick, J. B.; Saunders, E. K. *Tetrahedron Lett.* **1979**, *20*, 4009–4012.

(11)　Radiolysis of diluted aqueous solution at around pH 7.0 produces primary water radicals such as oxidizing hydroxyl radicals ($^\bullet$OH), reducing hydrated electrons (e_{aq}^-) and reducing hydrogen atoms ($^\bullet$H) with the *G* values of $G(^\bullet OH) = 280$ nmol J^{-1}, $G(e_{aq}^-) = 280$ nmol J^{-1}, and $G(^\bullet H) = 60$ nmol J^{-1}, respectively.

(12)　The number of molecules produced or changed per 1 J of radiation energy absorbed by the reaction system.

(13)　Tanabe, K.; Makimura, Y.; Tachi, Y.; Imagawa-Sato, A.; Nishimoto, S. *Bioorg. Med. Chem. Lett.* **2005**, *15*, 2321–2324.

(14)　Zhang, Z.; Tanabe, K.; Hatta, H.; Nishimoto, S. *Org. Biomol. Chem.* **2005**, *3*, 1905–1910.

(15)　Yu, L. J.; Matias, J.; Scudiero, D. A.; Hite, K. M.; Monks, A.; Sausville, E. A.; Waxman, D. J. *Drug Metab. Dispos.* **2001**, *29*, 304–312.

(16)　(a) Green, N. M. *Biochem. J.* **1965**, *94*, 23c–24c. (b) Morpurgo, M.; Hofstetter, H.; Bayer, E. A.; Wilchek, M. *J. Am. Chem. Soc.* **1998**, *120*, 12734–12739.

Chapter 3

Development of a Novel Hypoxia Detectable Probe:
Synthesis and Properties of a Complex
of Avidin-FITC and Magnetic Nanoparticle
Conjugated with a Hypoxia-Response Indolequinone Derivative

Abstract: We have developed and characterized a new class of functional magnetic nanoparticles (MNPs) possessing a hypoxia-responsible indolequinone-biotin derivative (**C5-IQ-Btn**) and fluorescein isothiocyanate (FITC) labeled avidin (AF) complex (**AF-IQ-Btn@MNP**) for hypoxia-specific imaging systems. The indolequinone derivative conjugated with biotin at 3-position and C-5 linker at 5-positin (**C5-IQ-Btn**) was preliminarily synthesized as reported in chapter 2. After the activation of the hydroxyl group at C-5 terminus of **C5-IQ-Btn** with *p*-nitrophenyl chloroformate (PNP-Cl), **C5-IQ-Btn** was incorporated onto MNPs (**IQ-Btn@MNP**). The amount of indolequinone-biotin units modified on an MNP was estimated to be 9.3–14.7 molecules by using HABA analysis. The AF fluorescence was decreased by existing **IQ-Btn@MNP**, suggesting that AF formed a complex with **IQ-Btn@MNP** (**AF-IQ-Btn@MNP**), and thus AF fluorescence was suppressed by the adjacent quencher units of indolequinone and MNP. Upon enzymatic reduction under hypoxic conditions, weak fluorescent **AF-IQ-Btn@MNP** was turned to be enhanced emission around 515 nm assigned AF chromophore, whereas an enhancement in fluorescence emission was suppressed upon aerobic treatment. With these reaction characteristics in a hypoxia-selective manner, **AF-IQ-Btn@MNP** might be applicable as a fluorescent imaging system for detecting tumor hypoxic microenvironments.

Introduction

A physiological hypoxia has been well known to be generated in solid tumor tissues due to an imbalance of rapid cell proliferation and neoangiogenesis.[1] Tumor hypoxia has been associated with the malignant phenotype of cancer cells and resistance to cancer therapies,[2] thus there has been increasing demand for hypoxia-specific molecular probes as useful indicators for a cancer diagnosis.

Indolequinone derivatives have been identified as quenchers for the adjacent fluorescent molecules[3] and removable substitutes *via* one-electron reduction under hypoxic conditions.[4] In view of these characteristics, we have developed a new class of hypoxia imaging probe consists of an indolequinone derivative and avidin-FITC chromophore. We conjugated with biotin at a 3-position and hydroxyalkyl group at a 5-position of indolequinone moiety (**C5-IQ-Btn**). Upon the X-radiolytic or enzymatic reduction, **C5-IQ-Btn** was activated to release biotin moieties from indolequinone units *via* one-electron reduction in a hypoxia selective manner, as were observed in the cases of indolequinone derivatives previously reported (IQ-Cou, IQ-FdUrd and CPT4 prodrugs).[5] **C5-IQ-Btn** was confirmed to retain the high affinity to an avidin protein, and thereby form a complex with avidin-FITC chromophore (**AF-IQ-Btn**). The **AF-IQ-Btn** complex showed a weak fluorescence because of the quenching function of the indolequinone unit, whereas upon the treatment by NADPH:cytochrome P450 reductase under hypoxic conditions, an enhanced fluorescence was observed due to release of the indolequinone unit *via* one-electron reduction. These hypoxia-selective fluorescent characteristics of the complex might be applicable as a fluorescent probe for the imaging of disease-relevant hypoxia; however, the **AF-IQ-Btn** system had some drawbacks in high background. To overcome this problem, we have newly designed the **AF-IQ-Btn** complex incorporated onto magnetic nanoparticles.

Magnetic nanoparticles (MNPs) attract the attention in magnetic resonance imaging (MRI) contrast agents, and are widely functionalized.[6] MNPs have been reported to have the following characteristics; first, MNPs accumulate in solid tumor tissues by the enhanced permeability and

retention (EPR) effect;[7] second, MNPs quench the adjacent fluorescence molecules mainly due to the strong absorption cross section of MNPs and to a lesser extent to the dynamic and static quenching of the fluorescence;[8] third, MNPs are readily introduced with various functional groups by conjugating at aminosilane coupling agents modified on MNPs.[9] These characteristics stimulated us to incorporate the **AF-IQ-Btn** complex onto MNPs. The introduction of **AF-IQ-Btn** onto MNPs is expected to have various benefits; (1) high-selectivity to solid tumor tissues by the EPR effect; (2) many optionalities changing multicolor fluorescent-labeled avidin chromophore for many purposes and situations; (3) low fluorescence background due to the combination of indolequinone and MNPs quenching; (4) high-contrast derived from a high molar ratio of modified **C5-IQ-Btn** molecules to an MNP; (5) dual-imaging based on fluorescence and MRI. In view of these benefits, we designed and incorporated the **C5-IQ-Btn** onto MNPs (**IQ-Btn@MNP**). The fluorescence of avidin-FITC chromophore (AF) was confirmed to be decreased by existing **IQ-Btn@MNP**, suggesting that AF formed a complex with **IQ-Btn@MNP** (**AF-IQ-Btn@MNP**), and thus AF fluorescence was suppressed by the adjacent quencher units of indolequinone and MNP. Upon enzymatic reduction under hypoxic conditions, weak fluorescent **AF-IQ-Btn@MNP** was observed to be enhanced emission around 515 nm assigned AF chromophore, whereas an enhancement in fluorescence emission was suppressed upon aerobic treatment. In light of these reaction characteristics in a hypoxia-selective manner, **AF-IQ-Btn@MNP** might be applicable as a fluorescent probe for detecting tumor hypoxic microenvironments.
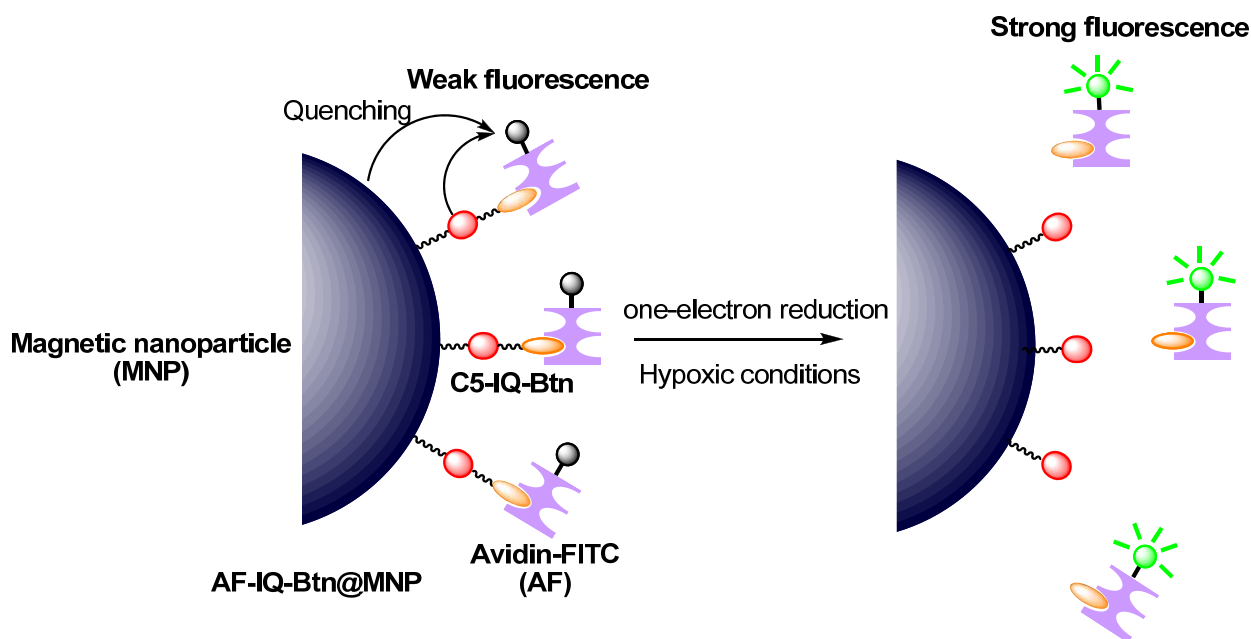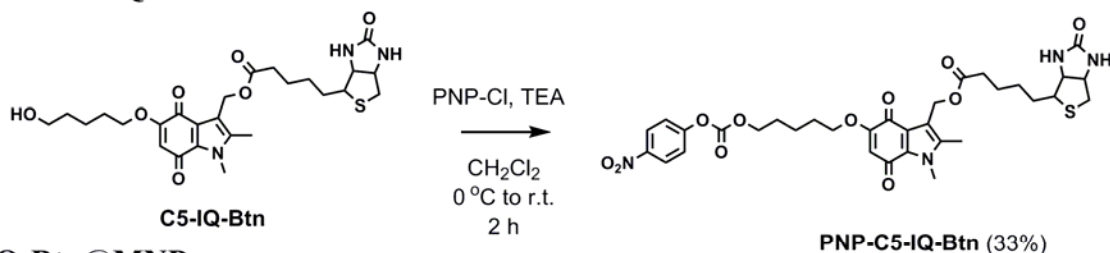
Figure1. Schematic illustration of an **AF-IQ-Btn@MNP** system including avidin-FITC (AF) and a magnetic nanoparticle (MNP) conjugated with indolequinone-biotin linkers (**C5-IQ-Btn**). The **AF-IQ-Btn@MNP** system is activated to enhance the AF fluorescence due to the cleavage between indolequinone and biotin moieties *via* one-electron reduction under hypoxic conditions.

Results and discussion

Fe$_3$O$_4$ magnetic nanoparticles (MNPs), modified with a 3-aminopropyltrimethoxysilane coupling agent, was synthesized as described.[10] The indolequinone derivative conjugated with biotin at a 3-position and C-5 linker at a 5-positin (**C5-IQ-Btn**) was synthesized as reported in chapter 2. To introduce indolequinone-biotin unit (**C5-IQ-Btn**) onto MNPs, the hydroxyl group at the C-5 terminus of **C5-IQ-Btn** was activated with *p*-nitrophenyl chloroformate (PNP-Cl). The activated compounds, **PNP-C5-IQ-Btn**, conjugated with amino groups on the surface of MNPs, to give a new class of MNPs possessing a hypoxia-responsible indolequinone-biotin derivative (named **IQ-Btn@MNP**).
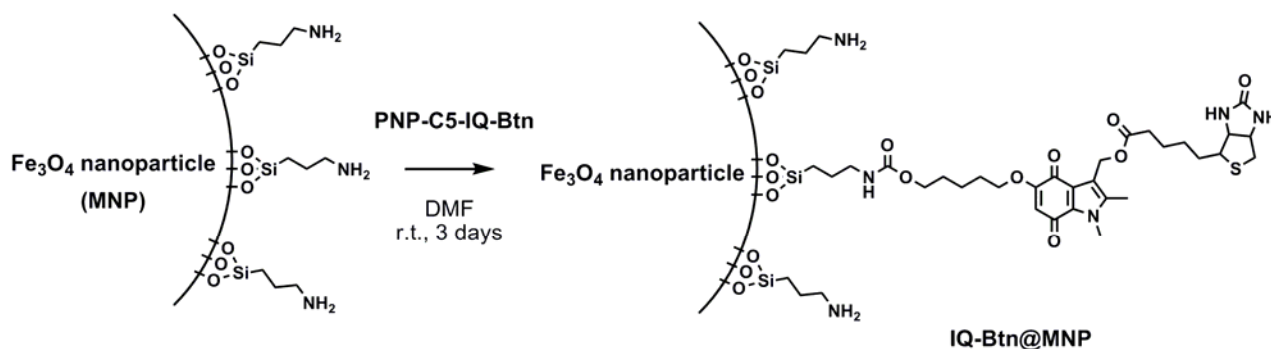
Scheme 1. Synthesis of (A) **PNP-C5-IQ-Btn** and (B) **IQ-Btn@MNP**. (A) **C5-IQ-Btn**, *p*-nitrophenyl chloroformate (PNP-Cl), triethylamine (TEA), CH₂Cl₂, 0 °C to room temperature, 2 h, (33%) (B) **PNP-C5-IQ-Btn**, DMF, room temperature, 3 days.

In order to confirm the incorporating of **C5-IQ-Btn** moieties on the surface of MNPs, FT-IR measurements were performed. Figure 2 shows the FT-IR spectra of unmodified MNP and **IQ-Btn@MNP**. The strong band at around 600 cm^{-1} was characteristics of the Fe-O stretching vibrations related to the magnetic core,[11] and the band at around 1000 cm^{-1} corresponds to Si-O stretching vibration.[11] In the case of **IQ-Btn@MNP**, the bands of 1600–1700 cm^{-1} were attributed to C=O stretching vibration,[12] indicating that **C5-IQ-Btn** units are modified on the surface of MNPs. Figure 3 shows TEM images of unmodified MNP and **IQ-Btn@MNP**. The average diameters of the unmodified MNP and **IQ-Btn@MNP** were 9.3 ± 1.8 and 9.5 ± 2.3 nm as measured by the TEM images, respectively. The obtained **IQ-Btn@MNP** was well-dispersed in DMF.
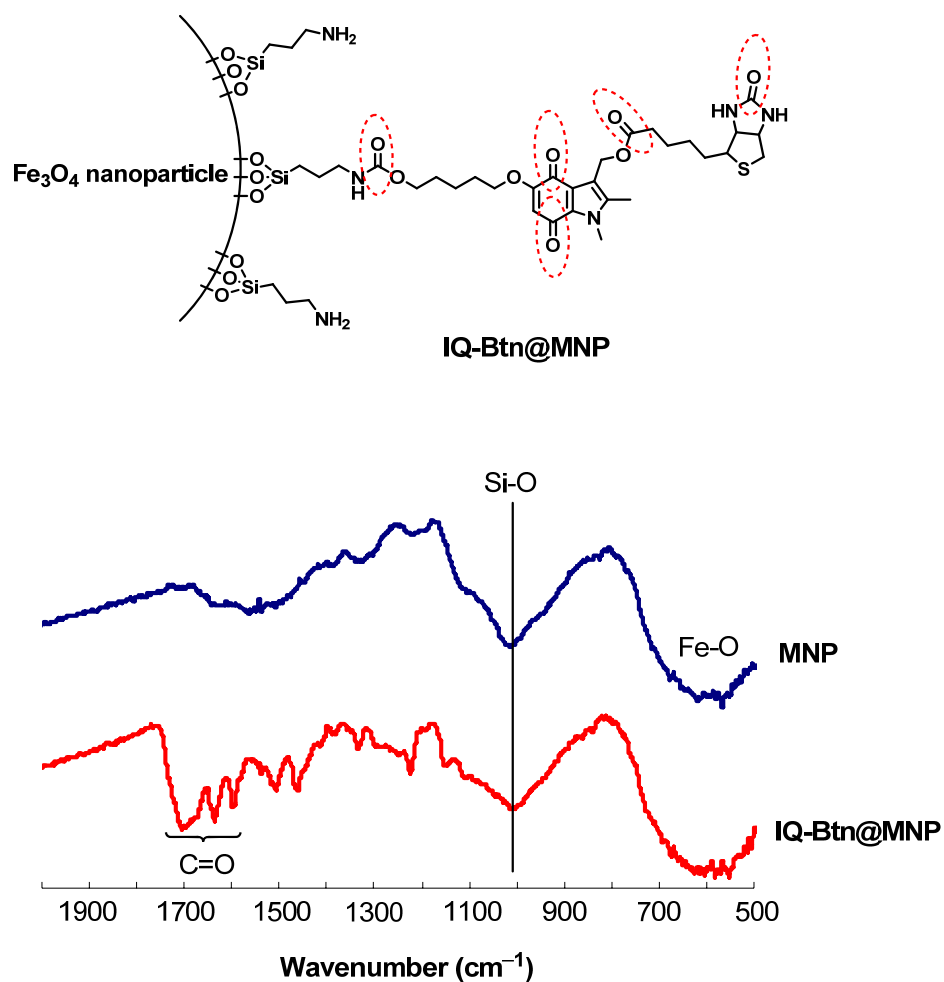
Figure 2. Comparison of FT-IR spectra of MNP (blue line) and **IQ-Btn@MNP** (red line). The strong band at around 600 cm^{-1} is characteristics of the Fe-O stretching vibrations related to the magnetic core, and the band at around 1000 cm^{-1} corresponds to Si-O stretching vibration. In the case of **IQ-Btn@MNP**, the bands of 1600–1700 cm^{-1} are attributed to C=O stretching vibration
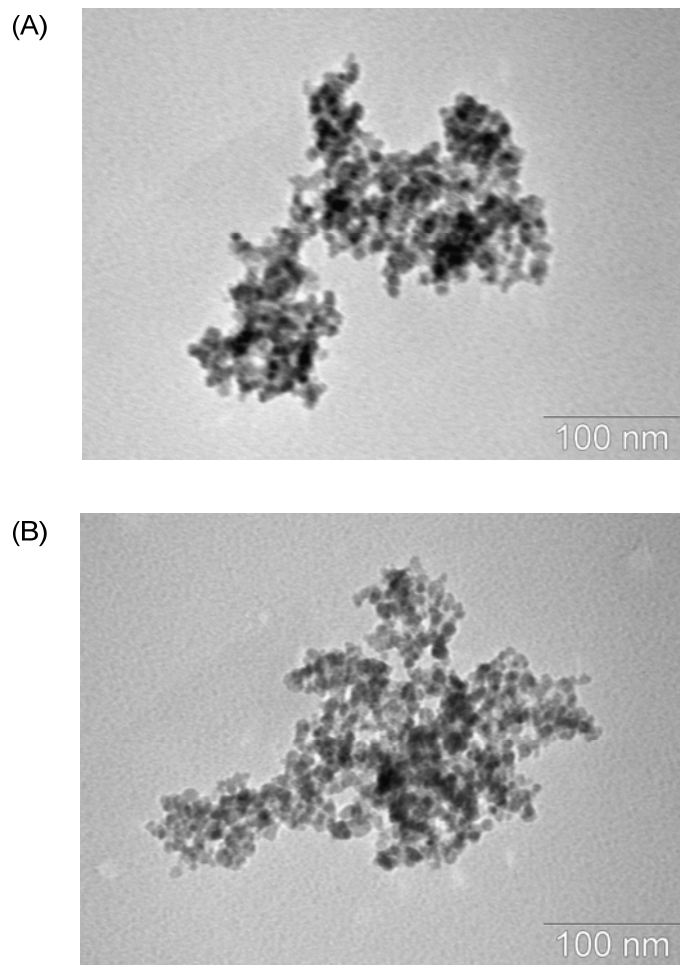
Figure 3. TEM images of (A) MNP (Avg. 9.3 nm, S.D. 1.8 nm) and (B) **IQ-Btn@MNP** (Avg. 9.5 nm, S.D. 2.3 nm)

To estimate the amount of the modified **C5-IQ-Btn** units on the surface of an MNP, we treated **IQ-Btn@MNP** with sodium dithionite[13] ($Na_2S_2O_4$) to release biotin molecules from the indolequinone derivatives, and quantified the released biotin by using 4-hydoroxyazobenzene-2'-carboxylic acid (HABA) analysis.[14] Indolequinone derivatives undergo two-electron reduction by $Na_2S_2O_4$ aqueous solution under basic conditions,[13] resulting that 3-substituted indolequinone derivatives are completely cleaved at the 3-position bond to release the substituents. Thus, the amount of **C5-IQ-Btn** modified on an MNP is evaluated by quantifying the released biotin with HABA analysis. It has been known that HABA forms a complex with avidin to enhance an absorbance at 500 nm. The interaction between HABA and avidin is comparatively weak, thus HABA incorporated into avidin is readily replaced with biotin, resulting that the intense absorbance at 500 nm is perceptively decreased. Therefore, the difference of the absorbance at 500 nm reflects quantitatively the amount of including biotin molecules.[14] Using these characteristics of $Na_2S_2O_4$ and HABA, the amount of **C5-IQ-Btn** units onto an MNP can be evaluated. To a solution of **IQ-Btn@MNP** (23.3 ± 0.9 mg in DMF) was added $Na_2S_2O_4$ solution (10 mM in 25 mM phosphate buffer pH 11.8) followed by addition of PBS to quench the reaction, and centrifugation to gather the supernatant solution, which includes the released biotin molecules. As a control sample, a treatment solution processed MNP (22.2 ± 1.3 mg in DMF) with $Na_2S_2O_4$ was prepared in a similar manner. To a solution of avidin including HABA was added the treatment solution processed **IQ-Btn@MNP** or MNP with $Na_2S_2O_4$, and the absorbance at 500 nm of these mixtures was monitored. Figure 4 shows the absorbance at 500 nm and a calibration curve evaluated by the HABA analysis. The absorbance including the treatment solution processed **IQ-Btn@MNP** with $Na_2S_2O_4$ was suppressed as same as the sample including biotin, whereas in the case of MNP, the absorbance at 500 nm didn't change as same as avidin-HABA sample without biotin. These results suggest that **C5-IQ-Btn** units are undoubtedly modified on the surface of MNPs. By fitting the calibration curve, the released biotin was determined as to 7.9 ± 1.5 μM, and thereby the number of biotin (**C5-IQ-Btn**) modified on MNPs (23.3 ± 0.9 mg) was calculated to be 197.5 ± 37.5 nmol. A molecular weight of an MNP is calculated to 1.4×10^6 with an average grain diameter of

IQ-Btn@MNP; (about 9.5 nm, Figure 3) and a density of Fe_3O_4 (5.1 g cm^{-3}), thus the number of MNP in 23.3 ± 0.9 mg is evaluated 16.6 ± 0.6 nmol. In view of these estimates, the number of **C5-IQ-Btn** conjugated on an MNP is determined to 9.3–14.7 molecules.
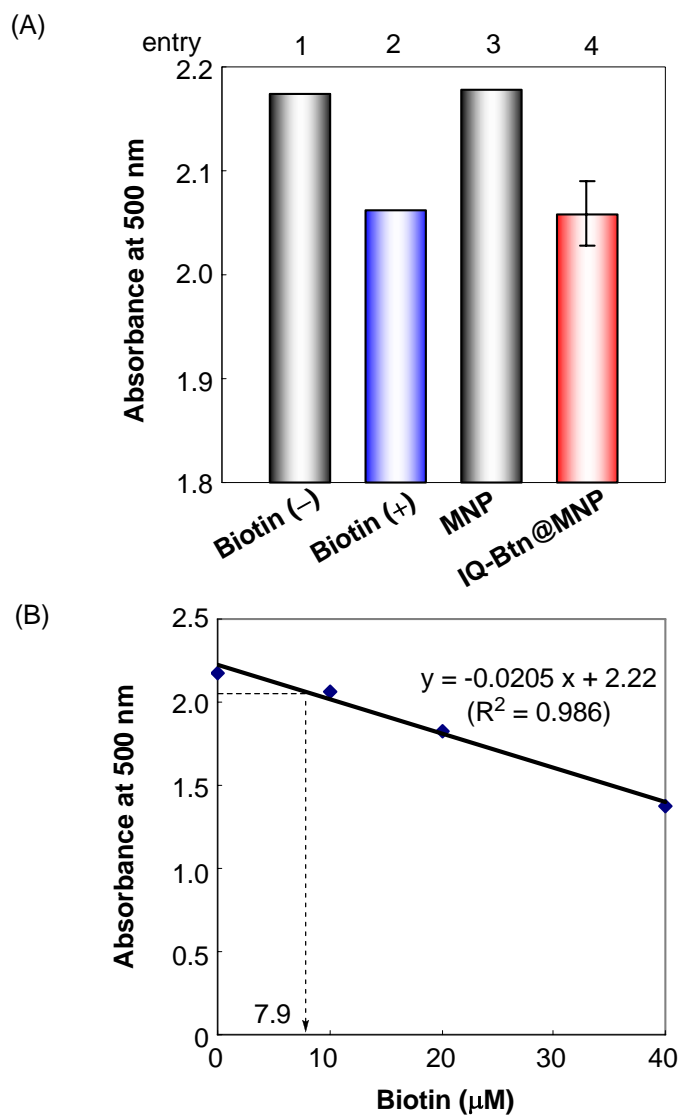

Figure 4. (A) Comparison of the absorbance at 500 nm of avidin-HABA complex (entry 1) containing biotin (entry 2) or the treatment solution of MNP (entry 3) and **IQ-Btn@MNP** (entry 4) processed with $Na_2S_2O_4$ agent. Result is shown with the mean ± S.D. (n = 3). (B) Calibration curve evaluated by the HABA analysis.

Figure 5 shows fluorescence characteristics of avidin-FITC (AF) with excitation at 495 nm in the presence of biotin, MNP or **IQ-Btn@MNP**. The intense fluorescence of AF including biotin was slightly decreased by existing MNP. In contrast, the AF fluorescence was dramatically

73

decreased by addition of **IQ-Btn@MNP**. These results suggest that AF units are contiguous to the quenchers of the indolequinone moieties and MNPs due to the modified biotin molecules on the MNPs, thus the AF fluorescence is suppressed compared to unmodified MNP.
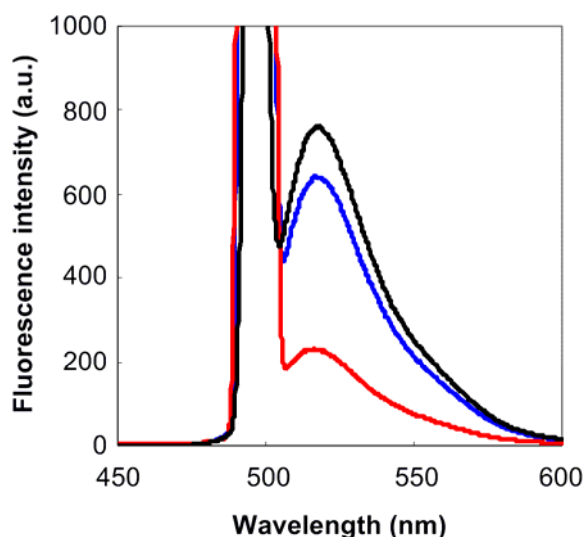

Figure 5. Fluorescence spectra of 500 ng mL^{-1} avidin-FITC containing with 72.2 nM biotin (black line), **IQ-Btn@MNP** (233 μg mL^{-1}, red line), and the mixutre of 72.2 nM biotin and MNP (222 μg mL^{-1}, blue line) in 25 mM phosphate buffer (pH 7.4).

We then similarly investigated the fluorescence characteristics using other fluorescent-labeled avidin chromophore; 7-amino-4-methylcoumarin-3-acetic acid-avidin (AvC, $\lambda_{max(ex)}$ = 350 nm, $\lambda_{max(em)}$ = 448 nm), rhodamine-avidin (AvR, $\lambda_{max(ex)}$ = 555 nm, $\lambda_{max(em)}$ = 572 nm), Texas Red-avidin (AvTx, $\lambda_{max(ex)}$ = 595 nm, $\lambda_{max(em)}$ = 610 nm), and FITC-streptavidin (SAvF, $\lambda_{max(ex)}$ = 495 nm, $\lambda_{max(em)}$ = 515 nm). These fluorescence characteristics are summarized in Figure 6. All spectra were normalized with the fluorescence intensity of each fluorescent-labeled avidin chromophore including biotin (left bar of each section). These fluorescence intensities were all suppressed by existing **IQ-Btn@MNP** (right bar of each section), whereas the strong fluorescence was observed for the samples of each fluorescent-labeled avidin chromophore including biotin and unmodified MNP (middle bar of each section). These results clearly suggest that fluorescent-labeled

avidin forms a complex with the qunechers of indoelquinone derivatives and MNPs, thus the fluorescence of these chromophores is supressed.
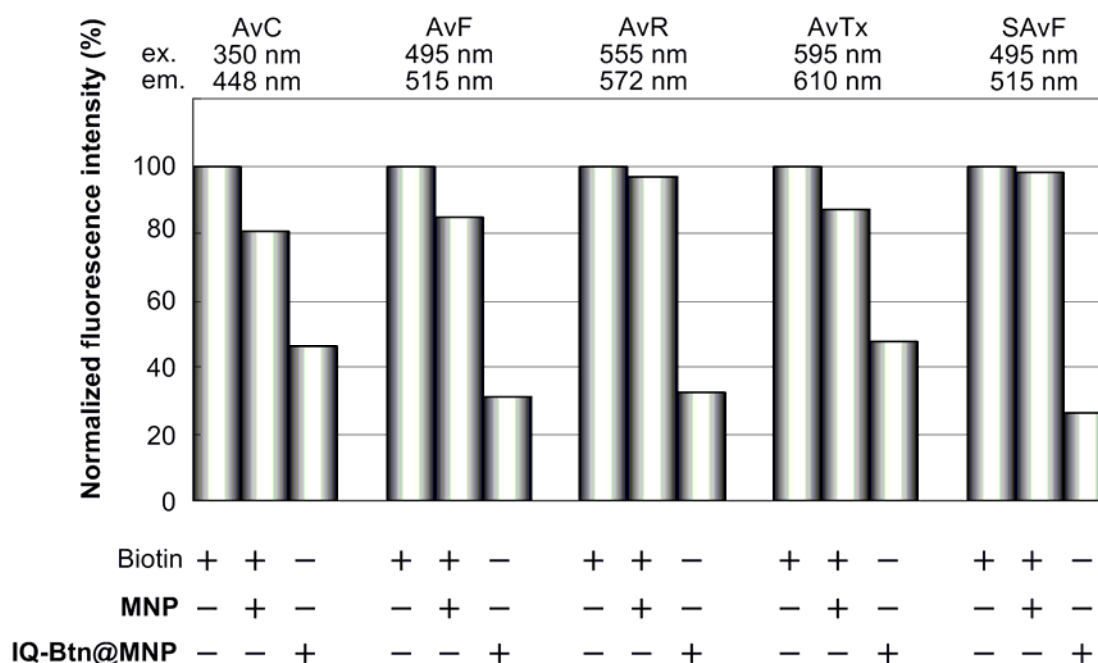

Figure 6. The fluorescence intensities of fluorescent-labeled avidin chromophore; 7-amino-4-methylcoumarin-3-acetic acid-avidin (AvC, ex. 350 nm, em. 448 nm), FITC-avidin (AvF, ex. 495 nm, em. 515 nm), rhodamine-avidin (AvR, ex. 555 nm, em. 572 nm), Texas Red-avidin (AvTx, ex. 595 nm, em. 610 nm), and FITC-streptavidin (SAvF, ex. 495 nm, em. 515 nm). All spectra were normalized with the fluorescence intensity of each fluorescent-labeled avidin chromophore including biotin (left bar of each section). The fluorescence intensities were all suppressed by existing the **IQ-Btn@MNP** (right bar of each section), whereas the strong fluorescence was observed in the case of each fluorescent-labeled avidin chromophore including biotin and MNP (middle bar of each section).

To assess the fluorescence activity of **IQ-Btn@MNP** including avidin-FITC (**AF-IQ-Btn@MNP**), we treated the **AF-IQ-Btn@MNP** with NADPH:cytochrome P450 redcutase under hypoxic or aerobic conditions, and evaluated fluorescence intensities at 515 nm. NADPH:cytochrome P450 redcutase has been known to be expressed in many patological tissues, and induce one-electron reduction to indolequinone derivatives.[15] We conducted the enzymatic reduction of **AF-IQ-Btn@MNP** under hypoxic or aerobic conditions. After the reaction for 5 min at 37 °C, aliquots were sampled and diluted 10% by 25 mM phosphate buffer (pH 7.4) to quench the reaction, and then fluorescent spectra were measured (excitation: 495 nm, detection: 515 nm).

The fluorescence intensities at 515 nm were normalized with the intensity of non-treatment sample. Figure 7 summarized the fluorescence intensities of hypoxic, aerobic or non-treatment samples. As shown in Figure 7, an enhanced fluorescence was observed in hypoxic treatment, while enhancement of fluorescent intensity was suppressed in aerobic treatment. These results clearly indicate that indolequinone units underwent one-electron reduction to lead to the cleavage between indolequinone and biotin units upon enzymatic treatment under hypoxic conditions. Consequently, fluorescence of AF was restored due to separation of the quencher units of indolequinone moieties and MNPs. In contrast, upon the aerobic treatment, the indolequinone can not be removed from **AF-IQ-Btn@MNP** due to the inhibition of one-electron reduction by intrinsic oxygen molecules. Thus, an enhanced emission of AF is still suppressed by the adjacent quencher units of indolequinone moieties and MNPs. In light of these hypoxia-selective reaction characteristics, **AF-IQ-Btn@MNP** might be applicable as a fluorescent probe for detecting tumor hypoxic microenvironments.
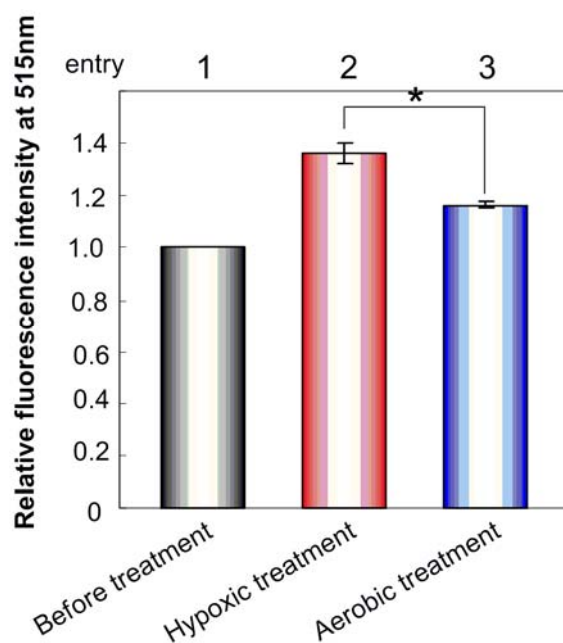

Figure 7. Relative fluorescence intensity normalized with the fluorescence intensity at 515 nm of 500 ng mL^{-1} avidin-FITC containing **IQ-Btn@MNP** (465 μg mL^{-1}, entry 1). Avidin-FITC containing with **IQ-Btn@MNP** in 25 mM phosphate buffer (pH 7.4) was treated by NADPH:cytochrome P450 reductase (22.7 μg mL^{-1}) existing with β-NADPH coenzyme (2 mM) at 37 °C under hypoxic (entry 2) and aerobic (entry 3) conditions. These fluorescence intensities were measured with excitation at 495 nm. Results are shown with the mean ± S.D. (n = 3) (* P < 0.01).

In this study, we have developed a new class of functional magnetic nanoparticles (MNPs) possessing a hypoxia-responsible indolequinone-biotin derivative (**C5-IQ-Btn**) and avidin-FITC (AF) complex (**AF-IQ-Btn@MNP**). **AF-IQ-Btn@MNP** was confirmed to enhance the fluorescence upon enzymatic treatment under hypoxic conditions, whereas the increase of the fluorescence was suppressed upon aerobic treatment. Therefore, **AF-IQ-Btn@MNP** could be a promising candidate as the imaging probe for the detection of hypoxic microenvironments. However, **AF-IQ-Btn@MNP** has some drawbacks: First, the AF fluorescence was not completely quenched by indolequinone and MNP units, therefore high background fluorescence would harm an actual application. Although indolequinone derivatives or magnetic nanoparticles respectively diminish the fluorescence of adjacent chromophore,[8] as shown in Figure 5, the fluorescence of **AF-IQ-Btn@MNP** was higher than expected. These results imply that the binding affinity of **C5-IQ-Btn** units for avidin proteins is weakened by the adjacent MNP units. Second, **AF-IQ-Btn@MNP** showed a low-reactivity for enzymatic reduction. As shown in Figure 5 and Figure 7, the enhanced emission of the **AF-IQ-Btn@MNP** after the enzymatic treatment under hypoxic conditions couldn't be completely recovered. The **C5-IQ-Btn** units are sufficiently reacted with NADPH:cytochrome P450 reductase for 5 min, therefore the low-reactivity for enzymatic reduction is attributed to a steric hindrance due to the macromolecules of avidin and MNP units. To overcome these problems, **AF-IQ-Btn@MNP** needs to be modified as incorporation of longer linkers between AF and MNP units.

Conclusion

In summary, we have designed and created a new class of functional magnetic nanoparticles (MNP) linked with hypoxia-responsible indolequinone-biotin derivative (**C5-IQ-Btn**) and avidin-FITC (AF) complex (**AF-IQ-Btn@MNP**). The amount of **C5-IQ-Btn** molecules modified on an MNP was confirmed to be 9.3–14.7 molecules by HABA analysis. The AF fluorescence was decreased in the presence of MNP modified with **C5-IQ-Btn** (**IQ-Btn@MNP**), indicating that AF formed a complex with **IQ-Btn@MNP** (**AF-IQ-Btn@MNP**), and thus AF fluorescence was suppressed by the adjacent quencher units of indolequinone derivatives and MNPs. **AF-IQ-Btn@MNP** showed enhanced emission upon enzymatic reduction under hypoxic conditions, whereas an enhancement in fluorescence emission was suppressed upon aerobic treatment. In view of these reaction characteristics in a hypoxia-selective manner, **AF-IQ-Btn@MNP** is a promising candidate as a hypoxia-specific imaging probe. However, this probe has some drawbacks in high background and low fluorescence reactivity due to the low binding affinity and the steric hindrance between AF and MNP units. Our current study focuses on modification of longer linkers between the macromolecules of AF and MNP units, and moreover, incorporation of Au-nanoparticles, multicolored quantum dots, or some functional proteins possessing avidin unit, instead of the combination of MNP and avidin-FITC.

Experimental Section

General Methods.

All reactions were carried out under a dry nitrogen atmosphere using freshly distilled solvents unless otherwise noted. Reagents were purchased from Aldrich, Wako pure chemical industries and Nacalai tesque, and used as received. NADPH:cytochrome P450 reductase and β-NADPH coenzyme were obtained from Oxford Biomedical Research and Oriental Yeast CO., respectively. Ultrapure water was obtained from YAMATO WR-600A. Precoated TLC (Merck silica gel 60 F_{254}) plates were used for monitoring the reactions. Column chromatography was carried out on Wakogel C-300 (Wako pure chemical industries). ^{1}H NMR spectra were measured with JEOL JMN-AL-400 (400 MHz) spectrophotometers at ambient temperature. ^{13}C NMR spectra were measured with JEOL JMN-AL-400 (100 MHz) spectrophotometers at ambient temperature. Coupling constants (J values) are reported in Hertz. The chemical shifts are expressed in ppm downfield from tetramethylsilane, using residual dimethylsulfoxide (DMOSO-d_6, δ = 2.49 in ^{1}HNMR, δ = 39.5 in ^{13}C NMR) as an internal standard. Multiplicity is designed as singlet (s), doublet (d), triplet (t), doublet-doublet (dd), or multiplet (m). FAB Mass spectra were recorded on JEOL JMS-SX102A spectrometer, using NBA matrix. Fluorescent spectra were recorded on Shimadzu RF-5300PC spectrofluorophotometer at ambient temperature. UV spectra were recorded with a Jasco V-530 UV/Vis spectrometer at ambient temperature. FT-IR spectra were recorded on a Shimadzu IR Prestage-21 infrared spectrophotometer using a KBr disk dispersed with the powdered sample. Transmission electron microscopy (TEM) measurements were performed using a JOEL JEM-100SX operated at 100 kV electron beam accelerating voltage. One drop of the sample solution was deposited onto a copper grid and the excess of the droplet was blotted off the grids with filter paper; then the sample was dried under ambient conditions.

Preparation of PNP-C5-IQ-Btn

To a solution of the **C5-IQ-Btn** as described in chapter 2 (93 mg, 0.174 mmol) in CH_2Cl_2 (5 mL)

cooled in ice-water bath (0 °C) were added *p*-nitrophenyl chloroformate (PNP-Cl, 211 mg, 1.047 mmol) and triethylamine (TEA, 144 μL, 1.035 mmol) followed by stirring at 0 °C to room temperature for 2 h. After the reaction, the resultant mixture was evaporated to remove the solvent. The residue was purified by flash column chromatography (silica gel, MeOH:CHCl$_3$ = 1:20) to give the title compound (40 mg, 33% yield). An orange oil; R_f = 0.31 (9% MeOH-CHCl$_3$); ^{1}H NMR (400 MHz, DMSO-d_6) δ 8.29 (d, 9.3 Hz, 2H), 7.55 (d, 9.3 Hz, 2H), 6.38 (s, 1H), 6.33 (s, 1H), 5.75 (s, 1H), 5.12 (s, 2H), 4.27 (t, 6.3 Hz, total 3H (2H overlapped with 1H)), 4.09 (t, 5.1 Hz, 1H), 3.94 (t, 6.3Hz, 2H), 3.83 (s, 3H), 3.04 (m, 1H), 2.79 (dd, 12.4 Hz, 4.9 Hz, 1H), 2.55 (d, 12.4 Hz, 1H), 2.23 (m, 5H), 1.78–1.73 (m, 4H), 1.52–1.27 (m, 8H); ^{13}C NMR (100 MHz, DMSO-d_6) δ 178.3, 177.1, 172.7, 162.6, 158.4, 155.3, 152.0, 145.1, 138.5, 128.1, 125.3, 122.6, 120.8, 114.8, 107.0, 79.1, 69.0, 61.0, 59.1, 56.0, 55.3, 40.1, 33.2, 32.1, 27.90, 27.87, 27.5, 27.4, 24.5, 21.7, 9.1; FABMS *m/z* 699 [(M + H)$^+$]; HRMS calcd. for C$_{33}$H$_{39}$N$_4$O$_{11}$S [(M + H)$^+$] 699.2331, found 699.2335.

Preparation of iron oxide magnetic nanoparticles (MNP)

Fe$_3$O$_4$ magnetic nanoparticles were prepared as reported.[10]

Preparation of IQ-Btn@MNP

To a precipitate of MNP (32 mg) was added **PNP-C5-IQ-Btn** (16 mg, 0.023 mmol) in DMF (16 mL) followed by stirring at room temperature for 3 days. After the reaction, the resultant mixture was centrifuged (6200 rpm, 30 min) to remove the solvent. Subsequently, the residue was washed by DMF and re-centrifuged (6200rpm, 30 min) to remove the solvent. This washing treatment was repeated as 7 times. After that, the residual MNP sample was dispersed in DMF (46.5 ± 1.7 mg mL^{-1}), and reserved or used for the experimental protocols. As a control sample, MNP (44.4 ± 2.5 mg mL^{-1}) without **PNP-C5-IQ-Btn** was prepared in a similar manner.

HABA analysis for quantitative determination of biotin modified of MNP

To a solution of 500 μL **IQ-Btn@MNP** (46.5 ± 1.7 mg mL^{-1} in DMF) was added 300 μL Na$_2$S$_2$O$_4$

solution (10 mM in 25 mM phosphate buffer pH 11.8) followed by vortex, adding PBS (200 μL) to quench the reaction, and centrifugation (6200 rpm, 30 min) to remove and gather the solvent, which includes a released biotin. This protocol was repeated twice. The gathered solvent was scaled up to 5 mL with PBS. As a control sample, a treatment solution processed MNP with $Na_2S_2O_4$ was prepared in a similar manner. To a solution of avidin (final concentration; 10 μM) including HABA (final concentration; 1.5 mM) was added the treatment solution processed **IQ-Btn@MNP** or MNP with $Na_2S_2O_4$ (20 μL picked up from 5 mL solution, respectively). The total volume of these mixtures was scaled up and integrated to 100 μL (resulting that the treatment solution was diluted by 20%). Subsequently, the absorbance at 500 nm of these mixtures was monitored by UV/Vis spectrometer.

A calibration curve was determined by the monitoring the change of the absorbance at 500 nm in adding biotin (10, 20, 30, 40 μM) to a solution of avidin (final concentration; 10 μM) including HABA (final concentration; 1.5 mM). Amount of released biotin was quantified by using the linear fit ($y = -0.0205 x + 2.22$, $R^2 = 0.986$; y: the absorbance at 500 nm, x: the concentration of biotin).

Fluorescence spectrophotometry

Fluorescence spectra of fluorescent-labeled avidin chromophores (AvC, 1.5 μg mL^{-1}; AvF, 0.5 μg mL^{-1}; AvR, 2.5 μg mL^{-1}; AvTx, 1.3 μg mL^{-1}; SAvF, 1.0 μg mL^{-1}) were taken in the presence of biotin (216.6 nM; 72.2 nM; 361.0 nM; 179.0 nM; 176.0 nM), **IQ-Btn@MNP** (233 μg mL^{-1}), and the mixutre of biotin and MNP (222 μg mL^{-1}), respectively. These biotin concentrations were adjusted to be ten times concentration of each fluorescent-labeled avidin chromophore.

Bioreductive activation of AF-IQ-Btn@MNP

A mixture of β-NADPH, avidin-FITC and **IQ-Btn@MNP** (final concentration: 2 mM, 500 ng mL^{-1} and 465 μg mL^{-1}, respectively) in 25 mM phosphate buffer (pH 7.4), which was preliminarily purged with argon for 30 min, were kept in anaerobic environmental glove box for 2 h at ambient temperature to establish hypoxia. To the resulting solution was added NADPH:cytochrome P450

reductase (final concentration: 22.7 μg mL^{-1}) and incubated for 5 min at 37 °C. After the reaction, aliquots were sampled and diluted 10% by 25 mM phosphate buffer (pH 7.4) for quenching the reaction and measuring the fluorescent spectra. Fluorescence spectra were taken with excitation at 495 nm and detected at 515 nm. As a control sample, air-saturated buffer was used and analyzed in a similar manner. All fluorescence intensities were normalized with intensity at 515 nm of avidin-FITC (final concentration; 500 ng mL^{-1}) containing **IQ-Btn@MNP** (final concentration; 465 μg mL^{-1}).

References and Notes

(1)   Vaupel, P.; Kallinowski, F.; Okunieff, P. *Cancer Res.* **1989**, *49*, 6449–6465.

(2)   (a) Kondoh-Kizaka., S; Inoue, M.; Harada, H.; Hiraoka, M. *Cancer Sci.* **2003**, *94*, 12, 1021–1028. (b) Harris, A. L. *Nat. Rev. Cancer.* **2002**, *2*, 38–47.

(3)   Everett, S. A.; Swann, E.; Naylor, M. A.; Stratford, M. R. L.; Patel, K. B.; Tian, N.; Newman, R. G.; Vojnovic, B.; Moody, C. J.; Wardman, P. *Biochem. Pharmacol.* **2002**, *63*, 1629–1639.

(4)   Newsome, J. J.; Swann, E.; Hassani, M.; Bray, K. C.; Slawin, A. M. Z.; Beall, H. D.; Moody, C. J. *Org. Biomol. Chem.* **2007**, *5*, 1629–1640.

(5)   (a) Tanabe, K.; Hirata, N.; Harada, H.; Hiraoka, M.; Nishimoto, S. *ChemBioChem.* **2008**, *9*, 426–432. (b) Tanabe, K.; Zhang, Z.; Ito, T.; Hatta, H.; Nishimoto, S. *Org. Biomol. Chem.* **2007**, *23*, 3721–3876. (c) Tanabe, K.; Makimura, Y.; Tachi, Y.; Imagawa-Sato, A.; Nishimoto, S. *Bioorg. Med. Chem. Lett.* **2005**, *15*, 2321–2324. (d) Zhang, Z.; Tanabe, K.; Hatta, H.; Nishimoto, S. *Org. Biomol. Chem.* **2005**, *3*, 1905–1910.

(6)   (a) Polito, L.; Colombo, M.; Monti, D.; Melato, S.; Caneva, E.; Prosperi, D. *J. Am. Chem. Soc.* **2008**, *130*, 12712–12724. (b) Yoon, T.; Kim, J. S.; Kim, B. G.; Yu, K. N.; Cho, M.; Lee, J. *Angew. Chem. Int. Ed.* **2005**, *44*, 1068–1071. (c) Zhao, L.; Wu, R.; Han, G.; Zhou, H.; Ren, L.; Tian, R.; Zou, H. *J. Am. Soc. Spectrom.* **2008**, *19*, 1176–1186. (d) Josephson, L.; Tung, C.; Moore, A.; Weissleder, R. *Bioconjugate Chem.* **1999**, *10*, 2, 186–191. (e) Babic, M.; Horak, D.; Trchova, M.; Jendelova, P.; Glogarova, K.; Lesny, P.; Herynek, V.; Hajek, M.; Sykova, E. *Bioconjugate Chem.* **2008**, *19*, 3, 740–750. (f) Barnett, B. P.; Arepally, A.; Karmarkar, P. V.; Qian, D.; Gilson, W. D.; Walczak, P.; Howland, V.; Lawler, L.; Lauzon, C.; Stuber, M.; Kraitchman, D. L.; Bulte, J. W. M. *Nat. Med.* **2007**, *13*, 8, 986–991.

(7)   (a) Matsumura, Y.; Maeda, H. *Cancer Res.* **1986**, *46*, 6387–6392. (b) Iyer, A. K.; Khaled, G.; Fang, J.; Maeda, H. *Drug Discovery Today* **2006**, *11*, 812–818.

(8)   (a) Li, L.; Choo, E. S. G.; Liu, Z.; Ding, J.; Xue, J. *Chem. Phys. Lett.* **2008**, *461*, 114–117. (b) Mandal, S. K.; Lequeux, N.; Rotenberg, B.; Tramier, M.; Fattaccioli, J.; Bibette, J.; Dubertret, B. *Langmuir* **2005**, *21*, 4175–4179.

(9)   Shen, X.; Fang, X.; Zhou, Y.; Liang, H. *Chem. Lett.* **2004**, *33*, 11, 1468–1469.

(10)   (a) Naka, K.; Narita, A.; Tanaka, H.; Chujo, Y.; Morita, M.; Inubushi, T.; Nishimura, I.; Hiruta, J.; Shibayama, H.; Koga, M.; Ishibashi, S.; Seki, J.; Kondoh-Kizaka., S.; Hiraoka, M. *Polym. Adv. Technol.* **2008**, *19*, 1421–1429. (b) Narita, A.; Naka, K.; Chujo, Y. *Colloids and Surface, A.* **2009**, *336*, 46–56.

(11)   (a) Bruce, I. L.; Sen, T. *Langmuir* **2005**, *21*, 7029–7035. (b) Ma, M.; Zhang, Y.; Yu, W.; Shen, H.; Zhang, H.; Gu, N. *Colloids and Surface, A.* **2003**, *212*, 219–226.

(12)   Itoh, S.; Takada, N.; Ando, T.; Haranou, S.; Huang, X.; Uenoyama, Y.; Ohshiro, Y.; Komatsu, M.; Fukuzumi, S. *J. Org. Chem.* **1997**, *62*, 5898–5907.

(13)   (a) Hernick, M.; Borch, R. F. *J. Med. Chem.* **2003**, *46*, 148–154. (b) Hernick, M.; Flader, C.; Borch, R. F. *J. Med. Chem.* **2002**, *45*, 3540–3548.

(14)   (a) Green, N. M. *Biochem. J.* **1965**, *94*, 23c–24c. (b) Morpurgo, M.; Hofstetter, H.; Bayer, E. A.; Wilchek, M. *J. Am. Chem. Soc.* **1998**, *120*, 12734–12739.

(15)   Yu, L. J.; Matias, J.; Scudiero, D. A.; Hite, K. M.; Monks, A.; Sausville, E. A.; Waxman, D. J. *Drug Metab. Dispos.* **2001**, *29*, 304–312.

Chapter 4

Radiolytic Activation of a Cytarabine Prodrug
Possessing a 2-Oxoalkyl Group:
One-Electron Reduction and Cytotoxicity Characteristics

Abstract: An anti-tumour agent of cytarabine (**ara-C**) was conjugated with a 2-oxopropyl group at the N(4) position to obtain a radiation-activated prodrug (**oxo-ara-C**) that targeted hypoxic tumour tissues with selective cytotoxicity. The parent anti-tumour agent, **ara-C**, was confirmed to be released from **oxo-ara-C** *via* one-electron reduction upon hypoxic X-ray treatment. The prodrug **oxo-ara-C** had dramatically reduced cytotoxicity against human lung adenocarcinoma A549 cells relative to **ara-C** because of the effect of 2-oxopropyl substituent. In contrast, X-ray treatment of hypoxic A549 cells containing **oxo-ara-C** enhanced the cytotoxic effect, indicating that toxic **ara-C** was preferentially released in hypoxic cells *via* radiolytic one-electron reduction by hydrated electrons (e_{aq}^-).

Introduction

Cytarabine (1-β-*D*-arabinofuranosyl-cytosine; **ara-C**) synthesized by Walwick and coworkers is one of a family of antimetabolites.[1] This deoxycytidine analog undergoes phosphorylation by intrinsic kinases, and is subsequently incorporated into DNA during chain elongation mediated by polymerase, thereby resulting in the inhibition of DNA replication and elongation.[2] Because of its highly cytotoxic effect, **ara-C** has been widely used as an antineoplastic and antiviral agent. However, **ara-C** has drawbacks in clinical applications: typically, a high dose of **ara-C** causes serious side effects, including encephalopathy and cerebellar dysfunction.[3] Therefore, there is a need for giving a target-specific feature to **ara-C** that would allow it to discriminate between tumour and normal cells. In view of the hypoxic microenvironment specific to tumours (generated from an imbalance between supply and consumption of oxygen[4]), we have attempted to exploit a new class of anti-tumour prodrugs that target the hypoxic microenvironment, resulting in a selective anti-tumour effect.[5]

We have thus far identified a series of 2-oxoalkyl groups that act as effective substituents for conjugation to nucleic acid derivatives, which are removable by X-ray treatment under hypoxic conditions in aqueous solution.[6] An activation mechanism has been proposed by which the 2-oxoalkyl group undergoes one-electron reduction by hydrated electrons (e_{aq}^-)[7] generated *via* radiolysis of water to form the corresponding π^* anion radical, followed by thermal activation into the σ^* anion radical, which is readily hydrolyzed to release the 2-oxoalkyl group.[8] We have applied these characteristics of the 2-oxoalkyl group to develop two prodrugs of anti-tumour agents, 1-(2'-oxopropyl)-5-fluorouracil and 2'-deoxy-5-fluoro-3-(2'-oxoalkyl)uridine, which are activated to release 5-fluorouracil (5-FU) and 5-fluoro-2'-deoxyuridine (5-FdUrd), respectively, upon hypoxic X-ray treatment.[6]

In this study, we designed an **ara-C** derivative possessing a 2-oxopropyl group at the N(4) position (**oxo-ara-C**) to obtain a novel radiation-activated prodrug. We performed radiolytic one-electron reduction of **oxo-ara-C** and evaluated its cytotoxic effect under hypoxic conditions.

The 2-oxopropyl group was readily removed from **oxo-ara-C** upon hypoxic X-ray treatment. Analysis of cell viability using an SF assay revealed that **oxo-ara-C** released the toxic parent **ara-C** *via* one-electron reduction when irradiated with X-rays under hypoxic conditions, thereby resulting in cytotoxic effects.

Results and discussion

The synthesis of **oxo-ara-C** is outlined in Scheme 1. The triazole group of **1**[9] was substituted with 1-amino-2,2-dimethoxypropane[10] to give the acetal derivative **2**. Hydrolysis of **2** furnished the desired **oxo-ara-C**. A control compound **3** lacking a carbonyl group at the N(4) position was prepared by the coupling of **1** with propylamine.
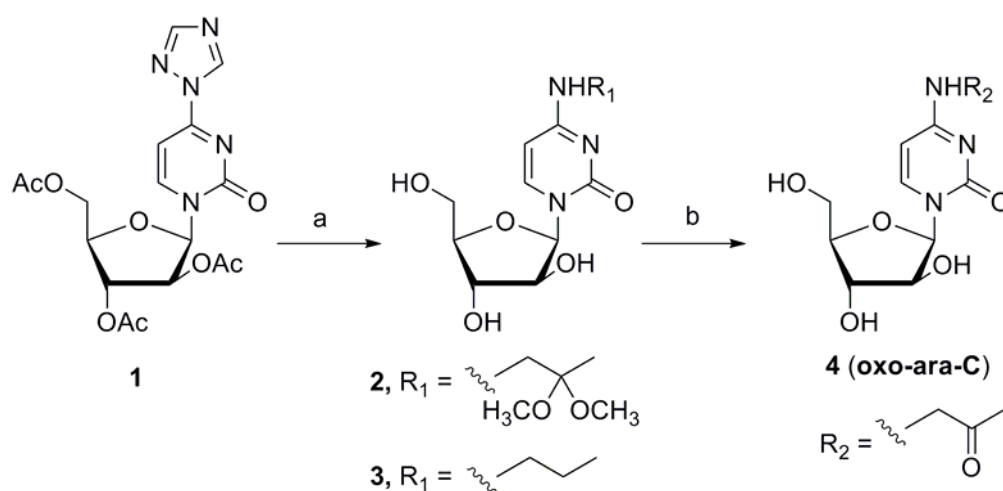
Scheme 1. Reagents and conditions: (a) 1-amino-2,2-dimethoxypropane, dioxane, 80 °C, 9.5 h (for **2**, 52%); propylamine, ethanol, room temperature, 4.5 h (for **3**, 71%); (b) **2**, oxalic acid, THF, room temperature, 5 h (44%).

We examined the efficiency of radiolytic one-electron reduction of **oxo-ara-C** for controlled release of **ara-C** in an argon-purged aqueous solution containing 2-methyl-2-propanol (10 mM) as the scavenger of oxidizing hydroxyl radicals ($^\bullet$OH).[7,11] Under these radiolysis conditions, reducing hydrated electrons (e_{aq}^-) were generated as the major active species. Figure 1 shows a representative reaction profile analyzed by HPLC of the radiolytic one-electron reduction of **oxo-ara-C** by the e_{aq}^- under hypoxic conditions. The appearance of a single new peak in Figure 1 was attributed to the formation of the parent **ara-C**, as confirmed by the overlapped injection of authentic samples in the HPLC analysis. The *G* values[12] were 151 nmol J^{-1} for the decomposition of **oxo-ara-C** and 69 nmol J^{-1} for the formation of the corresponding **ara-C**; thus, 46% of the decomposed **oxo-ara-C** was converted to **ara-C** upon hypoxic X-ray treatment. In contrast, the radiolytic decomposition of **oxo-ara-C** was dramatically suppressed under aerobic conditions; the *G* values were 27 nmol J^{-1} for the decomposition of **oxo-ara-C** and 4 nmol J^{-1} for the formation of the corresponding **ara-C**. These results indicate that **oxo-ara-C** was activated to release **ara-C** in a hypoxia-selective manner, as was observed in the case of the 5-FU and 5-FdUrd prodrugs possessing 2-oxoalkyl groups.[6,11]

To confirm the mechanistic validity of one-electron reduction of **oxo-ara-C** by e_{aq}^-, we conducted a control experiment in which **oxo-ara-C** was irradiated in an aqueous solution purged with nitrous oxide (N_2O)[13] gas, which efficiently captures the reducing species of e_{aq}^- to produce oxidizing species $^\bullet$OH. As shown in Table 1, the formation of **ara-C** was suppressed to greater extent in the presence of N_2O relative to the argon-purged aqueous solution, while efficient decomposition of **oxo-ara-C** occurred due to the $^\bullet$OH reaction (see also Figures 2 and 3). Thus, it is reasonable to conclude that reducing species e_{aq}^- is essential for the activation of **oxo-ara-C** and the concomitant release of **ara-C**.

In a separate experiment, we carried out radiolytic reduction of N(4)-substituted **ara-C** lacking a carbonyl group **3** in aqueous solution. As shown in Table 1, hypoxic irradiation of **3** failed to release **ara-C**, indicating that the carbonyl moiety is a key structural unit necessary for the release of **ara-C** *via* one-electron reduction of **oxo-ara-C** by e_{aq}^-.
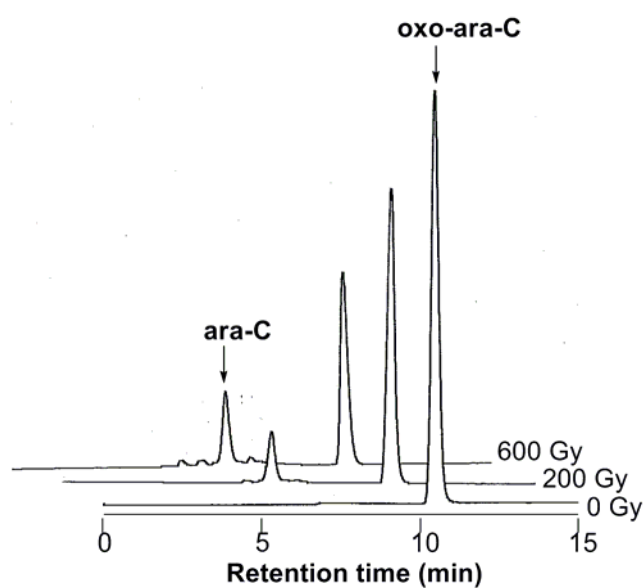
Figure 1. HPLC profiles for the one-electron reduction of **oxo-ara-C** (100 μM) under hypoxic X-ray treatment (0, 200, and 600 Gy) of an aqueous solution containing 2-methyl-2-propanol (10 mM).

Table 1. *G* Values for the Decomposition of **Oxo-ara-C** and for the Formation of **ara-C** upon X-ray Treatment in Several Gas-saturated Solutions.

| Compound | Saturating gas | *G* value / nmol J^{-1} | |
		Decomposition	Formation
oxo-ara-C	Aargon	151	69
oxo-ara-C	Air	27	4
oxo-ara-C	Nitrous oxide	141	5
3	Argon	130	ND[a]

[a] Not detected.
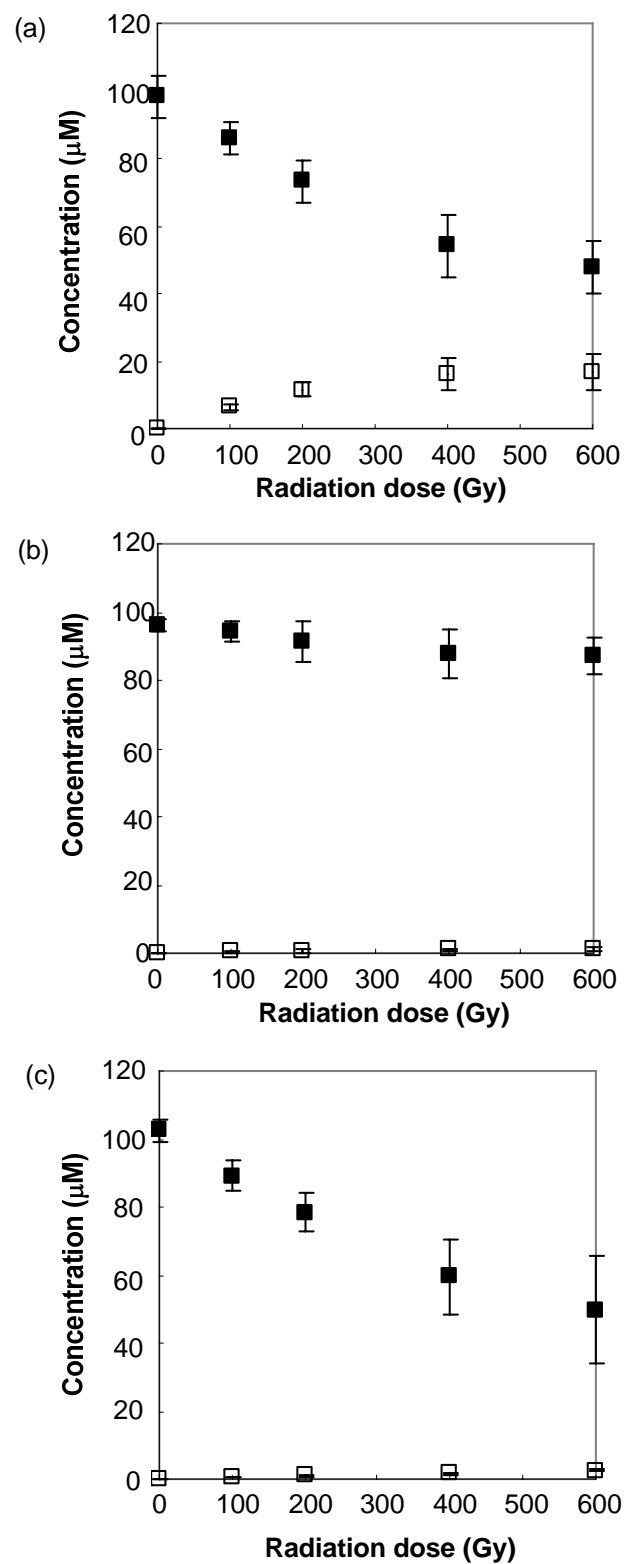
Figure 2. Radiolytic reduction of 100 μM **oxo-ara-C** (closed square) to release **ara-C** (open square) in hypoxic (a), aerobic (b) and N$_2$O-saturated (c) aqueous solutions containing 2-metyl-2-propanol (10 mM) Results are shown with the mean ± S.D. (n = 3)
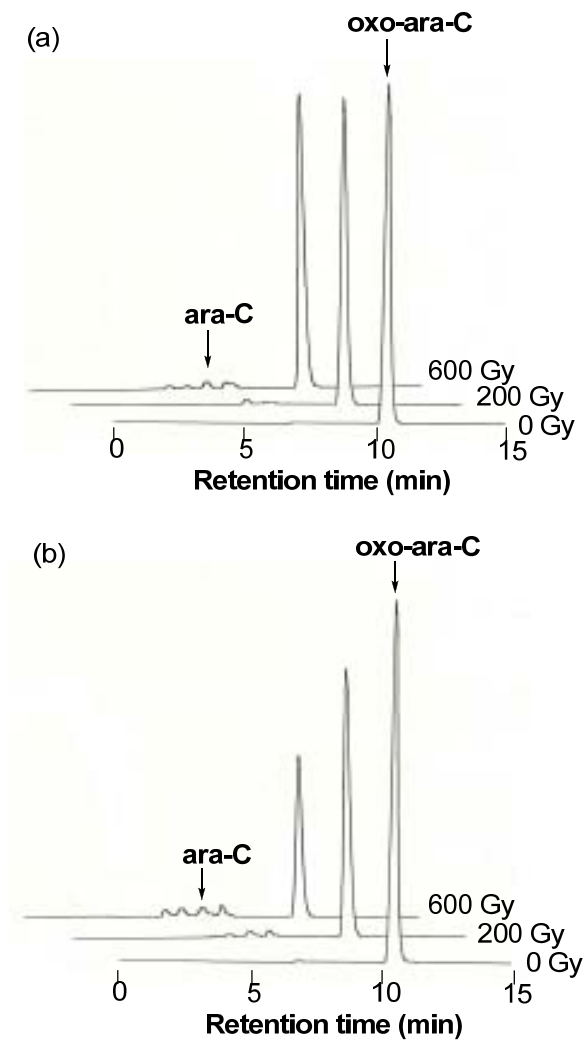
Figure 3. HPLC profiles for the X-radiolysis (0, 200, and 600 Gy) of **oxo-ara-C** (100 μM) in aerobic (a) and N_2O-saturated (b) aqueous solutions containing 2-methyl-2-propanol (10 mM)

An understanding of the function of **oxo-ara-C** in living cells is important for its biological applications. We therefore assessed the cytotoxic properties of **ara-C** and **oxo-ara-C** toward A549 cells (human lung adenocarcinoma). A549 cells were cultured for 72 h in the presence of various concentrations of **ara-C** or **oxo-ara-C** under aerobic conditions, and were subsequently subjected to a cell viability assay (Figure 4). The IC_{50} values were 20.7 and 0.38 μM for **oxo-ara-C** and **ara-C**, respectively, indicating that a small modification of **ara-C** by addition of a substituent such as the 2-oxopropyl group can effectively reduce the cytotoxicity of the parent anti-tumour agent. This result may be promising for further investigations to identify whether the dose of **oxo-ara-C** could be more increased without considerable side effects, compared to **ara-C**.
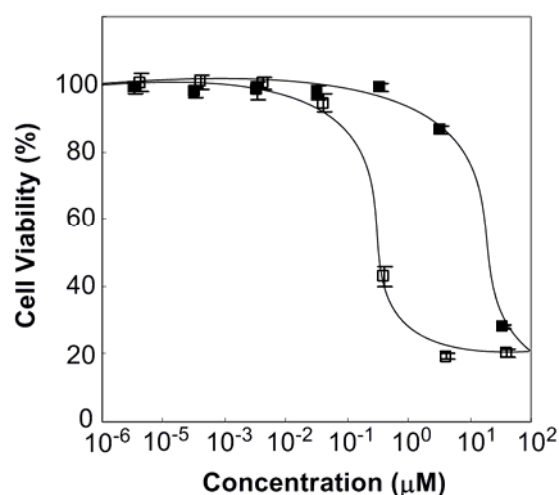

Figure 4. Cytotoxicity of **ara-C** and **oxo-ara-C** against A549 tumor cells. A549 cells were incubated with indicated concentrations of **ara-C** or **oxo-ara-C** under aerobic conditions for 72 hours. To calculate the cell viability in each conditions, SF counts (OD_{450}) for each drug concentration were compared to those in minimal drug concentrations. **ara-C** (open square); **oxo-ara-C** (filled square). Results are shown with the mean ± S.D (n = 3).

We subsequently exposed A549 cells to varying doses of X-rays in the presence or absence of **oxo-ara-C** under aerobic or hypoxic conditions, and characterized the hypoxia- and radiation-dependent cytotoxic effects of **oxo-ara-C** (Figure 5). In accordance with the suppression of cytotoxic effects described above, the cells were viable even in the presence of 3.3 μM **oxo-ara-C** without X-ray treatment (compare entries 1 and 2).[14] Although the A549 cells were practically resistant to radiation under hypoxic conditions (entry 7), **oxo-ara-C** showed the striking property to significantly enhance the radiation sensitivity of A549 cells (entry 8). In contrast, **oxo-ara-C** had little effect on the radiation sensitibity under aerobic conditions (compare entries 5 and 6). These results strongly suggest that **oxo-ara-C** preferentially releases toxic **ara-C** *via* radiolytic one-electron reduction in hypoxic cells and thereby results in enhanced cytotoxicity, consistent with the chemical reactivity upon irradiation.
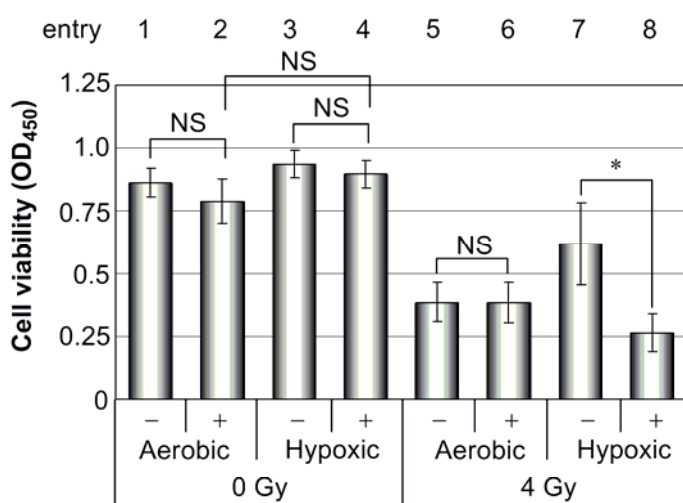

Figure 5. Radiation-induced cytotoxicity of **oxo-ara-C** against A549 cells under hypoxic conditions. A549 cells were cultured in the presence (+) or absence (−) of 3.3 μM **oxo-ara-C**, and treated with X-rays (4 Gy) under aerobic or hypoxic conditions. Results are shown with the mean ± S.D (n = 3) (* P < 0.05; NS: not significant).

We have demonstrated that **oxo-ara-C** is a useful radiation-activated prodrug that shows a cytotoxic effect upon hypoxic tumour cells. Incorporation of a 2-oxoalkyl group into **ara-C** dramatically reduced its cytotoxicity, while the toxic activity was recovered upon hypoxic irradiation. Although the suppression mechanism of the intrinsic cytotoxicity of **oxo-ara-C** in the presence of the 2-oxoalkyl group remains unclear, it can be presumed that the steric hindrance and/or disturbance of hydrogen bonding at the N(4) position may inhibit the recognition of intracellular DNA polymerases, which are key enzymes involved in the cytotoxicity of **ara-C**. Further mechanistic studies using DNA polymerase and triphosphate of **oxo-ara-C** are currently in progress to confirm this hypothesis.

Conclusion

In summary, we designed and synthesized an **ara-C** derivative possessing a 2-oxopropyl group at the N(4) position (**oxo-ara-C**) as a radiation-activated prodrug. **Oxo-ara-C** releases **ara-C** upon reaction with e_{aq}^-, generated during the radiolysis of water under hypoxic conditions. Assessment of the viability of A549 cells revealed that incorporation of the 2-oxoalkyl group into **ara-C** resulted in a dramatic suppression of the cytotoxic effect, while hypoxic X-ray ttreatment recovered the cytotoxicity *via* removal of the 2-oxoalkyl group to re-generate active **ara-C**. Thus, **ara-C** derivatives possessing 2-oxoalkyl groups are promising candidates as a new class of radiation-activated prodrugs for the treatment of hypoxic tumour tissues.

Experimantal Section

General Methods.

All reactions were carried out under a dry nitrogen atmosphere using freshly distilled solvents unless otherwise noted. Reagents were purchased from Aldrich, Wako pure chemical industries and Nacalai tesque, and used as received. Ultrapure water was obtained from YAMATO WR-600A. Precoated TLC (Merck silica gel 60 F_{254}) plates were used for monitoring the reactions. Column chromatography was carried out on Wakogel C-300 (Wako pure chemical industries). ^{1}H NMR spectra were measured with JEOL JMN-AL-300 (300 MHz) or JEOL JMN-AL-400 (400 MHz) spectrophotometers at ambient temperature. ^{13}C NMR spectra were measured with JEOL JMN-AL-300 (75.5 MHz) or JEOL JMN-AL-400 (100 MHz) spectrophotometers at ambient temperature. Coupling constants (J values) are reported in Hertz. The chemical shifts are expressed in ppm downfield from tetramethylsilane, using residual methanol ($\delta = 3.30$ in ^{1}H NMR, $\delta = 49.0$ in ^{13}C NMR) as an internal standard. Multiplicity is designed as singlet (s), doublet (d), triplet (t), doublet-doublet (dd), or multiplet (m). FAB Mass spectra were recorded on JEOL JMS-SX102A spectrometer, using glycerol matrix. A Rigaku RADIOFLEX-350 was used for X-ray treatment. High-performance liquid chromatography (HPLC) was performed with Shimadzu LC-6A system. Sample solutions were injected on a reversed phase column (Inertsil ODS-3, GL Science Inc., ϕ 4.6 $\times$ 150 mm). The 0.1 M triethylamine (TEA) 5 vol% acetonitrile/water solution containing acetic acid, pH 7.0 was delivered as the mobile phase at a flow rate of 0.6 mL min^{-1} at 40 °C. The elution peaks were monitored at 260 nm wavelength.

4-(2,2-Dimethyoxypropylamino)-1-(β-D-arabinofuranosyl)pyrimidine-2-(*1H*)-one (2)

1-Amino-2,2-dimethoxypropane[10] (796 mg 6.68 mmol) was added to a solution of **1**[9] (4-(1,2,4-Triazol-yl)-1-(β-D-2,3,5-tri-O-acetylarabinofuranosyl)pyrimidine-2(*1H*)-one, 167 mg, 0.40 mmol) in dioxane (1.2 ml) and stirred for 9.5 h at 80 °C. The solvent was removed under reduced pressure. The crude product was purified by column chromatography (SiO$_2$ 6%

methanol-chloroform) to give **2** (71 mg, 52%) as a white solid; mp 171–173 °C; ^{1}H NMR (CD$_3$OD, 400 MHz) δ 7.75 (d, 1H, J = 7.6 Hz), 6.16 (d, 1H, J = 4.0 Hz), 5.93 (d, 1H, J = 7.6 Hz), 4.16 (dd, 1H, J = 2.4, 3.6 Hz), 4.04 (dd, 1H, J = 2.4, 2.4 Hz), 3.92 (m, 1H), 3.79 (m, 2H), 3.58 (s, 2H), 3.23 (s, 6H), 1.28 (s, 3H); ^{13}C NMR (CD$_3$OD, 75.5 MHz) δ 165.9, 158.7, 143.0, 101.8, 95.7, 88.3, 86.4, 78.2, 76.8, 62.8, 48.8, 48.8, 45.3, 20.5; FABMS (glycerol) m/z 346 [(M + H)$^+$]; HRMS calcd. for C$_{14}$H$_{24}$N$_3$O$_7$ [(M + H)$^+$] 346.1614, found 346.1611.

4-Propylamino-1-(β-D-arabinofuranosyl)pyrimidine-2-(*1H*)-one (3)

Propylamine (0.23 ml, 2.80 mmol) was added to a solution of **1**[9] (4-(1,2,4-Triazol-yl)-1-(β-D-2,3,5-tri-*O*-acetylarabinofuranosyl)pyrimidine-2(*1H*)-one, 43.5 mg, 0.103 mmol) in ethanol (0.3 ml) at room temperature. After 4.5 h the product was concentrated under reduced pressure. The crude product was purified by column chromatography (SiO$_2$ 1% TEA, 9% methanol-chloroform) to give **3** (21 mg, 71%) as a white solid; mp 194–195 °C; ^{1}H NMR (CD$_3$OD, 300 MHz) δ 7.72 (d, 1H, J = 7.5 Hz), 6.17 (d, 1H, J = 3.9 Hz), 5.79 (d, 1H, J = 7.8 Hz), 4.16 (m, 1H), 4.07 (m, 1H), 3.93 (m, 1H), 3.80 (m, 2H), 3.32 (m, 2H), 1.60 (m, 2H, J = 7.2 Hz), 0.96 (t, 3H, J = 7.2 Hz); ^{13}C NMR (CD$_3$OD, 100 MHz) δ 165.4, 158.6, 142.5, 95.6, 88.2, 86.3, 78.2, 76.8, 62.8, 43.4, 23.3, 11.7; FABMS (glycerol) m/z 286 [(M + H)$^+$]; HRMS calcd. for C$_{12}$H$_{20}$N$_3$O$_5$ [(M + H)$^+$] 286.1403, found 286.1394.

4-(2-Oxopropylamino)-1-(β-D-arabinofuranosyl)pyrimidine-2-(*1H*)-one (4) (oxo-ara-C)

2 (20 mg 0.058 mmol) was hydrolyzed by treatment with aqueous 1 M oxalic acid in THF (0.3 ml) at room temperature for 5 h. The solvent was evaporated under reduced pressure and the crude product was purified by column chromatography (SiO$_2$ 1% TEA, 12% methanol-chloroform) to give **oxo-ara-C** (7.7 mg, 44%) as a white solid; mp 180–182 °C; ^{1}H NMR (CD$_3$OD, 300 MHz) δ 7.79 (d, 1H, J = 7.5 Hz), 6.15 (d, 1H, J = 3.8 Hz), 5.93 (d, 1H, J = 7.5 Hz), 4.26 (s, 2H), 4.16 (dd, 1H, J = 2.4, 3.6 Hz), 4.04 (dd, 1H, J = 2.8, 2.6 Hz), 3.92 (m, 1H), 3.79 (m, 2H), 2.18 (s, 3H); ^{13}C NMR (CD$_3$OD, 75.5 MHz) δ 206.0, 165.6, 158.5, 143.4, 95.4, 88.4, 86.6, 78.2, 76.8, 62.8, 51.3,

27.1; FABMS (glycerol) m/z 300 [(M + H)$^+$]; HRMS calcd. for $C_{12}H_{18}N_3O_6$ [(M + H)$^+$] 300.1196, found 300.1189.

Radiolytic reduction

Aqueous solutions of **oxo-ara-C** and **3** (100 μM), containing 2-methyl-2-propanol (10 mM), were purged with argon or nitrous oxide for 15 min and then irradiated in a sealed glass ampoule at ambient temperature with an X-ray source (4.0 Gy min^{-1}). After the X-irradiation, the solution was immediately subjected to HPLC analysis.

Assessment of cytotoxicity toward A549 cells

A549 cells were cultured in Dulbecco's modified Eagle's minimum essential medium (DMEM) containing 10% fetal bovine serum (FBS). The cells were seeded into 96-well plates (2000 cells/well) and cultured at 37 °C in a well-humidified incubator with 5% CO_2 and 95% air (aerobic condition) for 24 hours. The cells were then incubated with the various concentrations of **ara-C** or **oxo-ara-C** under aerobic conditions for 72 hours, and added with 11 μL of Cell Count Reagent SF[15] (Nacalai, Japan). The plates were further incubated at 37 °C for 2 hours and the cell viability assay was performed using Microplate Reader (BIO-RAD).

Radiation-induced cytotoxicity of oxo-ara-C

A549 cells were seeded into 96-well plates (2000 cells/well) and incubated at 37 °C for 24 hours under aerobic or hypoxic conditions. For the hypoxic treatment (< 0.02% of oxygen), the cells were treated in a hypoxic chamber, BACTRON-Ⅱ(Sheldon Manufacturing Inc., Cornelius, OR, USA). The plates kept under aerobic or hypoxic conditions using Anaeron Pack System (Mitsubishi Gas Chemical Company Inc., Japan) were treated with X-rays at a dose of 4 Gy and incubated for 72 hours under aerobic conditions. After adding 12 μL of Cell Count Reagent SF solution (Nacalai, Japan) to each well, and the cell viability assay was performed as described above.

References and Notes

(1)   (a) Evans, J. S.; Musser, E. A.; Bostwick, L.; Mengel, G. D. *Cancer Res.* **1964**, *24*, 1285–1293. (b) Ooi, K. *Yakugaku Zasshi* **2002**, *122*, 471–480.

(2)   (a) Furth, J. J.; Cohen, S. S. *Cancer Res.* **1968**, *28*, 2061–2067. (b) Major, P. P.; Egan, E. M.; Herrick, D. J.; Kufe, D. W. *Biochem. Pharmacol.* **1982**, *31*, 2937–2940. (c) Kufe, D.; Spriggs, D.; Egan, E. M.; Munroe, D. *Blood* **1984**, *64*, 54–58.

(3)   Macdonald, D. R. *Neurol. Clin.* **1991**, *9*, 955–967.

(4)   (a) Harris, A. L. *Nat. Rev. Cancer*, **2002**, *2*, 38–47. (b) Kizaka-Kondo, S.; Inoue, M.; Harada, H.; Hiraoka, M. *Cancer Sci*. **2003**, *94*, 1021–1028.

(5)   Tanabe, K.; Zhang, Z.; Ito, T.; Hatta, H.; Nishimoto, S. *Org. Biomol. Chem.* **2007**, *5*, 3745–3757.

(6)   (a) Tanabe, K.; Kanezaki, H.; Ishii, H.; Nishimoto, S. *Org. Biomol. Chem.* **2007**, *5*, 1242–1246. (b) Shibamoto, Y.; Zhou, L.; Hatta, H.; Mori, M.; Nishimoto, S. *Int. J. Radiat. Oncol. Biol. Phys.* **2001**, *49*, 407–413. (c) Shibamoto, Y.; Tachi, Y.; Tanabe, K.; Hatta, H.; Nishimoto, S. *Int. J. Radiat. Oncol. Biol. Phys.* **2004**, *58*, 397–402. (d) Tanabe, K.; Mimasu, Y.; Eto, A.; Tachi, Y.; Sakakibara, S.; Mori, M.; Hatta, H.; Nishimoto, S. *Bioorg. Med. Chem.* **2003**, *11*, 4551–4556.

(7)   Radiolysis of diluted aqueous solution at around pH 7.0 produces primary water radicals such as oxidizing hydroxyl radicals ($^{\bullet}$OH), reducing hydrated electrons (e_{aq}^{-}) and reducing hydrogen atoms ($^{\bullet}$H) with the G values of $G(^{\bullet}OH) = 280$ nmol J^{-1}, $G(e_{aq}^{-}) = 280$ nmol J^{-1}, and $G(^{\bullet}H) = 60$ nmol J^{-1}.

(8)   Mori, M.; Ito, T.; Teshima, S.; Hatta, H.; Fujita, S.; Nishimoto, S. *J. Phys. Chem.* **2006**, *110*, 12198–12204.

(9)   Divakar, K. J.; Reese, C. B. *J. Chem. Soc. Perkin Trans*. **1982**, *5*, 1171–1176.

(10)   Calabretta, R.; Giordano, C.; Gallina, C.; Morea, V.; Consalvi, V.; Scandurra, R. *Eur. J. Med. Chem*. **1995**, *30*, 931–941.

(11)   Mori, M.; Hatta, H.; Nishimoto, S. *J. Org. Chem.* **2000**, *65*, 4641–4647.

(12) The number of molecules produced or changed per 1 joule of radiation energy absorbed by the reaction system.

(13) Dissolved N_2O exclusively scavenges reducing hydrated electrons to produce hydroxyl radicals, as follows: $e_{aq}^- + N_2O \rightarrow {}^\bullet OH + OH^- + N_2$ (k = 9.1×10^9 dm^3 mol^{-1} s^{-1})

(14) Without X-ray treatment, the effect of oxygen on the cell viability is negligible irrespective of the presence or the absence of **oxo-ara-C** (Figure 5, entry 1–4).

(15) Ishiyama, M.; Miyazono, Y.; Sasamoto, K.; Ohkura, Y.; Ueno, K. *Talanta* **1997**, *44*, 1299–1305.

Chapter 5

Radiolytic One-Electron Reduction Characteristics of Tyrosine Derivative Caged by 2-Oxopropyl Group

Abstract: We employed X-irradiation to activate a caged amino acid with a 2-oxoalkyl group. We designed and synthesized tyrosine derivative caged by a 2-oxoalkyl group (Tyr(Oxo)) to evaluate its radiolytic one-electron reduction characteristics in aqueous solution. Upon hypoxic X-irradiation, Tyr(Oxo) released a 2-oxopropyl group to form the corresponding uncaged tyrosine. In addition, radiolysis of dipeptides containing Tyr(Oxo) revealed that the efficiency of radiolytic removal of 2-oxopropyl group increased significantly in the presence of neighboring aromatic amino acids.

Introduction

Caged amino acids and proteins, the functions of which can be regulated by external triggers, are applied widely to biological research.[1–5] The activities of these molecules can be blocked by chemical modification, while their intrinsic activities are recovered by external stimulation such as photoirradiation[6] and enzymatic treatment.[4] In view of a feature that their functions are easily regulated both temporally and spatially, these caged amino acids are useful for studying protein chemistry in biological systems.

Recently we have proposed caged drugs (prodrugs) that are activated by hypoxic X-irradiation.[7–11] Our studies illustrated that a 2-oxoalkyl group has an effective functionality for caging antitumor drugs such as 5-fluorouracil (5-FU)[8,9] and 5-fluorodeoxyuridine (5-FdUrd),[10] and for radiolytic activation of the resultant caged drugs. This class of radiation activated caged drugs release the 2-oxoalkyl group by reducing hydrated electrons, which are generated as the major active species along with hydrogen atoms and hydroxyl radicals upon radiolysis of an aqueous solution. An activation mechanism has been proposed by which the 2-oxoalkyl group undergoes one-electron reduction by hydrated electrons to form corresponding π^* anion radical, followed by thermal activation into σ^* anion radical that has a weakened N-C bond between the 5-FU unit and the 2-oxoalkyl group and is readily hydrolyzed to release the 2-oxoalkyl group. In this study, we designed and synthesized an amino acid caged by a 2-oxopropyl group on tyrosine (Tyr), which has a high affinity for hydrated electrons.[12] Under hypoxic conditions, radiolytic one-electron reduction of tyrosine derivative possesssing 2-oxopropyl group (Tyr(Oxo)) resulted exclusively in releasing of 2-oxopropyl group to recover the corresponding uncaged Tyr. In the case of dipeptides bearing Tyr(Oxo), the neighboring amino acid was identified to have a strong influence on the overall efficiency of radiolytic one-electron reductive release of the 2-oxopropyl group from Tyr(Oxo).

Results and discussion

The synthetic procedure of Tyr(Oxo) is outlined in Scheme 1. Coupling of *N*-(*tert*-butoxycarbonyl)tyrosine methyl ester **1** with α-bromoacetone and deprotection of the terminal amino group gave Tyr(Oxo) (**3**).

We initially performed one-electron reduction of Tyr(Oxo) by the X-radiolysis of an argon-purged aqueous solution containing excess 2-methyl-2-propanol as the scavenger of oxidizing hydroxyl radicals. Reducing hydrated electrons (e_{aq}^-) are generated as the major active species under these radiolysis conditions, in which the yield of reducing hydrogen atoms is much less than those of hydrated electrons and oxidizing hydroxyl radicals.[13] Figure 1 shows the reaction profiles of the radiolytic reduction of Tyr(Oxo) under hypoxic conditions. The appearance of a single new peak in Figure 1 is attributable to the formation of uncaged Tyr as confirmed by the overlap injection of authentic samples in the HPLC analysis. The *G* value (the number of molecules produced or changed per 1 J of radiation energy absorbed by the reaction system) were 223 nmol J^{-1} for the decomposition of caged Tyr(Oxo) and 130 nmol J^{-1} for the formation of the corresponding uncaged Tyr.[14] Theses results clearly indicated that the 2-oxopropyl group on the amino acid can be similarly removed as in the case of prodrugs.[10]
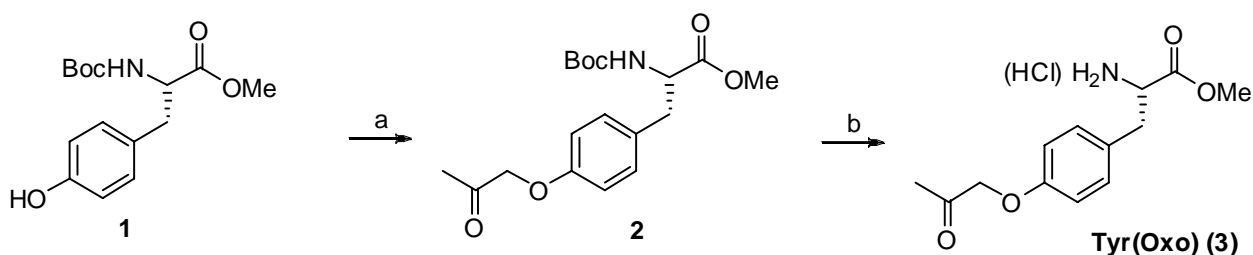
Scheme 1. Reagents and conditions: (a) K$_2$CO$_3$, KI, bromoacetone, acetone, reflux, quant.; (b) HCl in Et$_2$O, room temperature, 78%
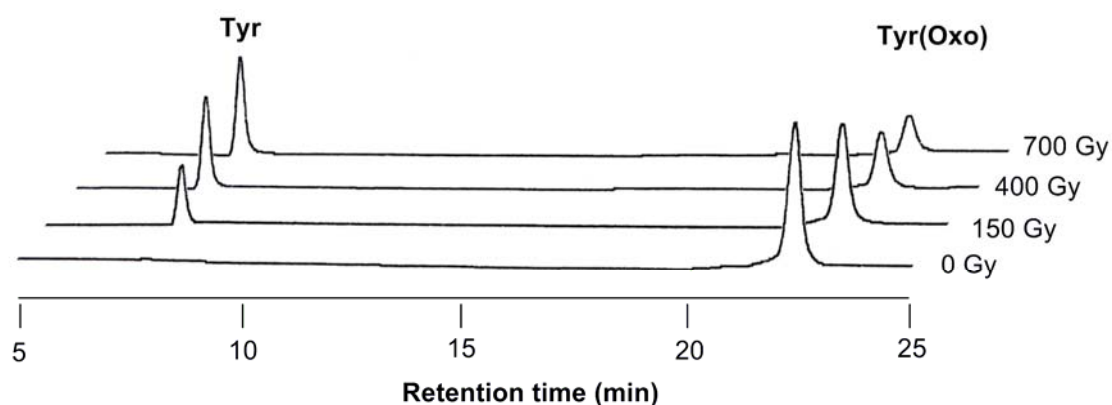
Figure 1. HPLC profiles for the one-electron reduction of Tyr(Oxo) (**3**) (95 μM) upon hypoxic X-radiolysis (0, 150, 400 and 700 Gy) of aqueous solution containing 10 mM 2-methyl-2-propanol.
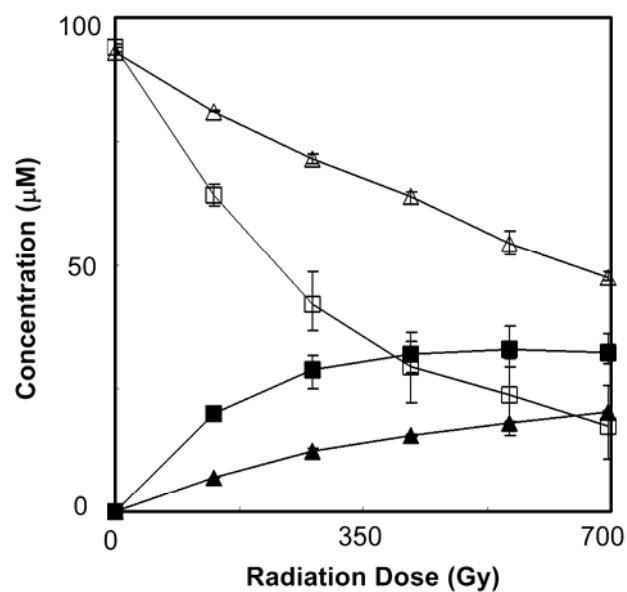

Figure 2. Decomposition of Tyr(Oxo) (**3**) (open symbol) and release of Tyr (filled symbol) in the hypoxic (circle) or aerobic (triangle) radiolysis of aqueous solution containing 10 mM 2-methyl-2-propanol. Each error bar represents the SE calculated from three experimental results.

To assess the effect of molecular oxygen on the radiolysis of Tyr(Oxo), we performed similar one-electron reduction under aerobic conditions. In contrast to the hypoxic X-radiolysis, the removal of the 2-oxopropyl group to convert Tyr(Oxo) into Tyr became considerably less efficient in the aerobic X-radiolysis (Figure 2). The G values were estimated as 81 nmol J^{-1} for decomposition of Tyr(Oxo) and 51 nmol J^{-1} for the formation of Tyr. In view of well-documented evidence that molecular oxygen efficiently inhibits radiolytic reduction due to the trapping of e_{aq}^- to form a super oxide anion radical,[15] the one-electron reduction of Tyr(Oxo) by e_{aq}^- is likely to occur in a hypoxia-selective manner.

To identify the effect of the neighboring amino acid on the radiolytic reduction of Tyr(Oxo), we compared one-electron reduction reactivity of dipeptides **7-13** comprising Tyr(Oxo) and seven types of natural amino acids upon hypoxic or aerobic X-irradiation. Dipeptides **7-13** were prepared from **4** (Ac-Tyr-OMe) as outlined in Scheme 2. The phenol group of **4** was alkylated by α-bromoacetone, and subsequent hydrolysis gave acid **6**. Coupling of **6** with the corresponding amino acids furnished the synthesis of dipeprides **7-13**.

Figure 3 shows representative reaction profiles of the radiolytic reduction of dipeptide Tyr(Oxo)-Gly under hypoxic conditions. Similar to the radiolysis of monomeric Tyr(Oxo), reductive removal of the 2-oxopropyl group occurred commonly for all dipeptides in hypoxia-selective manner. The dipeptides **10-13**, in which Tyr(Oxo) is linked to aromatic amino acids, showed higher G values than dipeptides **7-9** with a linkage between Tyr(Oxo) and aliphatic amino acids, as listed in Table 1. Thus, the neighboring amino acid has a marked effect on the one-electron reduction of Tyr(Oxo) to generate uncaged Tyr. It has been reported that aromatic amino acids are reduced by e_{aq}^- faster than aliphatic amino acids.[12] These reduction characteristics of e_{aq}^- could be responsible for the accelerated reduction of dipeptides bearing aromatic amino acids. It is most likely that capturing of e_{aq}^- by the aromatic amino acid residues in the caged dipeptides occurred more efficiently followed by rapid intramolecular electron transfer to Tyr(Oxo), thereby resulting in the efficient formation of an uncaged dipeptide.
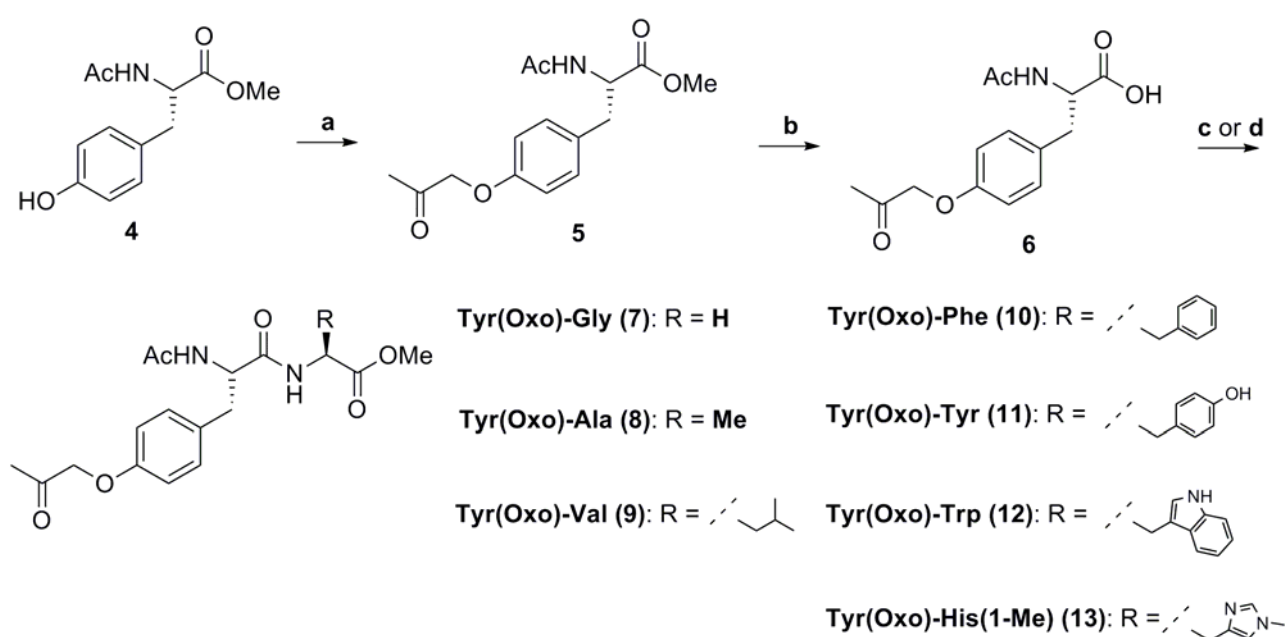
Scheme 2. Reagents and conditions: (a) K₂CO₃, KI, bromoacetone, acetone, reflux, 77%; (b) LiOH, MeOH-H₂O, room temperature, 76%; (c) amino acid methyl ester hydrochloride, HBTU, DIEA, THF, room temperature, 7–34% (for **7–12**); (d) 1-methylhistidine methyl ester hydrochloride, EDCI, triethylamine, DMF, room temperature, 28% (for **13**).
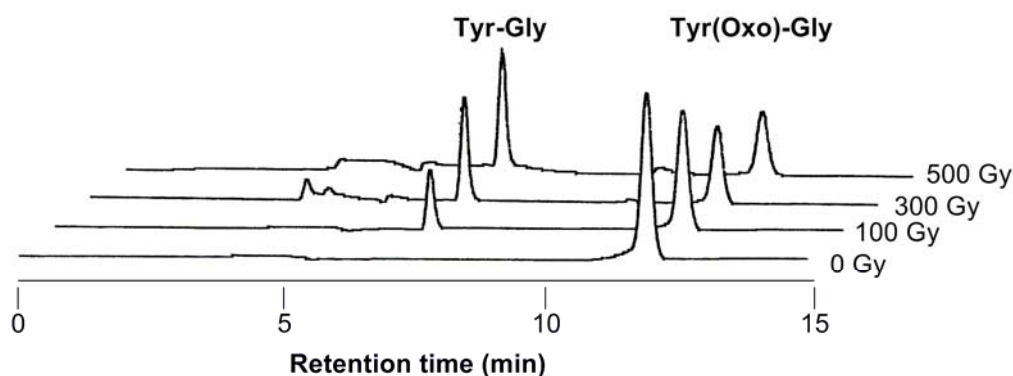
Figure 3. HPLC profiles for the one-electron reduction of Tyr(Oxo)-Gly (**7**) (100 μM) upon hypoxic X-radiolysis (0, 100, 300 and 500 Gy) of aqueous solution containing 10 mM 2-methyl-2-propanol.

Table 1. *G* Values (nmol J^{-1}) for the Decomposition of Tyr(Oxo) (**3**) and Dipeptides Bearing Tyr(Oxo) and the Formation of Corresponding Uncaged Tyr and Dipeptides upon X-radiolysis.[a]

	Hypoxic conditions		Aerobic conditions	
	Formation	Decomposition	Formation	Decomposition
Tyr(Oxo) (**3**)	130	223	51	81
Tyr(Oxo)-Gly (**7**)	55	212	11	52
Tyr(Oxo)-Ala (**8**)	96	232	20	72
Tyr(Oxo)-Val (**9**)	72	209	18	83
Tyr(Oxo)-Phe (**10**)	155	299	30	45
Tyr(Oxo)-Tyr (**11**)	196	258	37	52
Tyr(Oxo)-Trp (**12**)	131	295	24	55
Tyr(Oxo)-His(1-Me) (**13**)	158	282	42	96

[a] Aqueous solution of Tyr(Oxo) (**3**) and dipeptides (95–320 μM) containing excess amount of 2-methyl-2-propanol[16] were irradiated at ambient temperature with X-ray source (5 Gy min^{-1}).

Conclusion

In summary, we have demonstrated the activation of caged Tyr possessing a 2-oxoalkyl group by X-radiolytic one-electron reduction. Hypoxic X-irradiation caused the efficient removal of the 2-oxopropyl group on Tyr(Oxo), whereas the reaction efficiency decreased dramatically upon aerobic irradiation. More remarkable was that the neighboring aromatic amino acids increased the radiolytic reduction efficiency of Tyr(Oxo), presumably due to their high electron affinity. These results strongly indicate that functions of amino acids and proteins may be regulated by means of radiolytic reduction of 2-oxoalkyl group. Further exploration of the one-electron reduction of longer and higher-order peptides bearing Tyr(Oxo) by X-radiolysis is in progress.

Experimental Section

General Methods.

All reactions were carried out under a dry nitrogen atmosphere using freshly distilled solvents unless otherwise noted. Reagents were purchased from Aldrich, Wako pure chemical industries, Nacalai tesque and Watanabe chemical industries and used without purification. Ultra pure water was obtained from YAMATO WR-600A. The course of reactions was monitored by thin-layer chromatography (TLC) on fluorescent silica gel plates (Silica Gel 60 F254) using UV light. Wako gel (C-300, particle size 45-75 μm, Wako) was used for column chromatography. ^{1}H NMR spectra were measured with JEOL JNMAL 300 (300 MHz), or JEOL JMN-EX-400 (400 MHz) spectrometers. ^{13}C NMR spectra were measured with JEOL JNMAL 300 (75.5 MHz), or JEOL JMN-EX-400 (100 MHz). The chemical shifts are expressed in ppm downfield, using residual chloroform ($\delta = 7.26$ in ^{1}H NMR, $\delta = 77.0$ in ^{13}C NMR) and residual dimethylsulfoxide ($\delta = 2.50$ in ^{1}H NMR, $\delta = 39.5$ in ^{13}C NMR) as internal standards. The following abbreviations were used to explain the multiplicities: singlet (s); doublet (d); triplet (t); quartet (q); multiplet (m); broad (br). Melting points were obtained on YANAGIMOTO MICROMELTINGPOINT APPARATUS. Fast atom bombardment mass spectra and high-resolution mass spectra were recorded on JEOL JMN-SX102A spectrometer, using nitrobenzylalchol (NBA) matrix. UV-visible spectra were measured with JASCO V-530 UV/VIS spectrophotometer. High-performance liquid chromatography (HPLC) were performed with HITACHI HPLC system (pump: HITACHI L-2130, UV detector: HITACHI L-2400) and SHIMADZU HPLC system (pump: LC-10AS, UV detector: SPD-10A). Sample solution were injected on a reversed phase column (Inertsil ODS-3, GL Science Inc, ϕ 10 mm × 250 mm).

Boc-Tyr(2-oxopropyl)-OMe (2).

Boc-Tyr-OMe (1.51 g, 5.10 mmol), K$_2$CO$_3$ (906 mg, 6.35 mmol) and KI (167 mg, 1.01 mmol) were charged into a flask. 15 mL of acetone was added into the flask and reflux at 50 °C under an

atmosphere of nitrogen for 10 min. Then, bromoacetone (477 μL, 5.10 mmol) was added in one portion and the reaction mixture was refluxed at 50 °C for 7 hours. After reaction, the solvent was evaporated. The reaction mixture was extracted with ethylacetate, washed with water and brine, dried over anhydrous $MgSO_4$, and concentrated. The crude products were purified by silica gel column chromatography (hexane:ethyl acetate = 5:1 to 1:3 as eluent) to give Boc-Tyr(2-oxopropyl)-OMe (1810 mg, quant.) as a yellow oil. ^{1}H NMR ($CDCl_3$, 400 MHz) δ 7.05 (d, J = 8.8 Hz, 2H), 6.80 (d, J = 8.8 Hz, 2H), 4.96 (d, J = 7.6 Hz, 1H), 4.53 (m, 1H), 4.51 (s, 2H), 3.70 (s, 3H), 3.02 (m, 2H), 2.27 (s, 3H), 1.41 (s, 9H); ^{13}C NMR ($CDCl_3$, 75.5 MHz) δ 205.7, 156.9, 155.0, 130.5, 129.2, 117.1, 114.6, 79.8, 73.0, 54.4, 52.1, 37.4, 28.2, 26.5; FABMS: m/z 352 [(M + H)$^+$]; HRMS calcd. for $C_{18}H_{26}NO_6$ [(M + H)$^+$] 352.1760, found 352.1768.

Tyr(Oxo) (3)

Boc-Tyr(2-oxopropyl)-OMe (790 mg, 2.25 mmol) was charged into a flask and dissolved into a minimum amount of 0.5 M HCl / methanol. Then, 4 mL of 2 M HCl / diethyl ether was added into the flask and stirred at r.t. for 6 hours. After reaction, the mixture was concentrated. The crude products were washed with warm ethyl acetate to produce HCl·H-Tyr(2-oxopropyl)-OMe (503 mg, 77.8 %) as a white solid. mp 159–160 °C; ^{1}H NMR (DMSO-d_6, 300 MHz) δ 8.56 (s, 3H), 7.13 (d, J = 8.4 Hz, 2H), 6.85 (d, J = 8.4 Hz, 2H), 4.79 (s, 2H), 4.22 (t, J = 6.0 Hz, 1H), 3.68 (s, 3H), 3.07 (m, 2H), 2.15 (s, 3H); ^{13}C NMR (DMSO-d_6, 75.5 MHz) δ 204.1, 169.3, 157.0, 130.5, 126.8, 114.5, 72.0, 53.3, 52.5, 34.9, 26.2; FABMS: m/z 252 [(M + H)$^+$]; HRMS calcd. for $C_{13}H_{18}NO_4$ [(M + H)$^+$] 252.1236, found 252.1228.

Ac-Tyr(2-oxopropyl)-OMe (5)

Ac-Tyr-OMe (3.0 g, 12.6 mmol), K_2CO_3 (2.25 g, 15.8 mmol), and KI (208 mg, 1.26 mmol) were charged into a flask. 20 mL of acetone was added into the flask and reflux at 55 °C under an atmosphere of nitrogen for 10 min. Then, bromoacetone (1.18 mL, 12.6 mmol) was added in one portion and the reaction mixture was refluxed at 55 °C for 8 hours. After reaction, the solvent was

removed. The reaction mixture was extracted with ethyl acetate, washed with water and brine. The organic layer was dried over anhydrous Na_2SO_4 and concentrated. The crude products were purified by silica gel column chromatography (hexane : ethyl acetate = 1 : 5 to 100 % ethyl acetate as eluent) to give Ac-Tyr(2-oxopropyl)-OMe (2.86 g, 77.4 %) as a white solid. mp 85–86 °C; ^{1}H NMR (DMSO-d_6, 300 MHz) δ 8.30 (d, J = 7.7 Hz, 1H), 7.11 (d, J = 8.6 Hz, 2H), 6.80 (d, J = 8.6 Hz, 2H), 4.76 (s, 2H), 4.39 (m, 1H), 3.59 (s, 3H), 2.87 (m, 2H), 2.14 (s, 3H), 1.79 (s, 3H); ^{13}C NMR (DMSO-d_6, 75.5 MHz) δ 204.2, 172.2, 169.3, 156.5, 130.0, 129.5, 114.2, 72.0, 53.8, 51.7, 35.8, 26.2, 22.2; FABMS: m/z 294 [(M + H)[+]]; HRMS calcd. for $C_{15}H_{20}NO_5$ [(M + H)[+]] 294.1341, found 294.1343.

Ac-Tyr(2-oxopropyl)-OH (6)

Ac-Tyr(2-oxopropyl)-OMe (420 mg, 1.43 mmol) was charged into the flask and dissolved into methanol (2 mL). Then, 1 N LiOHaq (1 mL) was added into the flask and stirred at room temperature for 30 min. The reaction was quenched by adding water and the reaction mixture was evaporated to remove methanol. The water layer was washed with ethyl acetate, acidified by HCl, and extracted with ethyl acetate. The organic layer was dried over anhydrous Na_2SO_4 and concentrated to produce Ac-Tyr(2-oxopropyl)-OH (305 mg, 76.2 %) as a white solid. mp 138–139 °C; ^{1}H NMR (DMSO-d_6, 300 MHz) δ 12.5 (br, 1H), 8.14 (d, J = 8.0 Hz, 1H), 7.12 (d, J = 8.6 Hz, 2H), 6.80 (d, J = 8.6 Hz, 2H), 4.75 (s, 2H), 4.33 (m, 1H), 2.86 (m, 2H), 2.14 (s, 3H), 1.78 (s, 3H); ^{13}C NMR (DMSO-d_6, 75.5 MHz) δ 204.3, 173.5, 168.8, 156.2, 130.7, 130.1, 114.0, 72.1, 54.4, 36.2, 26.2, 22.5; FABMS: m/z 280 [(M + H)[+]]; HRMS calcd. for $C_{14}H_{18}NO_5$ [(M + H)[+]] 280.1185, found 280.1175.

Tyr(Oxo)-Gly (7)

Ac-Tyr(2-oxopropyl)-OH (100 mg, 0.358 mmol), HCl·H-Gly-OMe (89.9 mg, 0.716 mmol), and O-(benzotriazol-1-yl)-N, N, N', N'-tetramethyluronium hexafluorophosphate (HBTU) (272 mg, 0.716 mmol) were dissolved in THF (5 mL) and stirred at room temperature under an atmosphere of

nitrogen for 10 min. Then, *N, N*-diisopropylethylamine (DIEA) (122 μL, 0.716 mmol) was added to the solution and the solution was stirred at r.t. for 2 hours under N_2 atmosphere. After reaction, the solvent was removed by evaporation. The crude products were purified by silica gel column chromatography (chloroform:methanol = 5:1 as eluent), and further purification was carried out by HPLC on a column (Inertsil ODS-3, GL Science Inc, ϕ 10 × 250 mm), elution with a solvent (40 % acetonitrile / water) at a flow rate 3.0 mL min^{-1}, to give Ac-Tyr(2-oxopropyl)-Gly-OMe (20.5 mg, 15.4 %) as a colorless oil. ^{1}H NMR (DMSO-d_6, 300 MHz) δ 8.43 (t, *J* = 6.0 Hz, 1H), 8.08 (d, *J* = 8.4 Hz, 1H), 7.14 (d, *J* = 8.8 Hz, 2H), 6.78 (d, *J* = 8.8 Hz, 2H), 4.75 (s, 2H), 4.47 (m, 1H), 3.85 (d, *J* = 6.1 Hz, 2H), 3.63 (s, 3H), 2.94 (m, 1H), 2.65 (m, 1H), 2.14 (s, 3H), 1.75 (s, 3H); ^{13}C NMR (DMSO-d_6, 75.5 MHz) δ 204.3, 172.0, 170.2, 169.0, 156.2, 130.4, 130.0, 114.0, 72.1, 53.9, 51.7, 38.2, 36.7, 26.2, 22.5; FABMS: *m/z* 351 [(M + H)$^+$]; HRMS calcd. for $C_{17}H_{23}N_2O_6$ [(M + H)$^+$] 351.1556, found 351.1545.

Tyr(Oxo)-Ala (8)

Ac-Tyr(2-oxopropyl)-Ala-OMe was synthesized from Ac-Tyr(2-oxopropyl)-OH (100 mg, 0.358 mmol) and HCl·H-Ala-OMe (99.9 mg, 0.716 mmol) in the same way as Ac-Tyr(oxo)-Gly-OMe. The crude products were purified by silica gel column chromatography (chloroform:methanol = 5:1 as eluent), and further purification was carried out by HPLC, elution with a solvent (40 % acetonitrile / water) at a flow rate 3.0 mL min^{-1}, to give Ac-Tyr(2-oxopropyl)-Ala-OMe (11.6 mg, 8.9 %) as a white solid. mp 158–159 °C; ^{1}H NMR (DMSO-d_6, 300 MHz) δ 8.45 (d, *J* = 7.1 Hz, 1H), 8.03 (d, *J* = 8.6 Hz, 1H), 7.15 (d, *J* = 8.6 Hz, 2H), 6.79 (d, *J* = 8.6 Hz, 2H), 4.75 (s, 2H), 4.47 (m, 1H), 4.27 (m, 1H), 3.61 (s, 3H), 2.92 (m, 1H), 2.63 (m, 1H), 2.14 (s, 3H), 1.73 (s, 3H), 1.29 (d, *J* = 7.3 Hz, 3H); ^{13}C NMR (DMSO-d_6, 75.5 MHz) δ 204.3, 172.9, 171.5, 169.0, 156.2, 130.3, 130.1, 114.0, 72.1, 53.7, 51.8, 47.5, 36.9, 26.2, 22.4, 16.8; FABMS: *m/z* 365 [(M + H)$^+$]; HRMS calcd. for $C_{18}H_{25}N_2O_6$ [(M + H)$^+$] 365.1713, found 365.1726.

Tyr(Oxo)-Val (9)

Ac-Tyr(2-oxopropyl)-Val-OMe was synthesized from Ac-Tyr(2-oxopropyl)-OH (152 mg, 0.545 mmol) and HCl·H-Val-OMe (183 mg, 1.09 mmol) in the same way as Ac-Tyr(Oxo)-Gly-OMe. The crude products were purified by silica gel column chromatography (chloroform:methanol = 10:1 as eluent), and further purification was carried out by HPLC, elution with a solvent (50 % acetonitrile / water) at a flow rate 3.0 mL min^{-1}, to give Ac-Tyr(2-oxopropyl)-Val-OMe (22.7 mg, 10.6 %) as a white solid. mp 142–143 °C; ^{1}H NMR (DMSO-d_6, 300 MHz) δ 8.21 (d, J = 8.0 Hz, 1H), 8.03 (d, J = 8.4 Hz, 1H), 7.16 (d, J = 8.6 Hz, 2H), 6.79 (d, J = 8.6 Hz, 2H), 4.75 (s, 2H), 4.56 (m, 1H), 4.17 (m, 1H), 3.62 (s, 3H), 2.89 (m, 1H), 2.64 (m, 1H), 2.14 (s, 3H), 2.04 (m, 1H), 1.74 (s, 3H), 0.88 (t, J = 6.9 Hz, 6H) ; ^{13}C NMR (DMSO-d_6, 75.5 MHz) δ 204.3, 171.9, 171.8, 169.1, 156.2, 130.3, 130.1, 114.0, 72.1, 57.4, 53.7, 51.6, 36.6, 29.9, 26.2, 22.4, 18.9, 18.2; FABMS m/z 393 [(M + H)$^+$]; HRMS calcd. for C$_{20}$H$_{29}$N$_2$O$_6$ [(M + H)$^+$] 393.2026, found 393.2027.

Tyr(Oxo)-Phe (10)

Ac-Tyr(2-oxopropyl)-Phe-OMe was synthesized from Ac-Tyr(2-oxopropyl)-OH (135 mg, 0.484 mmol) and HCl·H-Phe-OMe (209 mg, 0.968 mmol) in the same way as Ac-Tyr(Oxo)-Gly-OMe. The crude products were purified by silica gel column chromatography (chloroform:methanol = 15:1 as eluent), and further purification was carried out by HPLC, elution with a solvent (50 % acetonitrile / water) at a flow rate 3.0 mL min^{-1}, to give Ac-Tyr(2-oxopropyl)-Phe-OMe (72.7 mg, 34.0 %) as a white solid. mp 107–108 °C; ^{1}H NMR (DMSO-d_6, 400 MHz) δ 8.40 (d, J = 7.6 Hz, 1H), 7.97 (d, J = 8.6 Hz, 1H), 7.24 (m, 5H), 7.12 (d, J = 8.8 Hz, 2H), 6.78 (d, J = 8.8 Hz, 2H), 4.73 (s, 2H), 4.47 (m, 2H), 3.58 (s, 3H), 2.95 (m, 3H), 2.61 (m, 1H), 2.14 (s, 3H), 1.72 (s, 3H); ^{13}C NMR (DMSO-d_6, 75.5 MHz) δ 204.3, 171.7, 171.6, 168.9, 137.0, 130.2, 130.1, 129.0, 128.2, 128.1, 126.5, 114.0, 72.1, 53.6, 53.5, 51.8, 36.5, 26.2, 22.4; FABMS: m/z 441 [(M + H)$^+$]; HRMS calcd. for C$_{24}$H$_{29}$N$_2$O$_6$ [(M + H)$^+$] 441.2026, found 441.2012.

Tyr(Oxo)-Tyr (11)

Ac-Tyr(2-oxopropyl)-Tyr-OMe was synthesized from Ac-Tyr(2-oxopropyl)-OH (152 mg, 0.542

mmol) and HCl·H-Tyr-OMe (251 mg, 1.08 mmol) in the same way as Ac-Tyr(Oxo)-Gly-OMe. The crude products were purified by silica gel column chromatography (chloroform:methanol = 10:1 as eluent), and further purification was carried out by HPLC, elution with a solvent (40 % acetonitrile / water) at a flow rate 3.0 mL min^{-1}, to give Ac-Tyr(2-oxopropyl)-Tyr-OMe (18.4 mg, 7.4 %) as a white solid. mp 77–78 °C; ^{1}H NMR (DMSO-d_6, 300 MHz) δ 9.21 (s, 1H), 8.32 (d, J = 7.5 Hz, 1H), 7.99 (d, J = 8.6 Hz, 1H), 7.12 (d, J = 8.6 Hz, 2H), 6.98 (d, J = 8.4 Hz, 2H), 6.78 (d, J = 8.6 Hz, 2H), 6.65 (d, J = 8.6 Hz, 2H), 4.74 (s, 2H), 4.42 (m, 2H), 3.57 (s, 3H), 2.89–2.27 (m, 4H), 2.14 (s, 3H), 1.72 (s, 3H); ^{13}C NMR (DMSO-d_6, 75.5 MHz) δ 204.3, 171.8, 171.5, 168.9, 156.2, 156.0, 130.3, 130.1, 130.0, 126.9, 115.0, 114.0, 72.1, 53.9, 53.6, 51.7, 36.6, 35.9, 26.2, 22.4; FABMS: m/z 457 [(M + H)$^+$]; HRMS calcd. for $C_{24}H_{29}N_2O_7$ [(M + H)$^+$] 457.1975, found 457.1981.

Tyr(Oxo)-Trp (12)

Ac-Tyr(2-oxopropyl)-Trp-OMe was synthesized from Ac-Tyr(2-oxopropyl)-OH (202 mg, 0.723 mmol) and HCl·H-Trp-OMe (369 mg, 1.45 mmol) in the same way as Ac-Tyr(Oxo)-Gly-OMe. The crude products were purified by silica gel column chromatography (chloroform:methanol = 10:1 as eluent), and further purification was carried out by HPLC, elution with a solvent (50 % acetonitrile / water) at a flow rate 3.0 mL min^{-1}, to give Ac-Tyr(2-oxopropyl)-Trp-OMe (14.7 mg, 4.2 %) as a white solid. mp 80–81 °C; ^{1}H NMR (DMSO-d_6, 300 MHz) δ 10.89 (s, 1H), 8.38 (d, J = 7.3 Hz, 1H), 8.00 (d, J = 8.6 Hz, 1H), 7.48 (d, J = 7.5 Hz, 1H), 7.33 (d, J = 7.7 Hz, 1H), 7.17–6.94 (m, 5H), 6.77 (d, J = 8.6 Hz, 2H), 4.74 (s, 2H), 4.51 (m, 2H), 3.56 (s, 3H), 3.12 (m, 2H), 2.91 (m, 1H), 2.63 (m, 1H), 2.14 (s, 3H), 1.73 (s, 3H); ^{13}C NMR (DMSO-d_6, 75.5 MHz) δ 204.3, 172.1, 171.6, 169.0, 156.2, 136.0, 130.3, 130.1, 127.0, 123.7, 120.9, 118.4, 117.9, 113.9, 111.4, 109.2, 72.1, 53.7, 53.0, 51.8, 36.6, 26.9, 26.2, 22.4; FABMS: m/z 480 [(M + H)$^+$]; HRMS calcd. for $C_{26}H_{30}N_3O_6$ [(M + H)$^+$] 480.2135, found 480.2126.

Tyr(Oxo)-His(1-Me) (13)

To the mixture of Ac-Tyr(Oxo)-OH (72 mg, 0.258 mmol) and H-His(1-Me)-OMe·HCl (52 mg,

0.283 mmol) in DMF (1.2 mL), triethylamine (39 μL, 0.283 mmol) and 1-ethyl-3-(3-dimethylaminopropyl)carbodiimide (EDCI, 99 mg, 0.516 mmol) were added at 0 °C, and then stirred at 0 °C to room temperature for 4 h. After concentrating the reaction mixture *in vacuo*, the crude product was purified by silica gel column chromatography (chloroform:methanol = 10:1 as eluent) to give **13** as a colorless oil (32 mg, 28%); ^{1}H NMR (DMSO-d_6, 400 MHz) δ 8.42 (d, J = 7.3 Hz, 1H), 8.07 (d, J = 7.3 Hz, 1H), 7.13 (d, J = 8.3 Hz, 2H), 6.77 (d, J = 8.3 Hz, 2H), 4.73 (s, 2H), 4.47–4.38 (2H), 3.58 (s, 3H), 3.56 (s, 3H), 2.96–2.53 (6H), 2.13 (s, 3H), 1.74 (s, 3H); ^{13}C NMR (DMSO-d_6, 100 MHz) δ 204.3, 171.8, 171.5, 169.0, 156.2, 137.3, 136.7, 130.1, 117.9, 114.0, 79.1, 72.1, 53.8, 52.3, 51.8, 36.4, 32.7, 29.7, 26.2, 22.4; FABMS: m/z 445 [(M + H)$^+$]; HRMS Calcd. for $C_{22}H_{29}N_4O_6$ [(M + H)$^+$] 445.2087, found 445.2089.

Radiolytic Reduction.

To establish hypoxia, aqueous solutions of Tyr(Oxo) (**3**) (95 μM) containing 10 mM 2-methyl-2-propanol (20% 2-methyl-2-propanol in the case of Tyr(Oxo)-Phe, Tyr(Oxo)-Tyr and Tyr(Oxo)-Trp for their insolubilities) were purged with argon for 15 min and then irradiated in a sealed Pyrex sample tube at ambient temperature with X-ray source (Rigaku RADIOFLEX-350, 5.0 Gy min^{-1}). After the irradiation, the solution was subjected to HPLC analysis.

References and Notes

(1)   Kaplan, J. H.; Forbush, B.Ⅲ.; Hoffman, J. F., *Biochemistry* **1978**, *17*, 1929–1935.

(2)   Rock, R. S.; Chan, S. I. *J. Org. Chem.* **1996**, *61*, 1526–1529.

(3)   Zou, K.; Cheley, S.; Givens, R. S.; Bayley, H. *J. Am. Chem. Soc.* **2002**, *124*, 8220–8229.

(4)   Santos, S. D.; Chandravarkar, A.; Mandel, B.; Mimna, R.; Murat, K.; Saucede, L.; Tella, P.; Tuchscherer, G.; Mutter, M. *J. Am. Chem. Soc.* **2005**, *127*, 11888–11889.

(5)   Kuner, T.; Li, Y.; Gee, K. R.; Bonewald, L. F.; Augustine, G. J. *Proc. Nat. Acad. Sci. USA.* **2008**, *105*, 347–352.

(6)   Mayer, G.; Heckel, A. *Angew. Chem. Int. Ed.* **2006**, *45*, 4900–4921.

(7)   Shibamoto, Y.; Zhou, L.; Hatta, H.; Mori, M.; Nishimoto, S. *Jpn. J. Cancer Res.* **2000**, *91*, 433–438.

(8)   Mori, M.; Hatta, H.; Nishimoto, S. *J. Org. Chem.* **2000**, *65*, 4641–4647.

(9)   Shibamoto, Y.; Zhou, L.; Hatta, H.; Mori, M.; Nishimoto, S. *Int. J. Radiat. Oncol. Biol. Phys.* **2001**, *49*, 407–413.

(10)   Tanabe, K.; Mimasu, Y.; Eto, Y.; Tachi, Y.; Sakakibara, S.; Mori, M.; Hatta, H.; Nishimoto, S. *Bioorg. Med. Chem.* **2003**, *11*, 4551–4556.

(11)   Mori, M.; Ito, T.; Teshima, S.; Hatta, H.; Fujita, S.; Nishimoto, S. *J. Phys. Chem.* **2006**, *110*, 12198–12204.

(12)   Rate constants for the reactions of hydrated electrons in aqueous solution around pH 7 was estimated as 8.8×10^6, 4.2×10^6, 5.0×10^6, 1.4×10^8, 3.4×10^8, 2.9×10^8, 6.0×10^7 and 1.8×10^{10} L mol^{-1} s^{-1} for Gly, Ala, Val, Phe, Tyr, Trp, His and O_2, respectively, see: Buxton, G. V.; Greenstock, C. V.; Helman, W. P.; Ross, A. B. *J. Phys. Chem. Ref. Data* **1988**, *17*, 513–886.

(13)   Radiolysis of a diluted aqueous solution at around pH 7.0 produces primary water radicals such as oxidizing hydroxyl radical ($^\bullet$OH), reducing hydrated electrons (e_{aq}^-) and reducing hydrogen atoms ($^\bullet$H) with the *G* values of $G(^\bullet OH) = 280$ nmol J^{-1}, $G(e_{aq}^-) = 280$ nmol J^{-1} and $G(^\bullet H) = 60$ nmol J^{-1}, respectively.

(14)   Reductive degradation of peptide main chain may lead to small *G* values for the formation of

uncaged Tyr. See: Garrison, W. M. *Chem. Rev.* **1987**, *87*, 381–398.

(15) Similar effect of oxygen was observed for the activation of 5-FdUrd prodrugs. See: Tanabe, K.; Makimura, Y.; Tachi Y.; Imagawa-Sato, A.; Nishimoto, S. *Bioorg. Med. Chem. Lett.* **2005**, *15*, 2321–2324. and Ref. 10.

(16) We carried out one-electron reduction of **13** in aqueous solution containing 10% or 20% 2-methyl-2-propanol. We compared one-electron reactivity and confirmed that both reactions showed similar profiles.

General Conclusions

Chapter 1 showed the development of a novel hypoxia detection probe, conjugating a reducing indolequinone moiety with fluorescent coumarin chromophore (IQ-Cou). Indolequinone derivatives have been identified as quenchers for the adjacent fluorescent molecules and removable substitutes *via* one-electron reduction under hypoxic conditions. Therefore, IQ-Cou showed a weak fluorescence due to an intramolecular electron-transfer quenching of indolequinone unit to coumarin chromophore. Under hypoxic conditions, however, IQ-Cou underwent a one-electron reduction triggered by X irradiation or the action of a reduction enzyme to release a fluorescent coumarin chromophore, whereupon an intense fluorescence emission with a maximum intensity at 420 nm was observed. The one-electron reduction of IQ-Cou was suppressed by molecular oxygen under aerobic conditions. IQ-Cou also showed intense fluorescence in a hypoxia-selective manner upon incubation with a cell lysate of the human fibrosarcoma cell line HT-1080. The IQ-Cou conjugate has several unique properties that are favorable for a fluorescent probe of hypoxia-specific imaging.

Chapter 2 substantiated the versatility of the hypoxia-specific reactivity of indolequinone derivatives. An indolequinone derivative possessing biotin and C-5 linker units was newly synthesized (named **C5-IQ-Btn**) and incorporated into FITC-labeled avidin systems. **C5-IQ-Btn** was revealed to have high affinity to avidin protein, thus **C5-IQ-Btn** formed a complex with avidin-FITC chromophore (**AF-IQ-Btn**), resulting that the fluorescence of FITC was suppressed due to the adjacent indoelquinone units. **C5-IQ-Btn** was confirmed to decrease the fluorescence of other fluorescent-labeled (7-amino-4methylcoumarin-3-acetic acid, Texas Red, and rhodamine) avidin chromophore in a similar way. In addition, **C5-IQ-Btn** could quench the emission of a FITC-labeled streptavidin chromophore, suggesting that indoelquinone derivatives could efficiently suppress the fluorescence of the adjacent chromophore in spite of the difference of fluorescent maximum or that of the structure between avidin and streptavidin. Upon the enzymatic treatment under hypoxic conditions, **AF-IQ-Btn** caused the enhanced emission of FITC, suggesting that

indolequinone moiety is removed *via* one-electron reduction. In contrast, an enhancement of emission derived from avidin-FITC was suppressed upon the aerobic treatment, indicating that avidin-FITC complex possessing hypoxia-responsible indolequinone-biotin derivative was applicable to a hypoxia detectable probe.

Chapter 3 demonstrated a new class of functional magnetic nanoparticles (MNP) possessing a hypoxia-responsible indolequinone-biotin derivative (**C5-IQ-Btn**) and avidin-FITC (AF) complex (**AF-IQ-Btn@MNP**) for hypoxia-specific imaging systems. After the activation of the hydroxyl group at C-5 terminus of **C5-IQ-Btn** with *p*-nitrophenyl chloroformate (PNP-Cl), **C5-IQ-Btn** was incorporated onto MNPs (**IQ-Btn@MNP**). The amount of indolequinone-biotin units modified on an MNP was estimated to be 9.3–14.7 molecules using HABA analysis. The AF fluorescence was decreased by existing **IQ-Btn@MNP**, suggesting that AF formed a complex with **IQ-Btn@MNP** (**AF-IQ-Btn@MNP**), and thus AF fluorescence was suppressed by the adjacent quencher units of indolequinone and MNP. Upon enzymatic reduction under hypoxic conditions, weak fluorescent **AF-IQ-Btn@MNP** was observed to be enhanced emission at about 515 nm assigned AF chromophore, whereas an enhancement in fluorescence emission was suppressed upon aerobic treatment. With these reaction characteristics in a hypoxia-selective manner, **AF-IQ-Btn@MNP** might be applicable as a fluorescent probe for the molecular imaging of disease-relevant hypoxia.

Chapter 4 illustrated the development of a novel radiation-activated prodrug, incorporating a 2-oxopropyl group to an anti-tumour agent of cytarabine (named **oxo-ara-C**) that targeted hypoxic tumour tissues with selective cytotoxicity. The parent anti-tumour agent, **ara-C**, was confirmed to be released from **oxo-ara-C** *via* one-electron reduction upon hypoxic X-ray treatment. The prodrug **oxo-ara-C** had dramatically reduced cytotoxicity against human lung adenocarcinoma A549 cells relative to **ara-C** because of the effect of 2-oxopropyl substituent. In contrast, X-ray treatment of hypoxic A549 cells containing **oxo-ara-C** enhanced the cytotoxic effect, indicating that toxic **ara-C** was preferentially released in hypoxic cells *via* radiolytic one-electron reduction by hydrated electrons (e_{aq}^-).

Chapter 5 characterized tyrosine derivative possessing a 2-oxoalkyl group (Tyr(Oxo)) to evaluate its radiolytic reactivity caged amino acids and proteins. Upon hypoxic X-irradiation, Tyr(Oxo) released a 2-oxopropyl group to form the corresponding uncaged tyrosine. In addition, radiolysis of dipeptides containg Tyr(Oxo) revealed that the efficiency of radiolytic removal of 2-oxopropyl group increased significantly by the presence of neighboring aromatic amino acids.

List of Publications

Chapter 1

Emission under Hypoxia: One-Electron Reduction and Fluorescence Characteristics of an Indolequinone-Coumarin Conjugate

Kazuhito Tanabe, Nao Hirata, Hiroshi Harada, Masahiro Hiraoka, and Sei-ichi Nishimoto

ChemBioChem **2008**, *9*, 426–432.

Chapter 2

Hypoxia Imaging Probe: One-electron Reduction and Fluorescence Characteristics of a Complex of Avidin-FITC and Biotin-Indolequinone Conjugate

In preparation.

Chapter 3

Development of a Novel Hypoxia Detectable Probe: Synthesis and Properties of a Complex of Avidin-FITC and Magnetic Nanoparticle Conjugated with a Hypoxia-Response Indolequinone Derivative

Submitted.

Chapter 4

Radiolytic Activation of a Cytarabine Prodrug Possessing a 2-Oxoalkyl Group: One-Electron Reduction and Cytotoxicity Characteristics

Nao Hirata, Kazuhito Tanabe, Hiroshi Harada, Masahiro Hiraoka, and Sei-ichi Nishimoto

Org. Biomol. Chem. **2009**, *7*, 651–654.

Chapter 5

Radiolytic One-Electron Reduction Characteristics of Tyrosine Derivative Caged by 2-Oxopropyl

Group

Kazuhito Tanabe, Masahiko Ebihara, Nao Hirata, and Sei-ichi Nishimoto

Acknowledgments